



IntechOpen

Vegetation Index and Dynamics

Methodologies for Teaching Plant Diversity
and Conservation Status

*Edited by Eusebio Cano Carmona
and Ana Cano Ortiz*



Vegetation Index and Dynamics - Methodologies for Teaching Plant Diversity and Conservation Status

*Edited by Eusebio Cano Carmona
and Ana Cano Ortiz*

Published in London, United Kingdom

Vegetation Index and Dynamics – Methodologies for Teaching Plant Diversity and Conservation Status
<http://dx.doi.org/10.5772/intechopen.111283>

Edited by Eusebio Cano Carmona and Ana Cano Ortiz

Contributors

Edinéia A. S. Galvanin, Natalia V. Revollo, Federico Javier Beron de la Puente, Veronica Gil, Sandra Mara Alves da Silva Neves, Paula Zapperi, Kohei Cho, Rushikesh Kulkarni, Kiyoshi Honda, Pius Yoram Kavana, Bukombe John Kija, Emmanuel Pagiti Reuben, Ally Kiyenze Nkwabi, Baraka Naftal Mbwambo, Simula Peres Maijo, Selemeni Rehani Moshi, Shabani Haruna Matwili, Victor Alexander Kakengi, Stephen Justice Nindi, Koji Shimano, Yui Oyake, Tsuyoshi Kobayashi

© The Editor(s) and the Author(s) 2024

The rights of the editor(s) and the author(s) have been asserted in accordance with the Copyright, Designs and Patents Act 1988. All rights to the book as a whole are reserved by INTECHOPEN LIMITED. The book as a whole (compilation) cannot be reproduced, distributed or used for commercial or non-commercial purposes without INTECHOPEN LIMITED's written permission. Enquiries concerning the use of the book should be directed to INTECHOPEN LIMITED rights and permissions department (permissions@intechopen.com).

Violations are liable to prosecution under the governing Copyright Law.



Individual chapters of this publication are distributed under the terms of the Creative Commons Attribution 3.0 Unported License which permits commercial use, distribution and reproduction of the individual chapters, provided the original author(s) and source publication are appropriately acknowledged. If so indicated, certain images may not be included under the Creative Commons license. In such cases users will need to obtain permission from the license holder to reproduce the material. More details and guidelines concerning content reuse and adaptation can be found at <http://www.intechopen.com/copyright-policy.html>.

Notice

Statements and opinions expressed in the chapters are those of the individual contributors and not necessarily those of the editors or publisher. No responsibility is accepted for the accuracy of information contained in the published chapters. The publisher assumes no responsibility for any damage or injury to persons or property arising out of the use of any materials, instructions, methods or ideas contained in the book.

First published in London, United Kingdom, 2024 by IntechOpen

IntechOpen is the global imprint of INTECHOPEN LIMITED, registered in England and Wales, registration number: 11086078, 5 Princes Gate Court, London, SW7 2QJ, United Kingdom

British Library Cataloguing-in-Publication Data

A catalogue record for this book is available from the British Library

Additional hard and PDF copies can be obtained from orders@intechopen.com

Vegetation Index and Dynamics – Methodologies for Teaching Plant Diversity and Conservation Status

Edited by Eusebio Cano Carmona and Ana Cano Ortiz

p. cm.

Print ISBN 978-0-85466-104-6

Online ISBN 978-0-85466-103-9

eBook (PDF) ISBN 978-0-85466-105-3

We are IntechOpen, the world's leading publisher of Open Access books Built by scientists, for scientists

6,800+

Open access books available

183,000+

International authors and editors

195M+

Downloads

156

Countries delivered to

Our authors are among the
Top 1%

most cited scientists

12.2%

Contributors from top 500 universities



WEB OF SCIENCE™

Selection of our books indexed in the Book Citation Index
in Web of Science™ Core Collection (BKCI)

Interested in publishing with us?
Contact book.department@intechopen.com

Numbers displayed above are based on latest data collected.
For more information visit www.intechopen.com



Meet the editors



Eusebio Cano Carmona obtained a Ph.D. in Science from the University of Granada, Spain. He is Professor of Botany at the University of Jaén, Spain. His fundamental line of research is flora and vegetation in Spain, Italy, Portugal, Palestine, the Caribbean islands, and Mexico. He has directed 13 doctoral theses and published 250 articles, books, and book chapters. He participates in national and international congresses and has presented about 200 papers and communications. He has held different academic positions, including Director of the Dean of the Faculty of Experimental Sciences and Founder and Director of the International Seminar on Management and Conservation of Biodiversity. Dr. Carmona is a member of the Spanish, Portuguese and Italian Geobotany societies. He is also a counselor at Instituto de Estudios Gien-nenses in Jaén, Spain.



Ana Cano Ortiz has a Ph.D. in Botany from the University of Jaen, Spain. She has worked in private business and higher education, including at the University of Complutense, Madrid. She is co-director of three doctoral theses. Her line of research is related to botanical bioindicators and the didactics of experimental sciences. She has worked in Spain, Italy, Portugal, and Central America. She has published more than 100 papers in various national and international magazines, as well as books and book chapters. She has also presented 100 papers and communications at national and international congresses. She is currently a professor in the Department of Didactics of Experimental, Social and Mathematical Sciences in Madrid. She is a journal co-editor and reviewer. Her research has focused mainly on edaphic bioindicators, bioclimatology, agriculture, and science education in European territories and locations in Central America and Palestine.

Contents

Preface	XI
Chapter 1	1
Monitoring and Mapping of the Brazilian Pantanal Wetland <i>by Edinéia A.S. Galvanin, Natalia V. Revollo, Federico Javier Beron de la Puente, Veronica Gil, Sandra Mara Alves da Silva Neves and Paula Zapperi</i>	
Chapter 2	17
Recovery Monitoring of Tsunami-Damaged Paddy Fields Using MODIS NDVI <i>by Kohei Cho</i>	
Chapter 3	41
Estimating Rice LAI Using NDVI: A Method for Plant Conservation Education <i>by Rushikesh Kulkarni and Kiyoshi Honda</i>	
Chapter 4	63
Plant Diversity in Agro-Pastoral Grasslands of Tanzania <i>by Pius Yoram Kavana, Bukombe John Kija, Emmanuel Pagiti Reuben, Ally Kiyenze Nkwabi, Baraka Naftal Mbwambo, Simula Peres Maijo, Selemani Rehani Moshi, Shabani Haruna Matwili, Victor Alexander Kakengi and Stephen Justice Nindi</i>	
Chapter 5	79
Methods and Practices for Analyzing Vegetation Shift Using Phytosociological Hierarchical Data <i>by Koji Shimano, Yui Oyake and Tsuyoshi Kobayashi</i>	

Preface

This book provides a comprehensive overview of vegetation and methodologies for teaching plant diversity and conservation. The information herein will serve to train future environmental managers about sustainable development and its benefits for the environment. The book reveals the state of conservation of different places in Asia and Africa and presents methodologies on education for nature conservation. In this sense, the teaching of vegetation, its dynamics, and the conservation of habitats will have an impact on a balanced, cultural, and socioeconomic development favorable to the population.

The editors would like to thank IntechOpen, especially Publishing Process Manager Mateo Belir for the unconditional help provided throughout the publication process.

Dr. Eusebio Cano Carmona

Professor of Botany,
Department of Animal and Plant Biology and Ecology,
Section of Botany,
University of Jaen,
Jaen, Spain

Dr. Ana Cano Ortiz

Professor of Experimental Sciences,
Department of Didactics of Experimental,
Social and Mathematical Sciences,
Complutense University of Madrid,
Madrid, Spain

Chapter 1

Monitoring and Mapping of the Brazilian Pantanal Wetland

*Edinéia A.S. Galvanin, Natalia V. Revollo,
Federico Javier Beron de la Puente, Veronica Gil,
Sandra Mara Alves da Silva Neves and Paula Zapperi*

Abstract

The Pantanal is one of the largest wetlands in the world. This natural region has fundamental importance for water supply and biodiversity conservation. In this paper, we apply a methodology to analyze multi-temporal water and vegetation changes in six different zones of land use/land cover and their relationship with humidity in the Brazilian Pantanal subregion of Cáceres, Mato Grosso. Meteorological data from the INMET Station in Cáceres was used. The Normalized Difference Vegetation Index (NDVI) and Normalized Difference Moisture Index (NDMI) were compared year to year (2019, 2020, 2021). The spatial variations revealed water changes according to the occurrence of wet and dry years. In dry years there was a remarkable increase in mean and maximum values linearly related to a decrease in water availability. Analyzing LULC change dynamics in these areas is crucial for developing new proposals for interventions to monitor the area and thus provide subsidies to goal 15 of the 2030 Sustainable Development Agenda, which aims to stop and restore degradation caused in the environment and to promote reforestation.

Keywords: wetland, Pantanal, remote sensing, NDVI, NDMI

1. Introduction

The Pantanal is an extraordinary and diverse natural region located in South America. It stands as one of the largest continuous wetland areas on the planet, encompassing territories of Brazil, Bolivia, and Paraguay. The hotspot holds significant importance as it has been designated both a World Heritage Site and a Biosphere Reserve by UNESCO (2000).

Renowned for its abundant biodiversity and landscapes, the Pantanal hosts an impressive array of ecosystems, including savannahs, forests, rivers, lagoons, and marshes. This diversity of habitats attracts a wide range of wildlife. In addition to its incredible fauna, the Pantanal holds significant ecological importance [1]. Its floodplains “act as a natural sponge, absorbing large amounts of water during the rainy season and gradually releasing it during the dry season” [2]. The storage capacity of

the rivers helps regulate the flow of water across the continent, which is essential for regional hydrological balance.

The Pantanal, however, faces many challenges. There are many threats to the ecosystem of this region including deforestation, fires, agricultural practices, and livestock farming [3].

Preserving the Pantanal and ensuring its sustainability is vital not just for conserving biodiversity but also for safeguarding water resources and the welfare of local communities. This research makes a significant contribution to advancing methods for detecting changes in land use, thereby facilitating studies that are in line with the objectives of the United Nations' 2030 Agenda for Sustainable Development [4], particularly regarding the indicators of Goal 6, "Clean Water and Sanitation," and Goal 13, "Action against global climate change."

Understanding the dynamics of land use and land cover (LULC) changes, as well as their impact on humidity levels, are crucial in the field of environmental research. Remote sensing techniques play a significant role in studying and monitoring these changes over time. The application of advanced remote sensing technologies and methodologies enables us to capture and analyze spatial and temporal patterns of LULC changes [5], providing valuable insights into the processes driving these transformations.

The integration of remote sensing with geographic information systems (GIS) Normalized Difference Vegetation Index (NDVI), and Normalized Difference Moisture Index (NDMI) enhances our ability to accurately identify and classify LULC changes. With this multidisciplinary approach, it is possible to develop robust models and predictive frameworks that can be applied to evaluating the impacts of land use adjustments on humidity patterns across a spectrum of scales, from local to regional. This knowledge is crucial for sustainable land management, water resource planning, and climate change adaptation measures.

This paper presents a methodology for analyzing multi-temporal land use/land cover changes and their relationship with humidity in the Cáceres Pantanal.

2. Material and methods

2.1 Study area

The Cáceres Pantanal occupies a privileged position among the sub-regions of the Pantanal biome's wetland plain, situated in the Upper Paraguay River Basin [6], in Brazil's Central-West region (**Figure 1**). It encompasses a diverse mosaic of savanna vegetation, including wooded Savanna, forested Savanna, woody-grass Savanna, as well as alluvial Forest [7], providing a habitat for a wide array of species uniquely adapted to the dynamic floodplain ecosystem [8]. Its altitude ranges from 90 to 150 meters [9, 10]. The Pantanal is primarily composed of Quaternary sediments that have accumulated over time.

The Upper Paraguay River Basin region is characterized by two primary aquifers: the Pantanal Aquifer (Quaternary) and the Guarani Aquifer (Jurassic-Triassic). While the waters from the Pantanal Aquifer drain into the Paraguay River, the deeper waters of the Guarani Aquifer flow towards the Paraná Basin [11].

In the Cáceres Pantanal region, the predominant soils are Plinthosols, Plinthosols, and Quartzarenic Neosols, influenced by hydromorphic processes [12]. The average annual temperature in the Cáceres Pantanal is 26.24°C, with an annual rainfall index

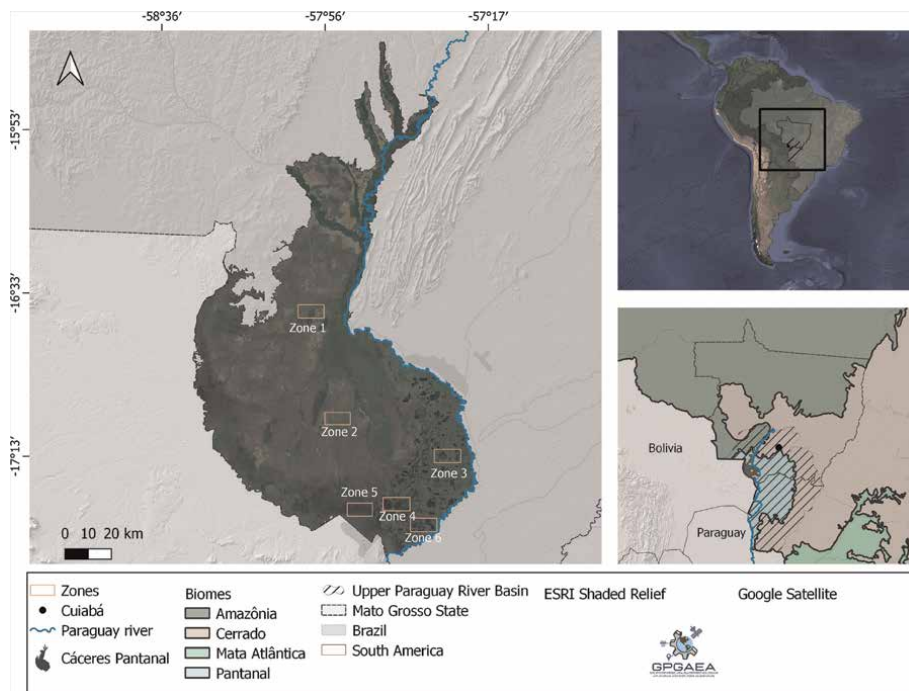


Figure 1.
 Study area: C  ceres Pantanal.

of 1335.00 mm [13, 14]. The Pantanal exhibits two distinct ecohydrological cycles: the dry season occurs from May to September and the rainy season spans from October to April, during this time, the region receives a substantial amount of precipitation, typically accounting for 70–80% of the total annual rainfall [13]. During the dry season, surface water becomes scarce and is mostly limited to perennial rivers with well-defined beds and large ponds [15].

2.2 Data pre-processing

Initially, we divided the Pantanal into six regions based on their morphological features (**Figure 1**). The six zones consist of mosaics, with Zone 1 comprising forested Savanna, woody-grass Savanna, and pioneer Formation. Zone 2 comprises wooded Savanna, woody-grass Savanna, and pioneer Formation. Zones 3, 4, 5, and 6 are characterized by bodies of water, vegetation influenced by rivers and/or lakes, and woody-grass Savanna. Zones 1 and 2 are located within the so-called seasonally inundated areas, while zones 3, 4, 5, and 6 belong to the frequently flooded and permanently flooded-hydromorphic zones [16].

The meteorological data used in this study were collected from the Meteorological Station of the National Institute of Meteorology (INMET) in C  ceres (code 01657000). This station is located at the Federal Institute of Mato Grosso (IFMT) at -16   13' S -57   69' W. For analysis, basic descriptive values were obtained for temperature, evapotranspiration, and relative humidity (sum, average) for monthly and seasonal (rainy season) values.

To enhance the knowledge of the Pantanal wetland dynamic, the study incorporated meteorological data and the Standardized Precipitation Evapotranspiration Index (SPEI) to assess the presence of drought periods occurring between 2018 and 2021. The data was obtained at a 12-month scale (SPEI 12) from the global model SPEI Global Drought Monitor and downloaded with a spatial resolution of 1° [17].

To calculate the SPEI, monthly mean temperature data were obtained from the NOAA NCEP CPC GHCN_CAMS gridded dataset [18]. Additionally, cumulative monthly precipitation data were sourced from the Global Precipitation Climatology Centre global model [19]. The SPEI Global Drought Monitor estimates reference evapotranspiration using the Thornthwaite method [20].

The SPEI time series were analyzed in conjunction with data from the weather station. The 12-month scale allows the identification of areas and time intervals with persistent drought conditions [21, 22]. According to the categorization of SPEI values, a dry event occurs when values are less than -0.5 , initiating drought. As values decrease, the magnitude of the drought increases. A drought event where the category is moderately dry takes values between -1 and -1.5 , while very dry is values between -1.5 and -2 and a drought magnitude of extremely dry is when the results are less than -2 [22].

The multispectral images from the Sentinel-2A satellite were acquired through the Earth Engine Catalog. The dataset comprises a total of eighteen images, with six images captured during each rainy season spanning from October 2018 to March 2019, October 2019 to March 2020, and October 2020 to March 2021, respectively. Each image represents the mean image of the rainy period, with a filtering process applied to exclude cloudy pixels, ensuring that they account for less than 10% of the image. Considering the annual weather variability in the Pantanal, we have selected the pre-fire images from 2018, as well as the post-fire images from 2020 and 2021.

In order to evaluate the green vegetation in the Pantanal regions, we employed the normalized difference vegetation index (NDVI). The NDVI is a widely used metric for quantifying the health and density of vegetation using satellite data. It is calculated by taking the normalized difference between the reflectance values in the red and near-infrared bands. The red band measures the amount of light reflected by vegetation in the visible red spectrum, while the near-infrared band captures the sunlight reflected by chlorophyll in plants in the near-infrared spectrum.

$$NDVI = \frac{NIR - Red}{NIR + Red} \quad (1)$$

For detecting moisture levels in the vegetation, we obtain the Normalized Difference Moisture Index (NDMI). This allows the combination of the near-infrared (NIR) and shortwave infrared (SWIR) spectral bands [23]. The SWIR bands depend on the changes in the vegetation water content and the spongy mesophyll structure of plant canopies [24]. Values between -1 to -0.4 indicate absent or very low ground vegetation cover, while values from -0.4 to 0.4 show different ranges of water stress, and values above 0.4 to 1 represent high-density cover with no water stress.

$$NDMI = \frac{NIR - SWIR}{NIR + SWIR} \quad (2)$$

To qualitatively analyze the changes in NDVI, a multi-temporal color composite image was generated. This technique combines the NDVI values from period 1, period 2,

and period 3 into the red, green, and blue channels, respectively, based on the temporal order. This approach is commonly used to visualize and analyze temporal dynamics, such as land cover changes, over a specific period.

In the composite image, high values of vegetation in one period are represented by red, green, or blue colors. Gray levels indicate features that remain stable across all periods. The absence of vegetation in all periods is represented by the black color. Regions with high vegetation values in two periods are indicated by a combination of yellow, cyan, or magenta colors. Situations, where the presence or absence of vegetation differs, are represented by the magenta and green colors. This approach enables a visual expert assessment of temporal changes in vegetation density and distribution, facilitating the identification of areas with consistent vegetation patterns, changes, or absence throughout the analyzed periods.

A linear regression trend analysis was conducted to assess NDVI evolution during the years 2018, 2019, 2020, and 2021. The analysis treated NDVI as the dependent variable and time as the independent variable. The regression model estimated the slope coefficients of the regression line, which provide insights into the trend of NDVI over time. By examining the slope of the regression line, it is possible to determine whether NDVI is increasing or decreasing. A positive slope indicates an increasing trend in NDVI, suggesting a rise in vegetation density or health. Conversely, a negative slope indicates a decreasing trend, indicating a decline in vegetation density or health. The input data for the regression model consisted of monthly NDVI images, with cloudy pixels filtered out. These NDVI images were organized as a two-band input image, with the first band representing the NDVI values and the second band representing the corresponding time information.

To apply the workflow, we used the geospatial processing service Google Earth Engine (GEE). The algorithms and the fit model were implemented using the Earth Engine (EE) Code Editor, a web-based IDE for the Earth Engine JavaScript API.

3. Results and discussion

The Pantanal region is of great significance due to its distinctive ecological characteristics and high vulnerability to climate change. Understanding the rainfall variability, temperature fluctuations, and hydrological dynamics, is essential for predicting and managing the impacts of climate change on the Pantanal's delicate balance.

In terms of precipitation, it is observed that for the period 2018–2021, the peaks of maximum accumulated monthly precipitation are found in the wet season, which is between the months of October to April. It is to be recognized that climatically a variation of rainfall can be found in the wet season although there are certain months where the monthly amounts usually exceed 80 mm, coinciding with the results of the 1971–2009 time series [25]. While the dry season is between the months of June to September, where monthly amounts do not usually exceed 10 mm per month.

On the other hand, if we talk about the average temperatures in the study area, they do not fall below 20°C and the maximum temperature peaks are found precisely at the beginning of the wet season, reaching 30°C. In contrast, the average monthly humidity percentage shows that the minimum peaks are distributed just before the beginning of the rainy season. Finally, evapotranspiration peaks coincidentally at the

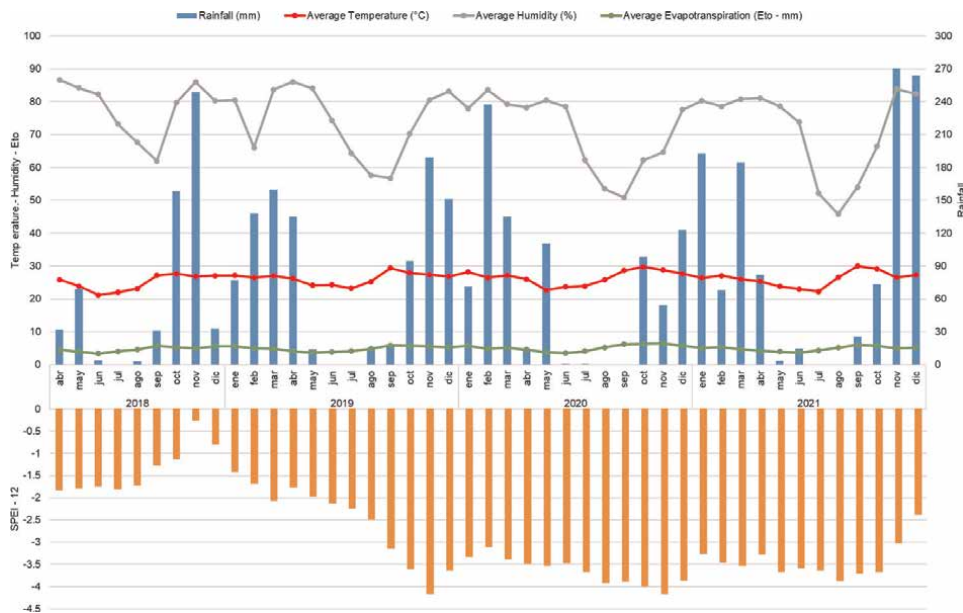


Figure 2. Annual distribution of the climatic variables (top). SPEI -12 values for the period (bottom).

beginning of the rainy season (September–October) and its lowest values in the dry season months.

In **Figure 2**, it is evident that most of the studied period, which spans from 2018 to 2021, was characterized by an extremely dry drought regime (SPEI value less than -2). This prolonged drought event persisted from June 2019 until the end of the climate data in December 2021, encompassing approximately 71% of the time series. Specifically, 18% of the months were classified as experiencing a very dry drought, 7% as moderately dry, and 2% as an incipient drought or a normal event.

By the other hand, the variations observed in precipitation may indicate the influence of climatic anomalies like El Niño–Southern Oscillation (ENSO), which can impact indirectly in the superficial hydrological regime of the Pantanal. The Oceanic Niño Index (ONI) is a primary indicator for monitoring the sea surface temperature (SST) of the equatorial Pacific Ocean part of the seasonal climate pattern. The NOAA's Climate Prediction Center monitoring system calculates them historically [26]. The ONI anomaly values for the period show that the SST anomaly was negative at the beginning of 2018 and during the period from 2021 to the end of 2022. From the end of 2018 to mid-2019 the SST anomaly was positive. This could be indicative of the fluctuations in precipitation shown in **Figure 2**.

Figure 3 focuses on the monthly values of rainy seasons between 2018 and 2021. Their values remain relatively stable without significant variation. However, precipitation exhibits the most significant fluctuations, with relative humidity values following these changes.

Table 1 presents the average values (Temperature, Evapotranspiration, and Humidity) and the accumulated Rainfall for each rainy season, confirming the findings mentioned in the previous paragraph. Additionally, an interesting observation can be made for the three periods: as the accumulated precipitation decreases, the mean values and standard deviations of the other variables tend to increase.

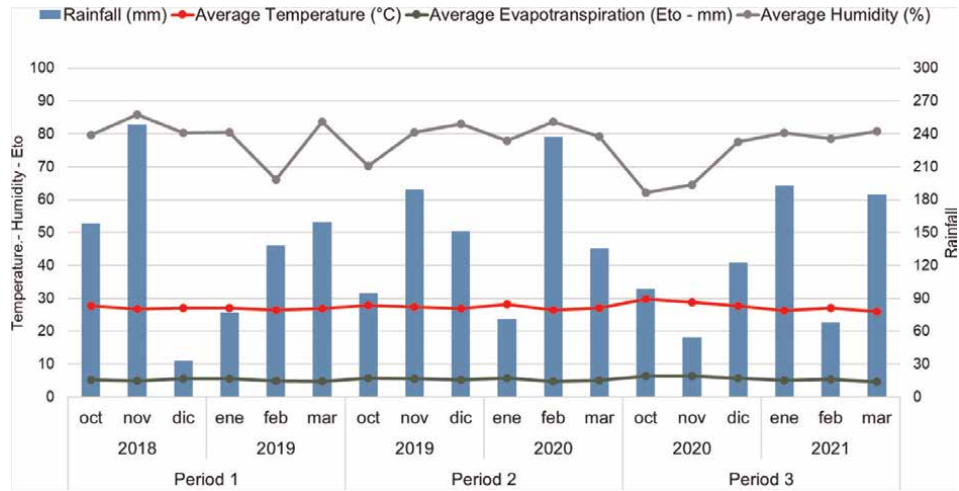


Figure 3.
Time slices detailing the rainy season.

Period	Rainfall (mm)	Average Temperature (°C)	Average Humidity (%)	Average Evapotranspiration (Eto - mm)
1) 10/2018 to 3/2019	814.6	27.0 +/- 1.27	79.6 +/- 8.21	5.2 +/- 0.81
2) 10/2019 to 3/2020	878.4	27.3 +/- 1.56	79.1 +/- 7.11	5.4 +/- 0.86
3) 10/2020 to 3/2021	720.4	27.6 +/- 2.03	90.9 +/- 11.22	5.6 +/- 1.12

Table 1.
Variability of meteorological data in the Pantanal of Cáceres: October 2018 to march 2019.

During the final period, a noteworthy decline in rainfall occurred. It is worth noting that this reduction can be attributed to the decreased transport of warm and humid air from Amazonia into the Pantanal. Notably, a substantial atmospheric shift took place during this period, characterized by the prevailing influence of warmer and drier air masses originating from subtropical latitudes. According to [27] this shift resulted in a considerable decrease in summer rainfall, particularly during the peak of the monsoon season. These changes in atmospheric conditions hold implications for the Pantanal’s hydrological dynamics and overall climate patterns.

To analyze the vegetation and humidity in the Pantanal region, we computed and gathered NDVI and NDMI images during the rainy periods for selected zones. These images were compiled into a multi-temporal map, covering the period from 2018 to 2021, for each specific region (**Figures 4** and **5**).

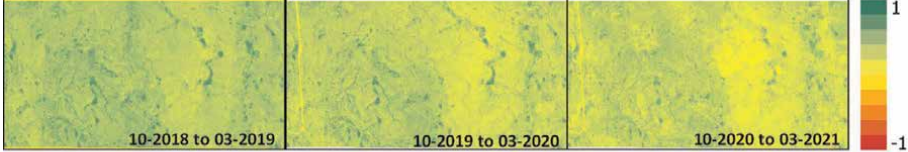
The multi-temporal map visually represents the changes in NDVI and NDMI values across various regions of the Pantanal throughout the specified period. The NDVI map indicates a stable vegetation density and health in the seasonally inundated areas, specifically in Zone 1 and Zone 2. The lowest NDVI values are observed in the flooded zones during period 1 and 2. However, period 3 exhibits the highest NDVI values, coinciding with the peak humidity level of 90.9%.

NDVI Images

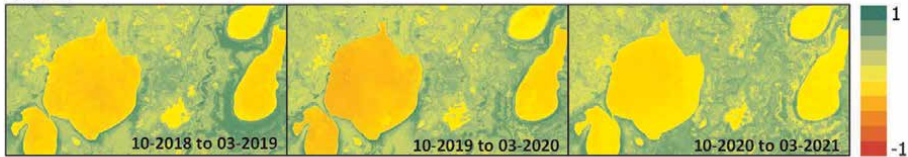
Zone 1:



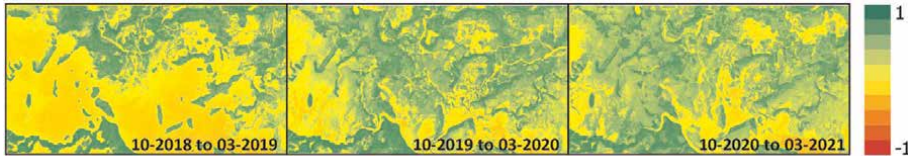
Zone 2:



Zone 3:



Zone 4:



Zone 5:

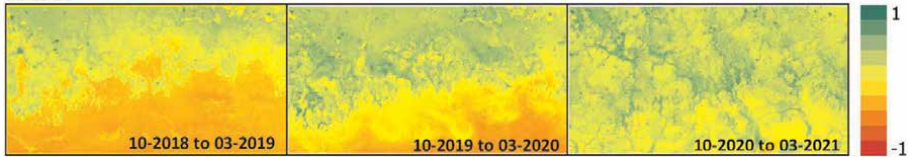


Figure 4.
NDVI multi-temporal map covering the period from 2018 to 2021, for each zone.

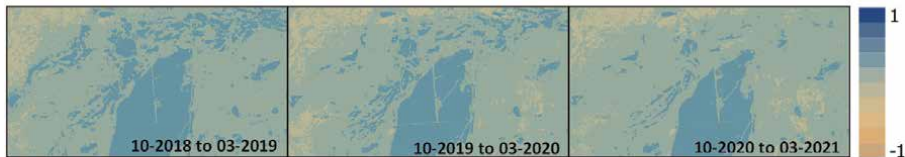
It is notable that the seasonally inundated areas (zones 1 and zone 2) have shown a decrease in the NDMI index over the last two years. The lowest values were observed in period 2 for zone 2, which coincided with the lowest average humidity of 79.1% recorded by the in-situ station. Zone 4 exhibited the highest NDMI values during period 2, which can be attributed to the hydromorphic features of the area. This coincides with the fact that period 2 also had the highest recorded precipitation values. In the frequently flooded and permanently flooded-hydromorphic zones, the maximum NDMI values are observed in zone 3 and zone 6 during period 3. This coincides with the highest recorded humidity values at the in-situ station location.

The multi-temporal images, generated by combining the NDMI index from the three different periods, are shown in **Figure 6**. The color scale on the images indicates the presence of vegetation in one, both, none, or all of the periods. By examining the images and referring to the color table, it is possible to quantitatively assess the fluctuations of vegetation across the six zones.

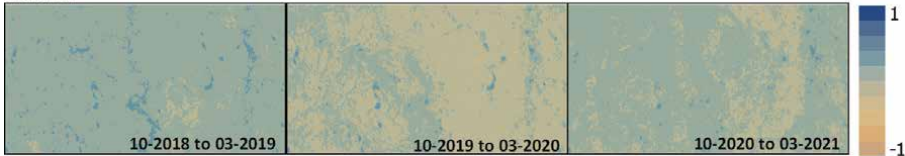
Zones 1 and 2 are represented by a significant portion of magenta-colored pixels in the image, indicating the presence of vegetation during periods 1 and 3, but the

NDMI Images

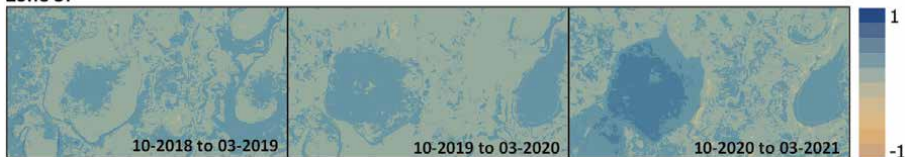
Zone 1:



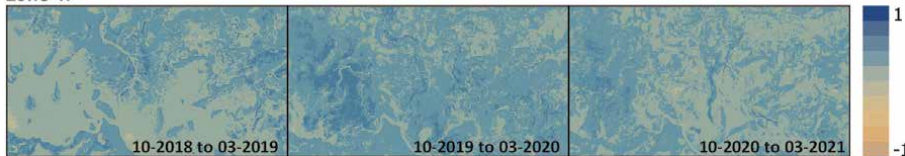
Zone 2:



Zone 3:



Zone 4:



Zone 5:

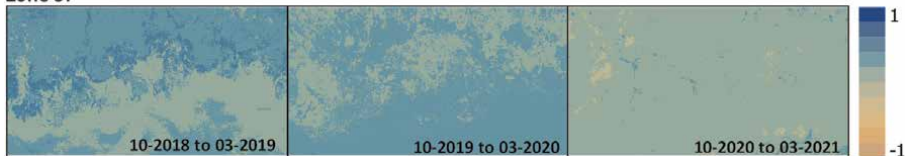


Figure 5.
 NDMI multi-temporal map covering the period from 2018 to 2021, for each region.

absence of vegetation in period 2. Zone 3 exhibits a lack of vegetation, which corresponds with the presence of prominent lakes in the area. Along the edges of these lakes, yellow-colored pixels appear, suggesting the absence of vegetation in recent periods. However, some areas along the lake edges show signs of vegetation presence.

Zones 4 and 5 display pixels in blue and cyan, indicating an increase in vegetation. These zones demonstrate a variety of color combinations, which signifies their dynamic nature, particularly in relation to the permanently flooded areas. Zone 5, located near the lake, exhibits a distinct pattern of vegetation along the perimeter of the lake. This pattern may indicate sediment deposition from the adjacent plateau areas, which contributes to the presence of vegetation in that specific zone.

In **Figure 7**, Zones 4 and 5 exhibited substantial growth in vegetation, which can be attributed to the enhanced sediment transport by the tributaries from the plateau region in these areas [28]. This sediment deposition has played a vital role in expanding vegetation cover and reducing water volume, considering that these zones experience frequent or permanent flooding. Conversely, zones 1, 2, and 3 visually showed minimal vegetation loss. Zones 1 and 2 are seasonally flooded areas.

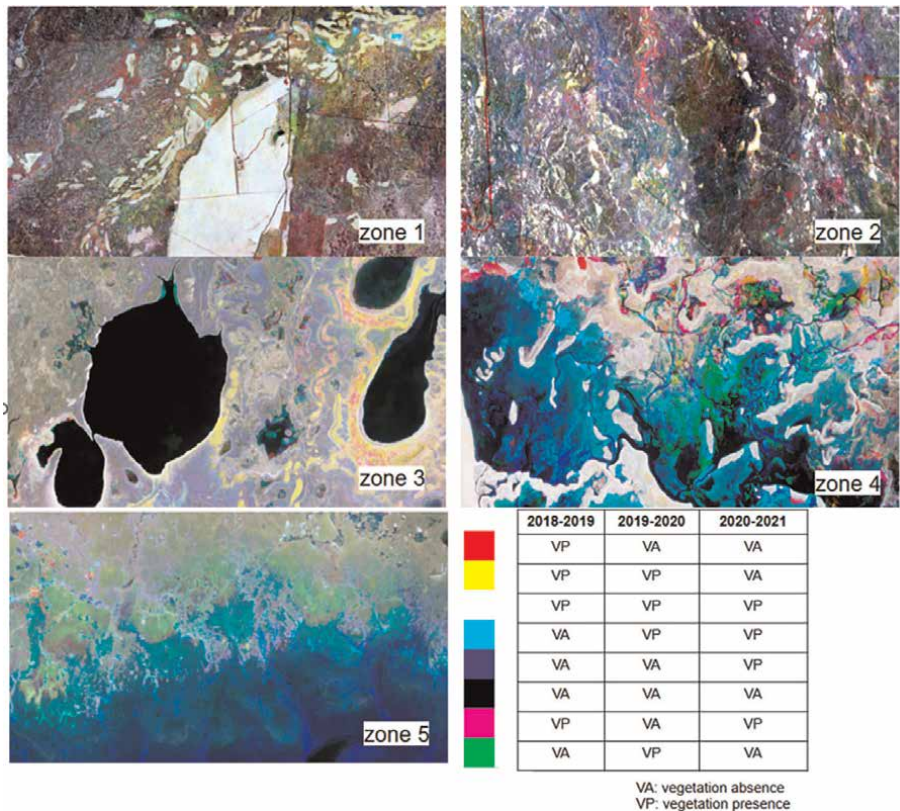


Figure 6. Multi-temporal image created by combining the NDVI index from three different periods: Period 1, period 2, and period 3. The color scale used in the image indicates the presence or absence of vegetation.

Understanding the impact of flooded areas is crucial as any decrease in the Pantanal's flooded areas can have significant consequences for the region's unique ecosystem and biodiversity. It can result in the loss of crucial habitats for aquatic species such as fish, amphibians, and water-dependent plants, disrupting their survival and overall ecological balance. Preserving the flooded areas is essential for maintaining the delicate equilibrium of the Pantanal [27, 28].

Furthermore, the decline in flooded areas can disrupt the natural water cycle and hydrological processes in the Pantanal. It may result in decreased water availability for wildlife, impacting their feeding and breeding patterns.

Figure 8 summarizes the results of the methodology applied in zone 6, which is characterized by frequently flooded and permanently flooded-hydromorphic zones. The multi-temporal map of NDMI and NDVI, along with the multi-temporal and NDVI slope images, provided valuable information for analyzing the dynamics of vegetation and water in the area.

The NDVI values for the last period indicated an increase in vegetation cover, suggesting a potential improvement in plant growth and density. Conversely, the NDMI values demonstrated a decrease in water presence, indicating a reduction in moisture levels within the studied regions, particularly during the peak of the monsoon season (**Figure 8**). A study conducted by [28] used the NDVI to compare monthly

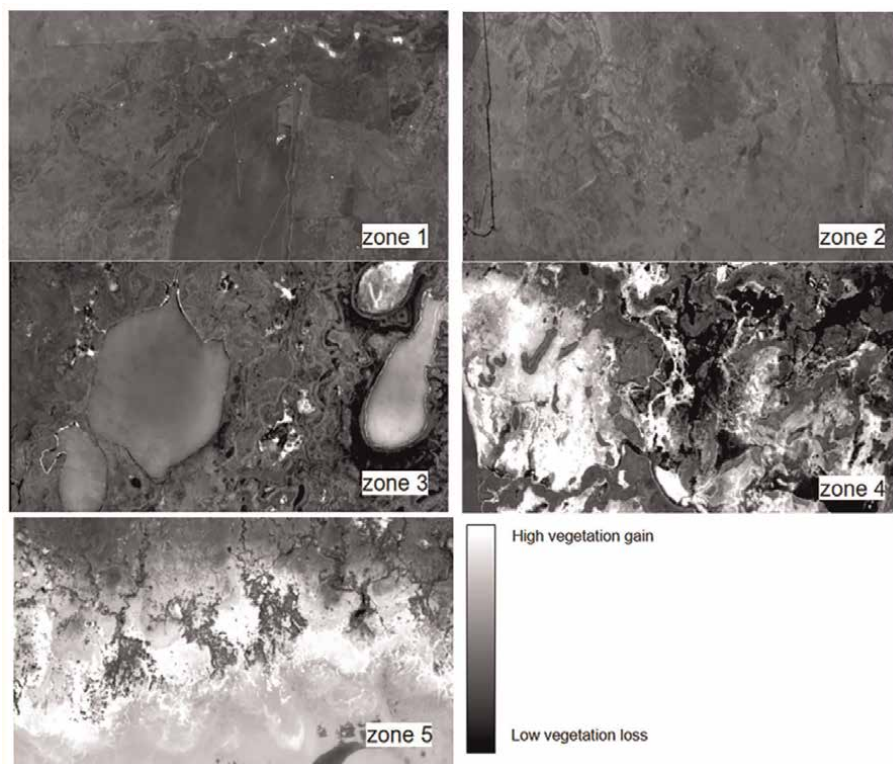


Figure 7.
 NDVI slope image provides insights into the trend of vegetation density or health (represented by a trend towards white). On the other hand, a negative slope indicates a decreasing trend in NDVI (represented by a trend towards black).

precipitation and water table depth. The study demonstrated a correlation between higher absolute NDVI values with wet years, during which a greater extent of woody vegetation covered the area [29]. While the study focused on a different environment from the Pantanal, the prevalence of vegetation remains consistent, allowing NDVI values to serve as an indicator of water in the soil.

In the second period (2019–2020) most of the NDMI values indicate water stress. However, this is not reflected in the NDVI, where vegetation coverage/density increases (showing more positive values) from the first period (2020–2021) to the second period. In the third period, the water stress measured by NDMI decreases, and there is an increase in vegetation gain according to the NDVI. In this particular zone, the vegetation is influenced by rivers and/or lakes and belongs to the frequently flooded and permanently flooded-hydromorphic zones. The findings appear to have been an imbalance in the water balance during the first period due to the prevailing conditions of rainfall, temperature, humidity, and evapotranspiration. This led to water stress in the second period, with a subsequent “recovery” observed in the third period.

4. Conclusion

This paper presents a methodology for analyzing multi-temporal land use/land cover changes and their relationship with humidity in the Caceres Pantanal. The

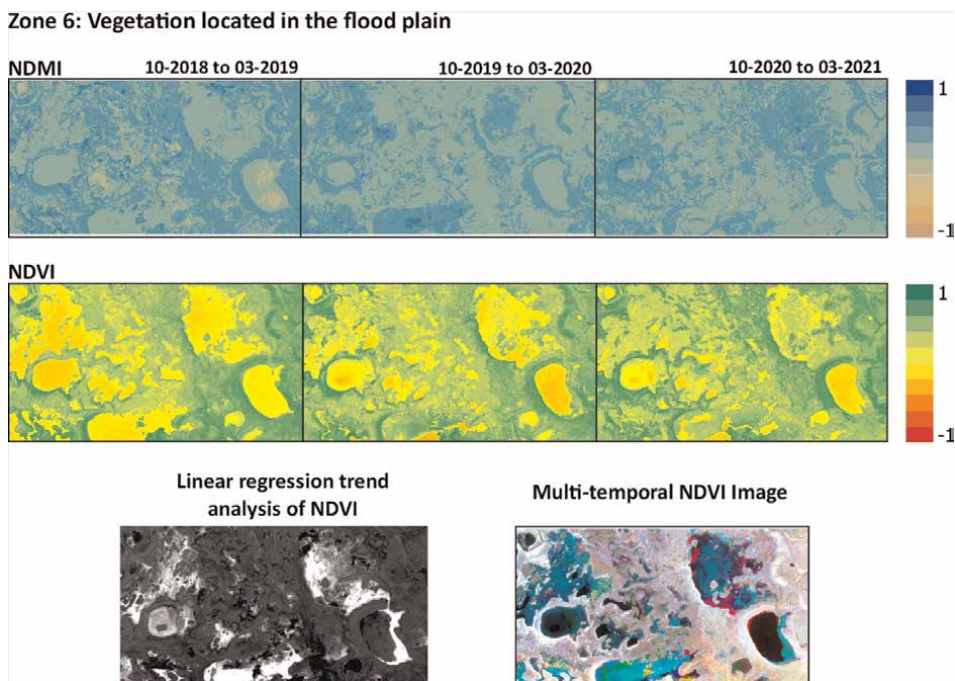


Figure 8.
Vegetation and humidity patterns using NDMI, and NDVI.

analysis reveals that the studied period in the Caceres Pantanal was predominantly characterized by an extremely dry drought regime. As the accumulated precipitation decreases for each period, both the mean and standard deviation exhibit an increasing trend. This indicates a noticeable impact on the overall variability and average values of rainfall during these specific periods. These results emphasize the importance of considering the variability and potential consequences of reduced rainfall seasons when studying the climate dynamics in the analyzed area.

The multi-temporal maps of NDMI and NDVI, along with the multi-temporal and slope images, demonstrate the importance of satellite data processing methodologies for analyzing the dynamics of land use/land cover (LULC) changes and their impact on humidity in the Brazilian Pantanal. This region remains largely pristine, and its ecological integrity is intricately linked to its hydrology. The methodology provides information to qualitatively analyze the dynamics of an interested region. All of this is achieved through the availability of data and processing tools offered by the GEE platform.

Analyzing land use change dynamics in these areas is crucial for developing new proposals for interventions to monitor the area and thus provide subsidies to goal 15 of the 2030 Sustainable Development Agenda, which aims to stop and restore degradation caused in the environment and to promote reforestation.

The alteration in flooded areas can influence the overall climate of the Pantanal. Wetlands play a crucial role in regulating temperature, humidity, and precipitation patterns. A decrease in flooded areas may disrupt these natural climate regulation mechanisms, leading to changes in local weather patterns and potentially affecting neighboring regions.

The findings of this study contribute to a better understanding of the Pantanal's hydrological dynamics and provide information for sustainable land management and conservation efforts in the region. Further research and monitoring are necessary to assess the long-term implications of LULC changes and develop effective strategies for preserving the ecological integrity of the Pantanal.

Acknowledgements

The work was supported by São Paulo State University, and National Council for Scientific and Technical Research (CONICET), Argentina.

Conflict of interest

The authors declare no conflict of interest.

Data availability

Data were collected from freely available images composites from the GEE catalog.

Code availability

QGIS software (version 3.22.14), GEE catalog.

Author details

Edinéia A.S. Galvanin^{1*}, Natalia V. Revollo², Federico Javier Beron de la Puente³, Veronica Gil³, Sandra Mara Alves da Silva Neves⁴ and Paula Zapperi³

1 Department of Geography and Planning, São Paulo State University, Ourinhos, Brazil


2 Institute for Computer Science and Engineering Universidad Nacional del Sur - CONICET, Bahía Blanca, Argentina

3 Department of Geography and Tourism, Universidad Nacional del Sur - UNS/ CONICET, Bahía Blanca, Argentina

4 Faculty of Human Sciences/Geography Course, University of Mato Grosso State, Cáceres, Brazil

*Address all correspondence to: edineia.galvanin@unesp.br

IntechOpen

© 2023 The Author(s). Licensee IntechOpen. This chapter is distributed under the terms of the Creative Commons Attribution License (<http://creativecommons.org/licenses/by/3.0>), which permits unrestricted use, distribution, and reproduction in any medium, provided the original work is properly cited. 

References

- [1] Brasil. Ministério do Meio Ambiente. Convenção de Ramsar. 2008. Available from: <http://www.mma.gov.br/biodiversidade/biodiversidade-aquatica/zonas-umidasconvencao-de-ramsar>
- [2] Wantzen KM et al. Towards a sustainable management concept for ecosystem services of the Pantanal wetland. *Ecohydrology & Hydrobiology*. 2008;**8**:115-138
- [3] Berlinck LCN et al. The Pantanal is on fire and only a sustainable agenda can save the largest wetland in the world. *Brazilian Journal of Biology*. 2022;**82**. DOI: 10.1590/1519-6984.244200
- [4] Nações Unidas no Brasil ONU BR: The Agenda 2030. Available from: <https://nacoesunidas.org/pos2015/agenda2030/> [Accessed: June 20, 2023]
- [5] Lu D, Li G, Moran E, Hetrick S. Spatiotemporal analysis of land use and land cover change in the Brazilian Amazon. *International Journal of Remote Sensing*. 2013;**34**:5953-5978
- [6] Silva JSV, Abdon MM. Delimitação do Pantanal brasileiro e suas sub-regiões. *Pesquisa Agropecuária Brasileira*. 1998, Brasília;**33**(Número Especial):1703-1711
- [7] IBGE Instituto Brasileiro de Geografia e Estatística. Manual Técnico de Uso da Terra. 3rd ed. Rio de Janeiro: IBGE; 2013
- [8] Tomas WM, Oliveira RF, Morato RG, Medici PE, Chiaravallotti R, Tortato F, et al. Sustainability agenda for the Pantanal wetland: Perspectives on a collaborative interface for science, policy, and decision-making. *Tropical Conservation Science*. 2019;**12**: 1940082919872634
- [9] Girard P, da Silva CJ, Abdon M. River-groundwater interactions in the Brazilian Pantanal. The case of the Cuiabá River. *Journal of Hydrology*. 2003;**283**(1-4):57-66
- [10] Alho CJR, Silva JSV. Effects of severe floods and droughts on wildlife of the Pantanal wetland (Brazil) - A review. *Animals*. 2012;**2**(4):591-610
- [11] ANA - Agência Nacional de Águas. Strategic Action Program for the Integrated Management of the Pantanal and the Upper Paraguay River Basin. Brasília, DF: ANA/GEF/PNUMA/OEA; 2005. p. 315
- [12] Embrapa. Centro Nacional de Pesquisa de Solos (Rio de Janeiro, RJ). Sistema Brasileiro de Classificação de solos. 2nd ed. Rio de Janeiro: EMBRAPA-SPI; 2006
- [13] Brasil Ministério do Meio Ambiente. Biomas. Pantanal: Fauna e Flora; 2007
- [14] Dallacort R, Neves SMAS, Nunes MCMN. Variabilidade da temperatura e das chuvas de Cáceres/ Pantanal Mato-Grossense - Brasil. *Geografia*. 2014;**23**(1):21-33
- [15] Alho CJR, Sabino J. A conservation agenda for the Pantanal's biodiversity. *Brazilian Journal of Biology*. 2011;**71**: 327-335
- [16] EAS G, CBM C, Vicens RS, MHX P, SMAS N. Study of the floodflow dynamics in the Pantanal of Cáceres/MT. In: *Proceedings of the 3rd International Conference on Geographical Information Systems Theory, Applications and Management (GISTAM 2017)*. Porto: SCITEPRESS – Science and Technology Publications; 2017. pp. 195-200. ISBN: 978-989-758-252-3

- [17] Standardised Precipitation-Evapotranspiration Index. Available from: <https://spei.csic.es/index.html>. [Accessed: July 07, 2023]
- [18] National Oceanic and Atmospheric Administration (NOAA). Available from: <https://www.noaa.gov/>. [Accessed: July 03, 2023]
- [19] Global Precipitation Climatology Centre (GPCC). Available from: <https://psl.noaa.gov/data/gridded/data.gpcc.html>. [Accessed: July 02, 2023]
- [20] Thorntwaite CW. An approach toward a rational classification of climate. *Geographical Review*. 1948;**38**: 55-94
- [21] McKee TB, Doesken NJ, Kleist J. The relationship of drought frequency and duration to time scales. In: 8th Conference on Applied Climatology. Boston: Am. Meteorol. Soc; 1993. pp. 179-184
- [22] Vicente-Serrano SM, Beguería S, López-Moreno JI. A multiscale drought index sensitive to global warming: The standardized precipitation evapotranspiration index. *Journal of Climate*. 2010;**23**(7):1696-1718. DOI: 10.1175/2009JCLI2909.1
- [23] Gao B. NDWI—A normalized difference water index for remote sensing of vegetation liquid water from space. *Remote Sensing of Environment*. 1996;**58**(3):257-266. DOI: 10.1016/S0034-4257(96)00067-3
- [24] European Drought Observatory. Available from: <https://edo.jrc.ec.europa.eu/>. [Accessed: July 12, 2023]
- [25] Neves SMAS, Nunes MCM, Neves RJ. Caracterização das Condições Climáticas de Cáceres/Mt-Brasil, No Período de 1971 a 2009: Subsídio às Atividades Agropecuárias e Turísticas Municipais. *Boletim Goiano de Geografia, Goiânia*. 2011;**31**(2):55-68. DOI: 10.5216/bgg.V31i2.16845
- [26] Climate Prediction Center. Available from: https://origin.cpc.ncep.noaa.gov/products/analysis_monitoring/ensostuff/ONI_v5.php. [Accessed: July 01, 2023]
- [27] Marengo JA et al. Extreme drought in the Brazilian Pantanal in 2019–2020: Characterization, causes, and impacts. *Frontiers in Water*. 2021;**3**:639204. DOI: 10.3389/frwa.2021.639204
- [28] Alho CJR. Biodiversidade do Pantanal: Resposta ao regime sazonal de enchente e à degradação ambiental. *Brazilian Journal of Biology*. 2008;**68**(4 suppl):957-966. DOI: 10.1590/S1519-69842008000500005
- [29] Aguilar C, Zinnert JC, Polo MJ, Young DR. NDVI as an indicator for changes in water availability to woody vegetation. *Ecological Indicators*. 2012; **23**:290-300

Recovery Monitoring of Tsunami-Damaged Paddy Fields Using MODIS NDVI

Kohei Cho

Abstract

On March 11, 2011, the Great East Japan Earthquake struck the Tohoku Region of Japan. A huge area along the northeast coast of Japan was seriously damaged by earthquake with a magnitude of 9.0 and subsequent tsunami. The view of the coast-line of the Tohoku Region was dramatically changed by the tsunami. Since then, the author and his group at Tokai University have been monitoring the recovery of the tsunami-damaged areas of Miyagi Prefecture through ground survey and satellite image data analysis. In this study, the authors have investigated how the NDVI seasonal variability of inundated paddy fields changed from year to year after the tsunami. The authors have selected two areas in Miyagi Prefecture in Japan for the test sites of the investigation. One is the paddy fields along the Kitakami River, and the other is the paddy fields in the Sennan Plain of Miyagi Prefecture. Usually, the NDVI of typical paddy fields in Miyagi Prefecture gradually increases from May to August and suddenly decreases in September due to harvesting. The NDVI trend analysis of both areas clarified how the location of paddy fields influenced recovery from the damages of the tsunami.

Keywords: remote sensing, Great East Japan Earthquake, Tohoku, MODIS, NDVI

1. Introduction

On March 11, 2011, the Great East Japan Earthquake with a magnitude of 9.0 struck the Tohoku Region of Japan. A huge area along the coast of the northeast coast of Japan was seriously damaged by the earthquake and subsequent tsunami. **Figure 1** shows the epicenter and the seismic intensity distribution of the earthquake [1]. The maximum height of the tsunami was 9.3 m recorded in Soma, Fukushima Prefecture (see **Figure 2**). A total of 561 sq. km was inundated by the tsunami [2]. More than 19,000 people were lost and more than 2592 people are still missing [3]. The Great East Japan Earthquake can be characterized by the heavy damages caused by the huge tsunami. **Figure 3** shows aerial photos of the paddy fields of Wakabayashi-ku, Sendai City, Miyagi Prefecture reflecting how seriously the area was damaged by the tsunami [4].

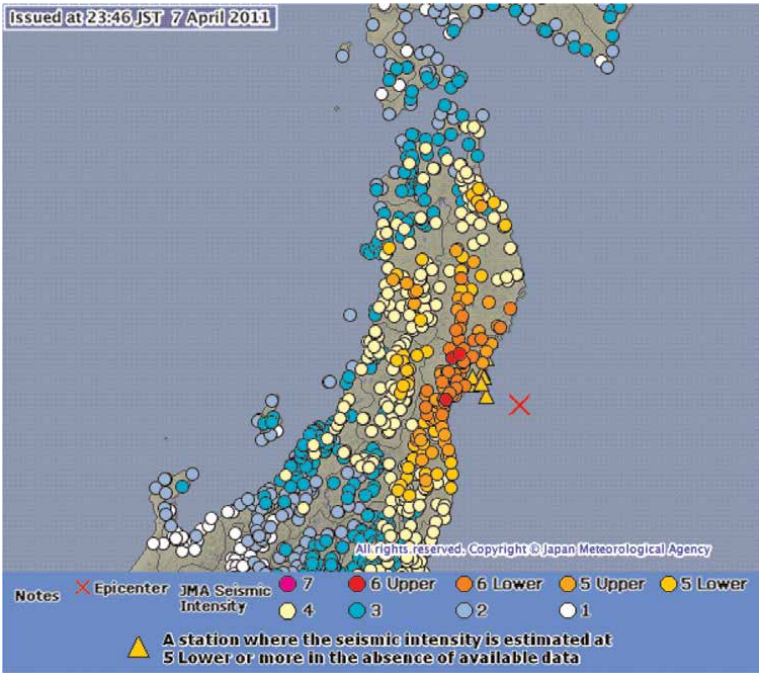


Figure 1.
Epicenter and seismic intensity distribution of the Japan Earthquake (Mar. 11, 2011, JMA) [1].

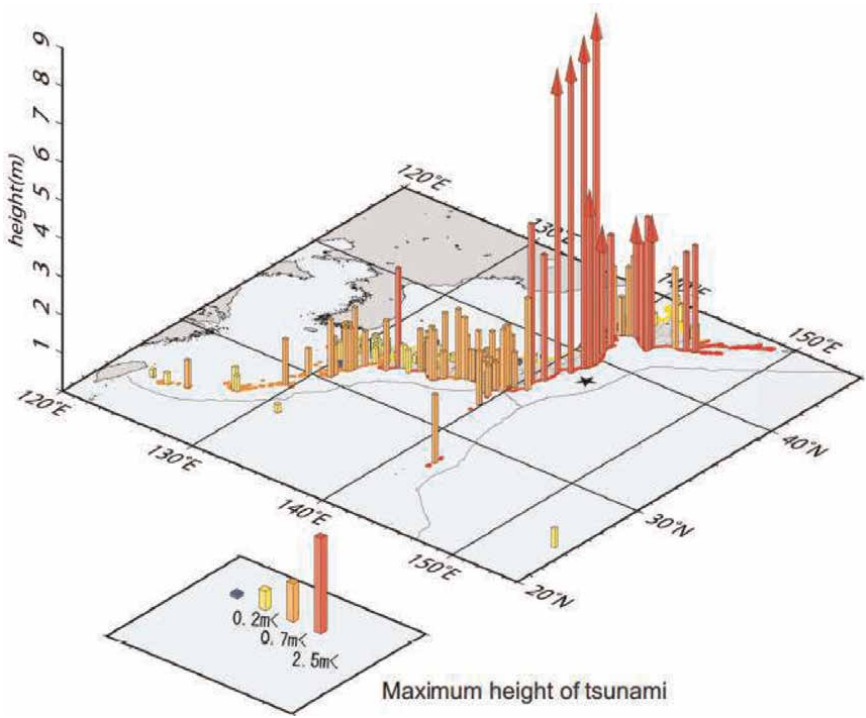


Figure 2.
Observed maximum height of tsunami (Mar. 11, 2011, JMA) [1].



(a)



(b)

Figure 3.
Aerial photos of Wakabayashi-ku, Sendai City, Miyagi Prefecture (provided by Sendai City). (a) Tsunami striking paddy fields (March 11, 2011) and (b) inundated paddy fields (March 14, 2011) [4].

More than 5000 satellite images were taken within 2 weeks after the disaster under international cooperation [5–7]. The comparison of the satellite images taken before and after the disaster enhanced the serious damages in the area. After the Great East Japan Earthquake, various studies on monitoring the damages of the earthquake and associated tsunami were performed. JAXA has taken a total of 643 images of the damaged areas using AVNIR2 and PALSAR onboard the ALOS satellite, and these images were used for damage analysis [8]. Koshimura et al. [9] reviewed how remote sensing methods have been used to contribute to post-tsunami disaster response. Remote sensing is a necessary technology for monitoring the damages of disasters. Liou et al. [10] analyzed MODIS data of before (2010) and after (2011) the tsunami, and evaluated the area of rice fields lost by the tsunami. They estimated the total loss area of paddy fields after the tsunami using MODIS data. However, remote sensing should also be used for monitoring the recovery of the damaged areas. Since 2011, the authors are monitoring the recovery of the tsunami-damaged areas of the Miyagi Prefecture by ground survey and satellite image data analysis [11–14]. In this study, the author and his team have applied a multitemporal analysis of MODIS NDVI to evaluate the recovery status of paddy fields [15].

2. Test site

The authors have selected two areas in Miyagi Prefecture in Japan as the test sites for the investigation. One is the paddy fields along the Kitakami River, and the other is the paddy fields in the Sennan Plain.

2.1 Kitakami River

The Kitakami River is the fourth largest river in Japan with a length of 249 km. The source of the river is in the northern part of Iwate Prefecture and it flows down to Miyagi Prefecture. In Miyagi Prefecture, the river bends to the east and flows into the Pacific Ocean (see **Figure 4**). **Figure 5** shows the optical sensor AVNIR2 images taken from the ALOS satellite of JAXA before and after the tsunami. It is clear that a huge area of paddy fields along the river was inundated by the tsunami. **Figure 6**



Figure 4.
Map of the Kitakami River before the tsunami (blue square frame corresponds to the area of **Figure 5**).
(Source: GSI Maps).

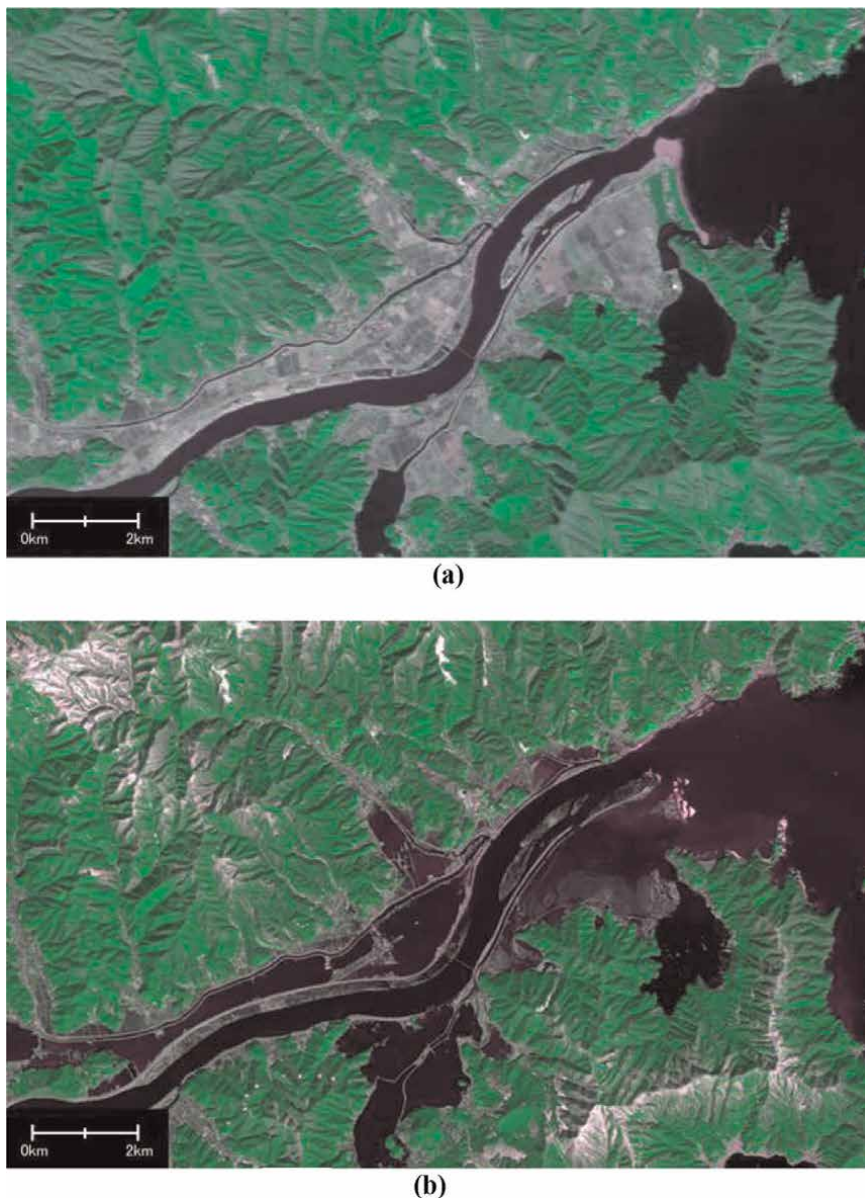
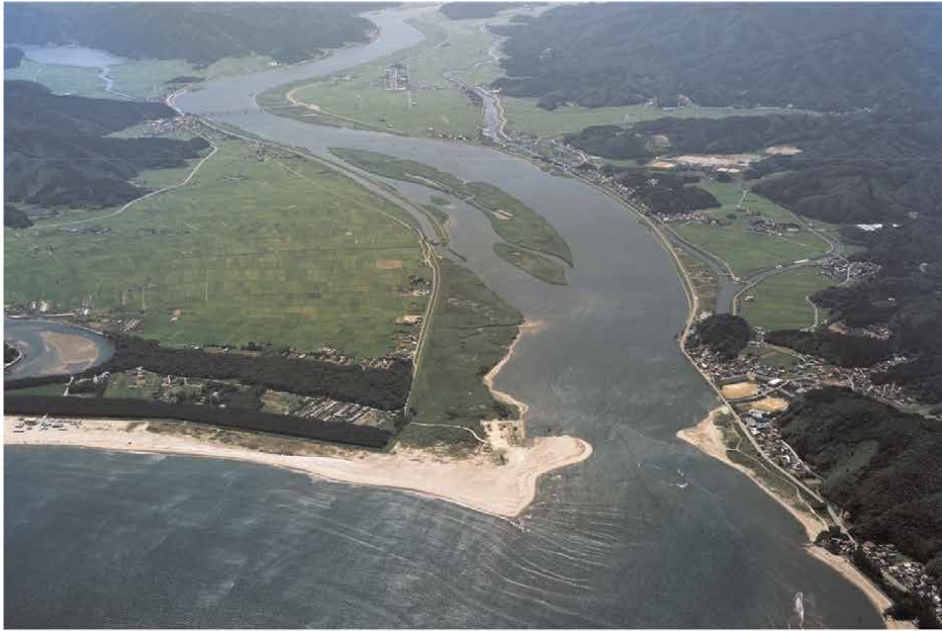


Figure 5. ALOS/AVNIR2 images of the Kitakami River taken before and after the tsunami (AVNIR2: Band 1: Blue, Band 3: Red, Band 4: Green, provided by JAXA). (a) February 27, 2011 and (b) March 19, 2011.

shows the aerial photos of the mouth of the river taken before and after the tsunami. It is shocking to see how the scenery of the mouth of the river is completely changed by the tsunami.

Figure 7 shows MODIS false composite images around the Kitakami River. By looking at the time series of MODIS images, we can recognize the changes in the form of the river reflecting the damage and recovery along the river. However, on the other hand, it is also clear that the 250-m special resolution of MODIS is not enough for spatially evaluating the damages and recovery of the paddy fields in this area. As a



(a)



(b)

Figure 6.
Aerial photos of the mouth of Kitakami River taken before and after the Tsunami [16]. (a) July, 1995 and (b) April 4, 2011.

result, considering that MODIS can observe the same area every day, the author has decided to monitor the damages and recovery by comparing the time series of MODIS NDVI of particular paddy fields.

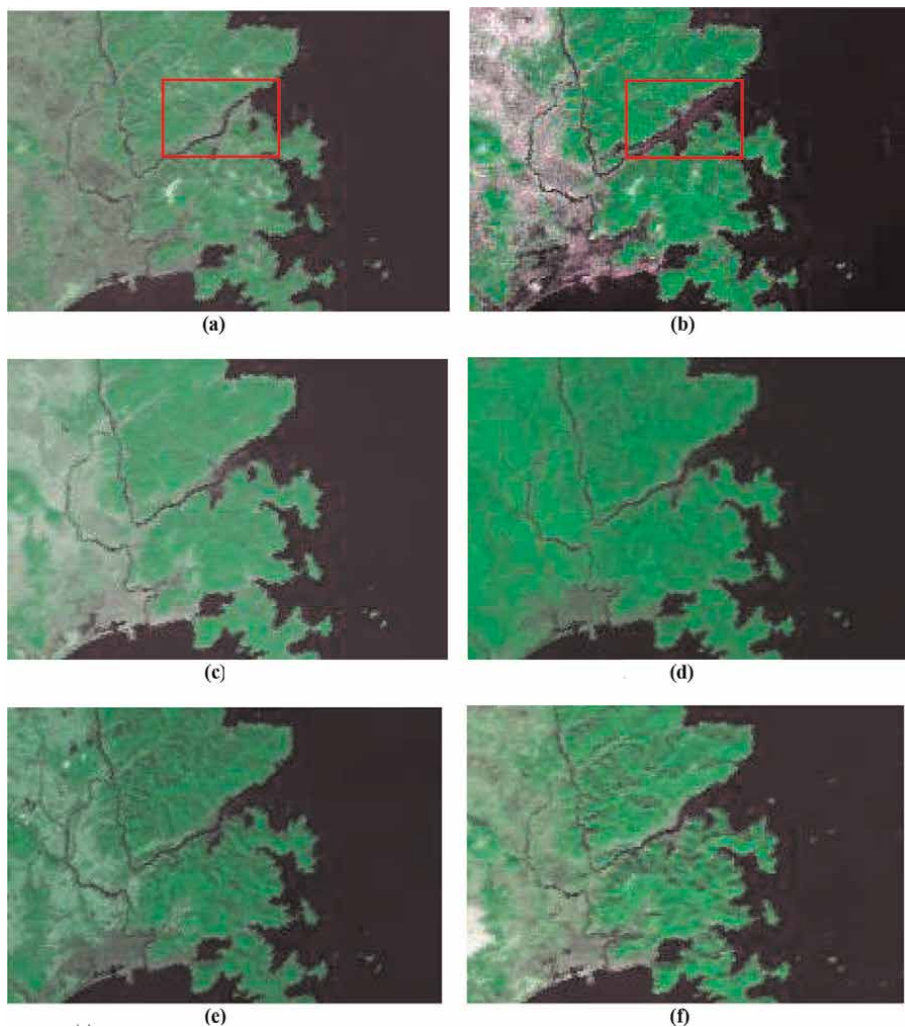


Figure 7.
 Time series of MODIS images of Kitakami River and its surroundings. The red rectangle corresponds to the area of **Figure 4** (MODIS Band 1: blue, red, Band 2: Green). (a) February 16, 2011, (b) March 13, 2011, (c) April 5, 2011, (d) August 13, 2011, (e) October 19, 2011 and (f) December 24, 2011.

2.2 Sennan Plain

The second test site we selected is Sennan Plain of Miyagi Prefecture. The Sennan Plain is located in the southeast along the coast of Miyagi Prefecture facing the Pacific Ocean as shown in **Figure 8**. Huge agricultural fields, mostly paddy fields, of the Sennan Plain were seriously inundated by the tsunami. **Figure 9** shows an aerial photo of Sendai Airport that was taken at the time when the tsunami inundated the area on March 11, 2011, after the earthquake. **Figure 10** shows the AVNIR2 images of this area taken before and after the tsunami. It is obvious that most of the paddy fields along the coast were inundated by the tsunami. The dotted line box in **Figure 8** shows the test site for evaluating how the 16 days of MODIS images were composed into a single image (see Chapter 3).



Figure 8.
Location of the test site. (Source: Google Maps).



Figure 9.
Aerial photo of the Sendai Airport and its surroundings (March 11, 2011 Japan Coast Guard).

3. Analyzed data

NDVI (Normalized Difference Vegetation Index) defined by the following formula is a typical index for estimating the condition of vegetation [17].

$$\text{NDVI} = (\text{NIR} - \text{VIS}) / (\text{NIR} + \text{VIS}) \quad (1)$$

Where NIR: near infrared band; VIS: visible red band.

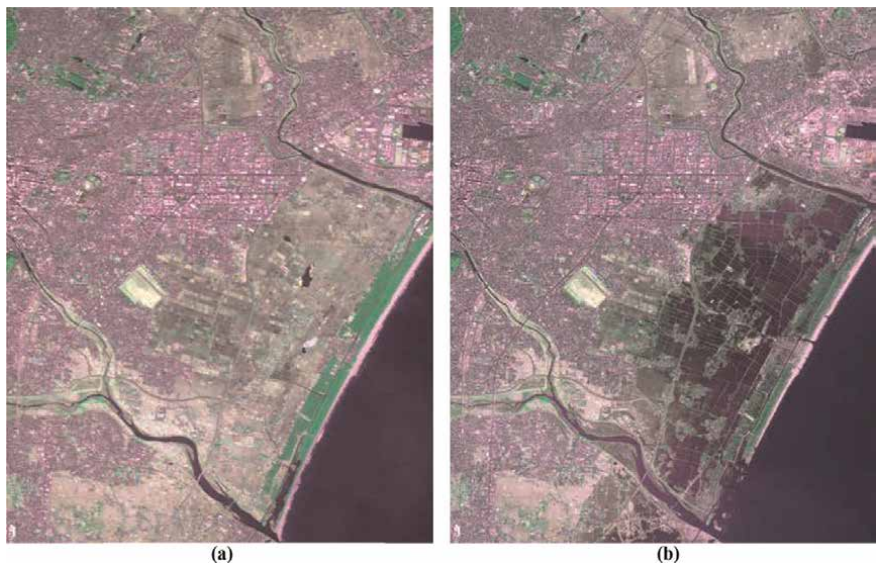


Figure 10.
ALOS/AVNIR2 images of the Wakabayashi-ku taken before and after the Tsunami (AVNIR2: Band 1: blue, Band 3: red, Band 4: green, provided by JAXA). (a) February 27, 2010 and (b) March 14, 2011.

Band	Wavelength	IFOV	Swath
1	0.620–0.670 μm	250 m	2330 km
2	0.841–0.876 μm		
3	0.459–0.479 μm	500 m	
4–7	0.545–2.155 μm		
8–36	0.405–14.385 μm	1000 m	

Table 1.
Specifications of MODIS [18].

Since inundated paddy fields are likely to reduce the reflectance of NIR, the damages may be enhanced in the value reduction of NDVI. In this study, NDVI derived from MODIS data of the Terra satellite was used for the analysis. **Table 1** shows the specifications of MODIS. For calculating NDVI with formula (1), MODIS Band 1 is used for VIS, and Band 2 is used for NIR. As for the test site of the Kitakami River, MODIS NDVI monthly composite data provided by GSI (Geospatial Information Authority of Japan) was used [19]. As for the test site of the Sennan Plain, the 16-day composite of MODIS NDVI dataset (MOD13Q1 [18, 20, 21]) provided by NASA [23] was analyzed. AVNIR2 images of the ALOS satellite of JAXA were used as the reference for selecting the sample areas. **Table 2** shows the specification of AVNIR2 [24].

Figure 11 shows 16 MODIS Band 1 images of the area of the dotted line box in **Figure 8** from July 28 to August 12, 2014. Certain areas of each image are covered with clouds. **Table 3** shows the pixel reliability key [22] of MODIS provided by NASA. This pixel reliability data is used in MOD13Q1 when calculating 16-day composite MODIS NDVI. In addition, Band 3 was used for detecting the bright area such as clouds or snow. For example, if only the data of three days among 16 days were Good Data (0)

Band	Wavelength	IFOV	Swath
1	0.42–0.50 μm	10 m	70 km
2	0.52–0.60 μm		
3	0.61–0.69 μm		
4	0.76–0.89 μm		

Table 2.
Specifications of AVNIR2 [23].

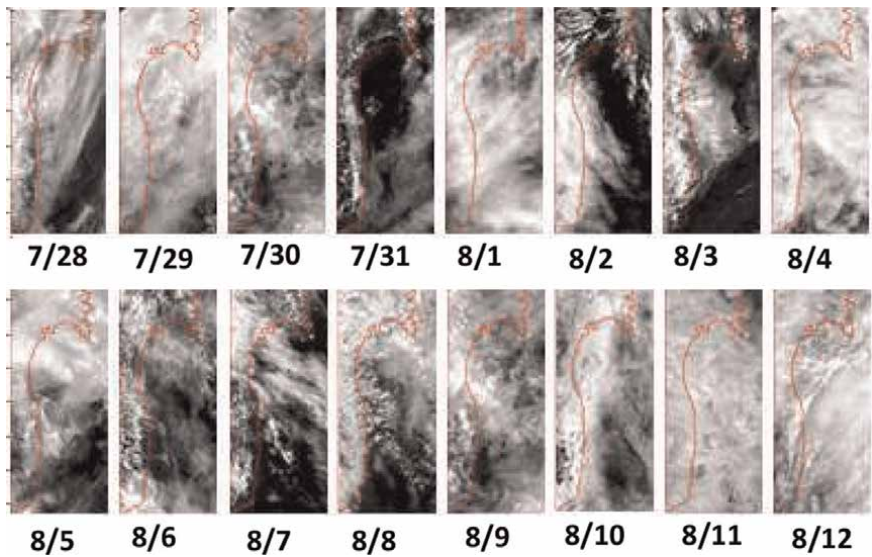


Figure 11.
MODIS Band 1 image (2017).

Rank key	Summary QA	Description
–1	Fill/no data	Not processed
0	Good data	Use with confidence
1	Marginal data	Useful, but look at other QA information
2	Snow/ice	Target covered with snow/ice
3	Cloudy	Target not visible, covered with cloud

Table 3.
MODIS pixel reliability key [22].

and the others were No Data (–1), the three days data are averaged for calculating the 16-day composite. **Figure 12(a)** shows the result of 16-day composite. Most of the clouds are well rejected. **Figure 12(b)** shows which day was used for each location. This image shows that though the image was acquired within 16 days, the exact observation dates of NDVI are quite different from pixel to pixel.

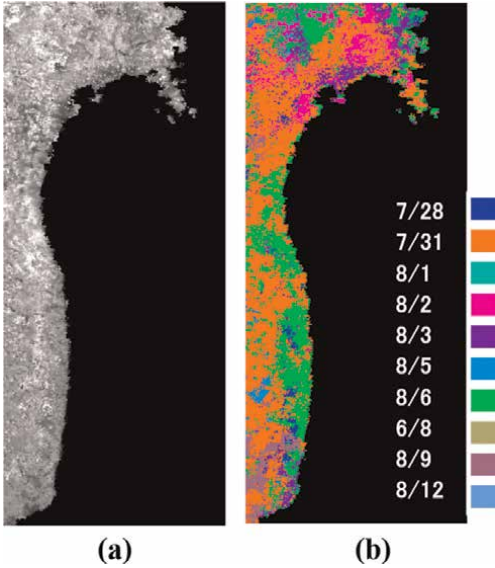


Figure 12.
MODIS 16 days composite. (a) Result and (b) day distribution.

4. Methodology

4.1 Seasonal variability evaluation

Figure 13 shows the typical MODIS NDVI seasonal variability of normal paddy fields in Miyagi Prefecture. This graph was derived by averaging monthly NDVI of

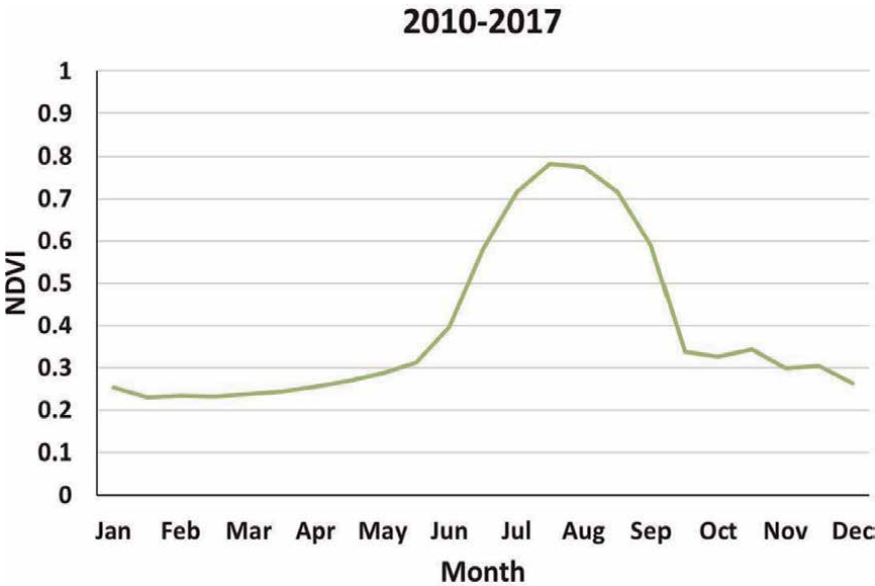
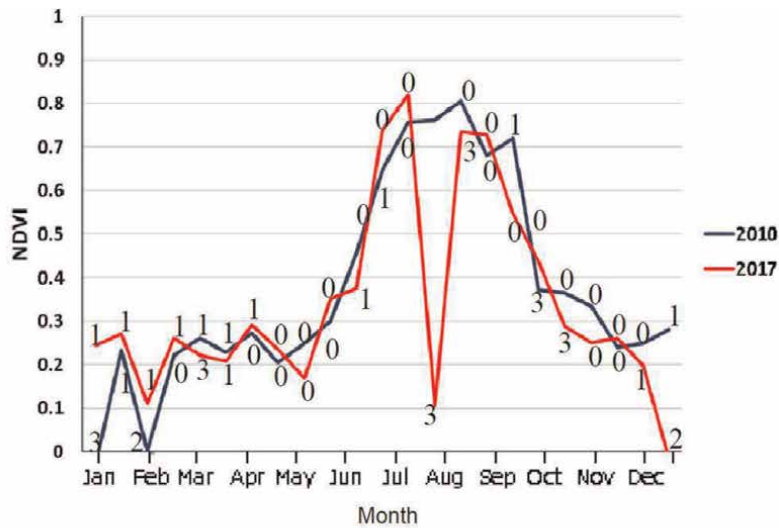


Figure 13.
MODIS NDVI seasonal variability of normal paddy field. (Monthly NDVI data were averaged from 2010 to 2017).

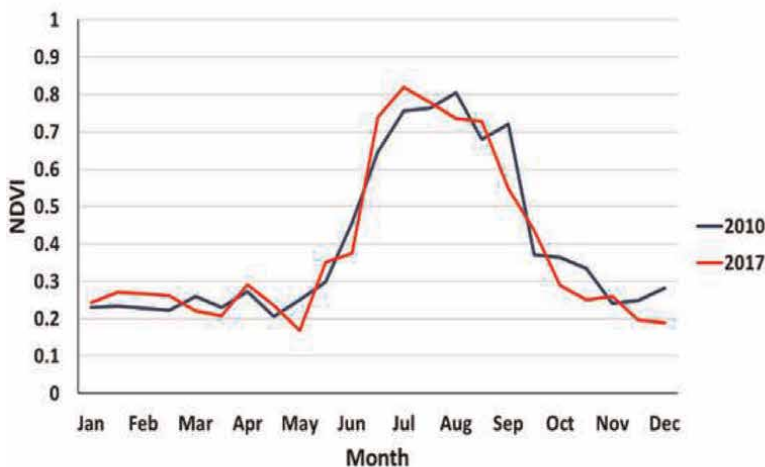
normal paddy fields that were not suffered by the Tsunami from 2010 to 2017. In Tohoku Region, the NDVI of a paddy field gradually increases from May after the rice planting and reaches to a peak in August. From September to October, NDVI suddenly goes down after the harvesting. The author has examined how this seasonal NDVI pattern changed before and after the Tsunami.

4.2 Interpolation of irregular value of NDVI in the 16-day composite

When we checked the NDVI seasonal variation of various paddy fields using the 16-day composite of MODIS NDVI, irregular reductions in NDVI value were often



(a)



(b)

Figure 14. MODIS NDVI seasonal variability of normal paddy field. (a) Original NDVI and (b) interpolated NDVI.

observed. **Figure 14** shows such an example. The graph for 2017 has an abnormal reduction of NDVI in July. The graph of 2010 also has reductions in January and February. The numbers in the graph correspond to the pixel reliability key described in **Table 3**. “2” corresponds to snow/ice and “3” corresponds to clouds. So, we can understand that a big reduction of NDVI values was caused by the snow or clouds cover during 16 days. These irregular values of NDVI make it difficult to understand the condition of the paddy fields. On the other hand, even though the pixel reliability key is “3” (cloudy), many of the NDVI values looked normal. So, simply using the pixel reliability key for extracting irregular values is not appropriate. Also, it has become clear that most of the points where the NDVI was 0 were the areas that were covered with snow. These problems had to be solved. The authors have examined ways to extract the irregular value of NDVI by comparing the NDVI value before and after the period. In this study, we defined the following two equations to interpolate the irregular value of NDVI.

If $\text{NDVI}(t-1) - \text{NDVI}(t) > 0.1$ and
 If $\text{NDVI}(t+1) - \text{NDVI}(t) > 0.1$
 or $\text{NDVI}(t) = 0$
 then

$$\text{NDVI}(t) = \{\text{NDVI}(t-1) + \text{NDVI}(t+1)\} / 2 \quad (2)$$

If $\text{NDVI}(t) < 0.1$ and If $\text{NDVI}(t+1) < 0.1$
 then

$$\text{NDVI}(t) = \{\text{NDVI}(t-1) + \text{NDVI}(t+2)\} / 2 \quad (3)$$

t: target period (1 to 23).

The result of applying this method is shown in **Figure 14(b)**. The seasonal variability became similar to the normal paddy field shown in **Figure 13**.

5. Result

5.1 Kitakami River

As shown in **Figures 5** and **6**, the Kitakami River was seriously damaged by the Tsunami. In order to evaluate the damage difference of the paddy fields located along the Kitakami River, the author have selected nine sample points, namely T1 to T9, as shown in **Figure 15**. The map is an inundated map produced by GSI after the Tsunami. The pink areas correspond to the inundated areas. **Figure 16** shows the seasonal NDVI variability graph of 2009 to 2012 for each sample point.

We compare seasonal NDVI graphs shown in **Figure 16**, all the graph patterns of 2009 and 2010, before the tsunami looks similar to the pattern of the normal paddy fields as shown in **Figure 13**. However, the patterns of 2011 and 2012 are quite different from one sample point to the other. Particularly, if we compare the patterns of the year 2011, it is clear that the NDVI values gradually reduced from T1 to T9. These changes can be explained as follows. The damages of the paddy fields far from the river mouth, namely sample points T1 to T4, were not much. The damages of the paddy fields in the middle, namely sample points T5 and T7, were quite serious. Finally, the damages of the paddy fields near in the mouth of the river, namely sample

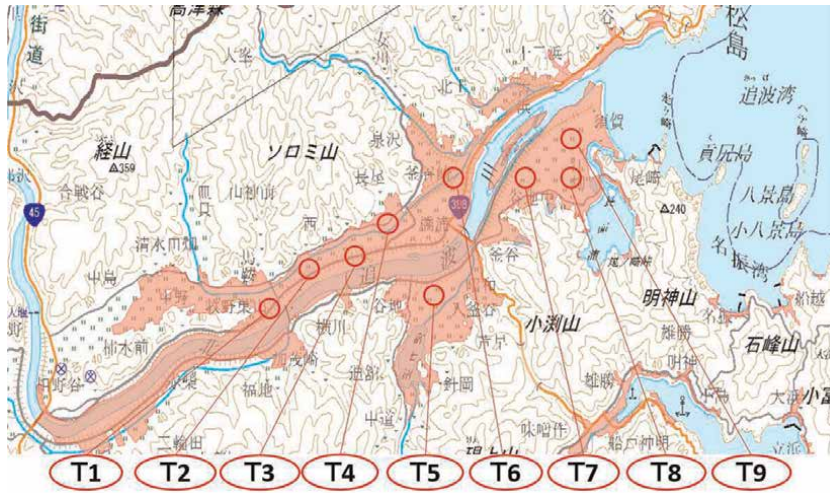
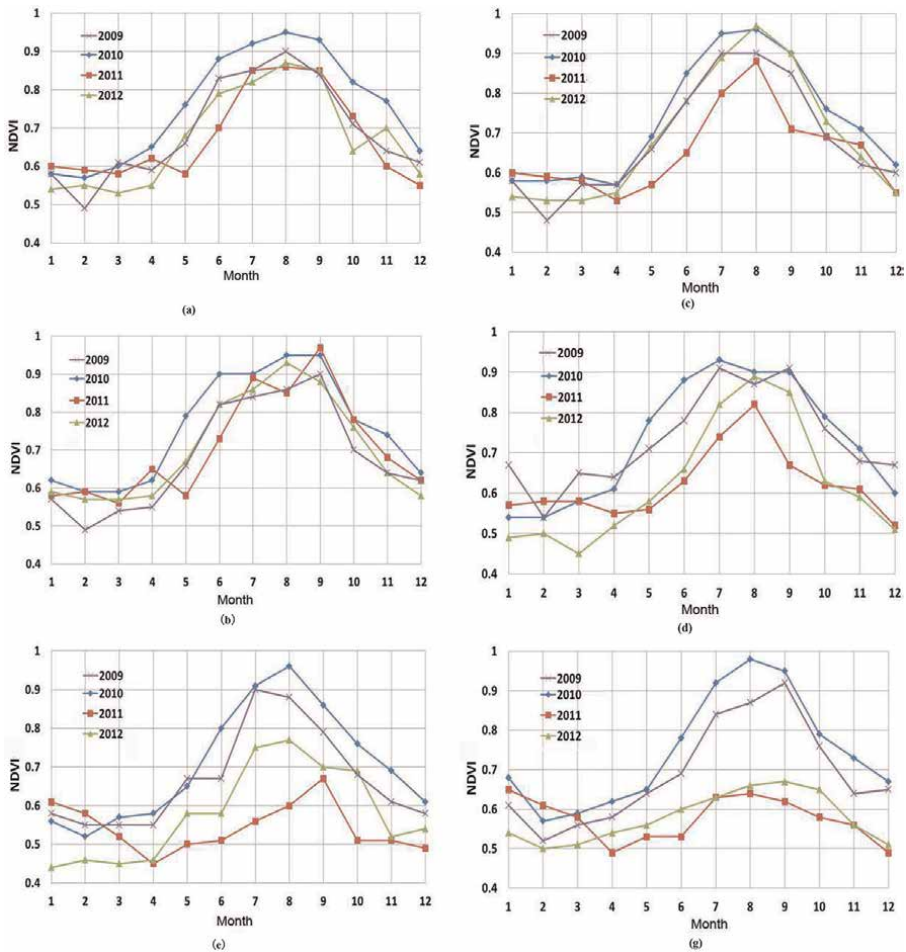


Figure 15.
Sample point of NDVI plotted on the inundated map of the Kitakami River.



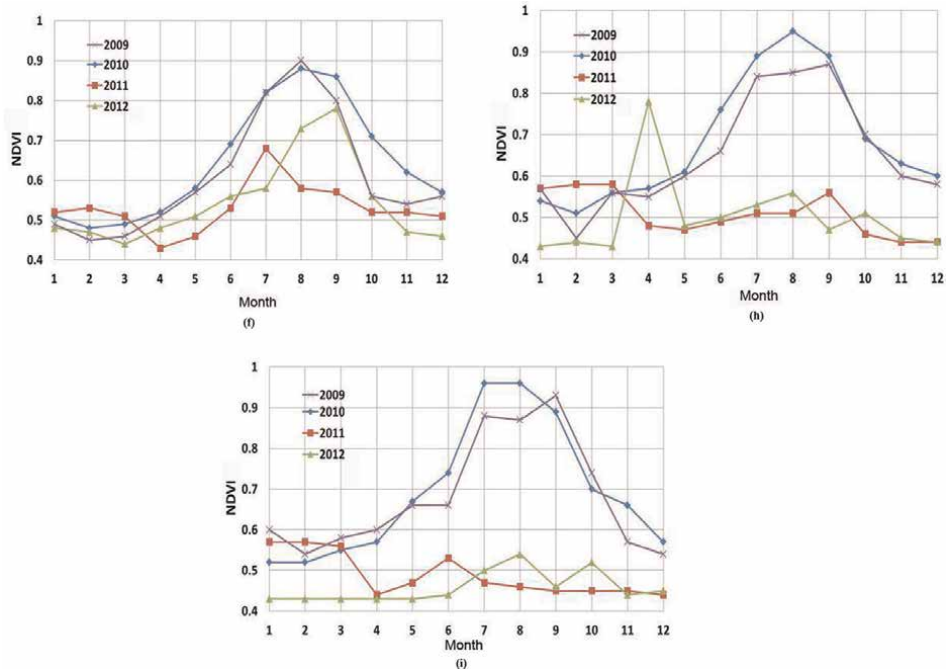


Figure 16.
Seasonal NDVI Variability comparison of the nine sample points. (a) T₁, (b) T₂, (c) T₃, (d) T₄, (e) T₅, (f) T₆, (g) T₇, (h) T₈ and (i) T₉.

points T₈ and T₉, were most serious, and NDVI value did not go up to more than 0.6 throughout the years of 2011 and 2012.

Figure 17 shows the NDVI comparison of August from T₁ to T₉ for 2009 to 2012. The NDVI values of T₁ to T₉ are almost the same for 2009 and 2010. However, as for

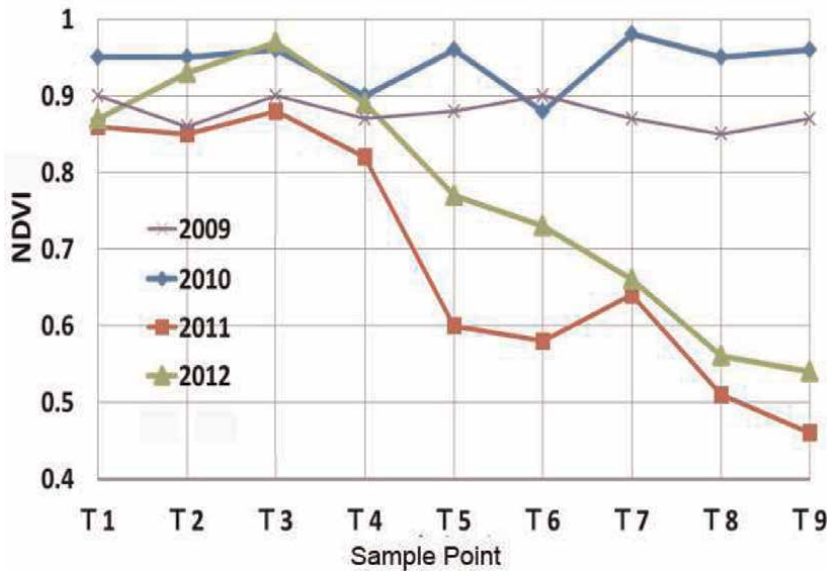


Figure 17.
NDVI comparison of August from 2009 to 2012 of the sample points T₁ to T₉.

2011, the NDVI value dramatically reduced from T1 to T9 reflecting the damage difference of paddy fields according to the distance from the mouth of the river. Though the pattern of 2012 is similar to the pattern of 2011, some increase of NDVI value can be observed reflecting the recovery of the paddy field. The paddy fields around the mouth of the river were completely destroyed and needed to be reclaimed to reconstruct the paddy fields, and the author terminated the NDVI comparison of the paddy fields around the Kitakami River and shifted to the detailed study of the paddy fields in the Sennan Plain.

5.2 Sennan Plain

Figure 18 shows a part of the agricultural recovery map of the Sendai Area prepared by the Miyagi Prefectural Government [25]. The area framed in red is the area that suffered from the Tsunami. The area colored in white corresponds to the area where the tsunami did not come or was not much affected by the tsunami. The area colored in yellow corresponds to the area where the recovery project started in 2011, the green area started in 2012, and the purple area started in 2013. It is quite reasonable that the agricultural recovery project started from the inland areas where the damages of the tsunami were lighter than the inshore areas. Then, the recovery project was expanded toward the inshore areas. To evaluate the status of the recovery project,

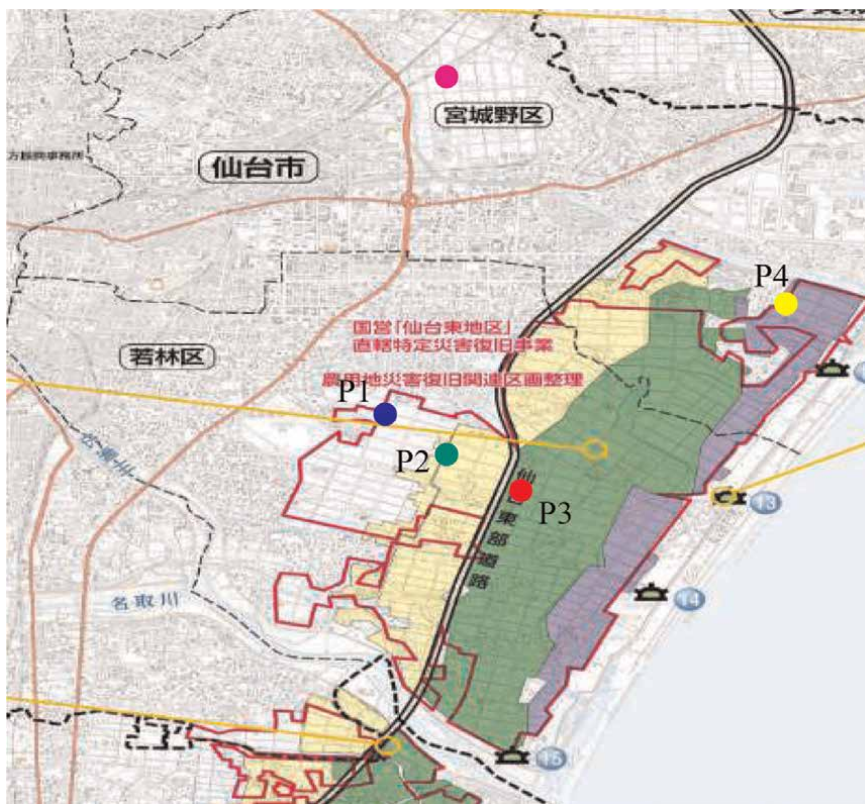


Figure 18.
Paddy Field Recovery Project Map [24].

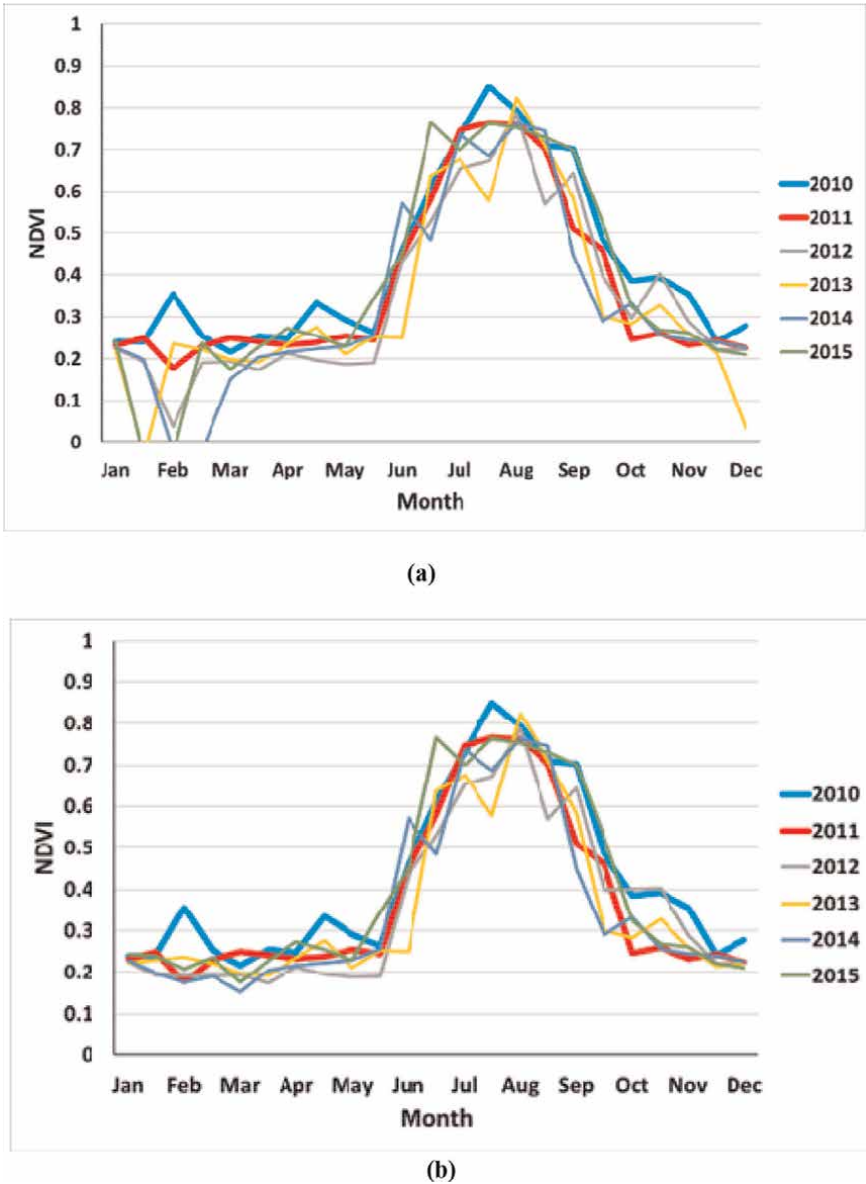
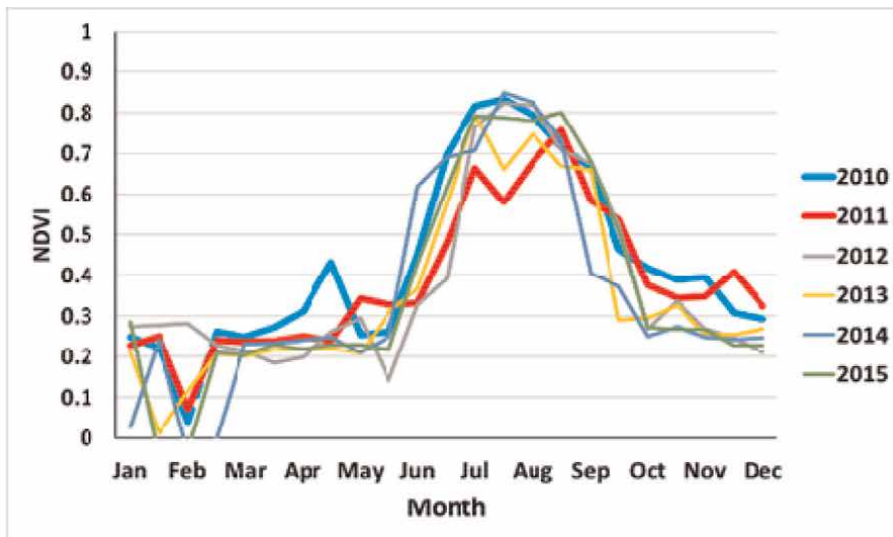


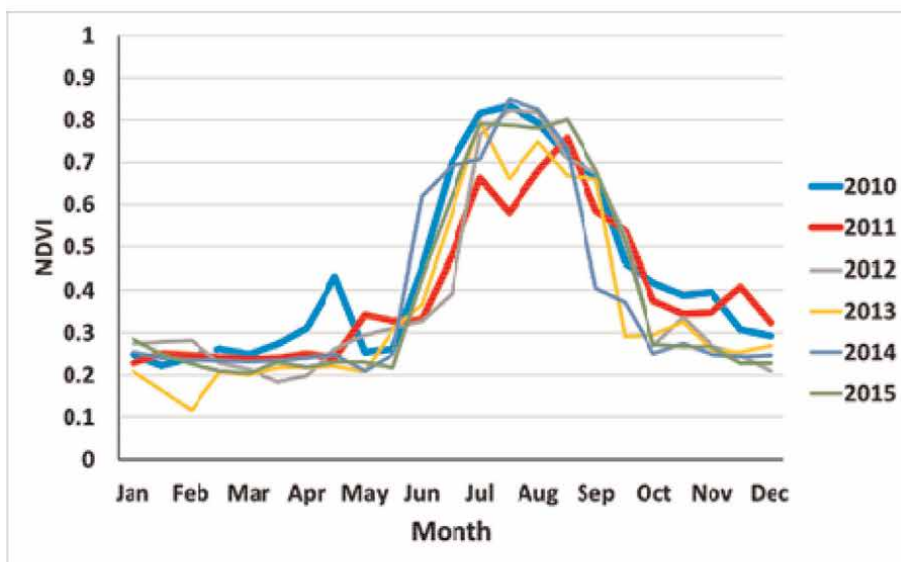
Figure 19. MODIS NDVI seasonal variability of a normal paddy field (sample point P1). (a) Before interpolation and (b) after interpolation.

the authors have selected four sample points as shown in **Figure 18**. ● shows the sample point P1 selected from the normal inland paddy field that was not affected by the tsunami. ● shows the sample point P2 selected in the area of recovery project started in 2011. ● shows the sample point P3 selected in the area of recovery project started in 2012, and ● shows the sample point P4 selected in the area of recovery project started in 2013.

The interpolation method was applied to the 16-day composite MODIS NDVI for the paddy fields selected in **Figure 18**. The result of before and after applying the



(a)



(b)

Figure 20. MODIS NDVI seasonal variability of inundated inland paddy field (sample point P2). (a) Before interpolation and (b) after interpolation.

method to the MODIS NDVI seasonal variabilities from 2010 to 2015 is shown in **Figures 19–22**. In all four figures, by applying the proposed interpolation method, irregular reduction of NDVI during the winter due to the snow cover (see (a) of each figure) was well interpolated by the data of before and after the period, and the normal paddy filed pattern became clear in (b) of each figure. At the same time, the

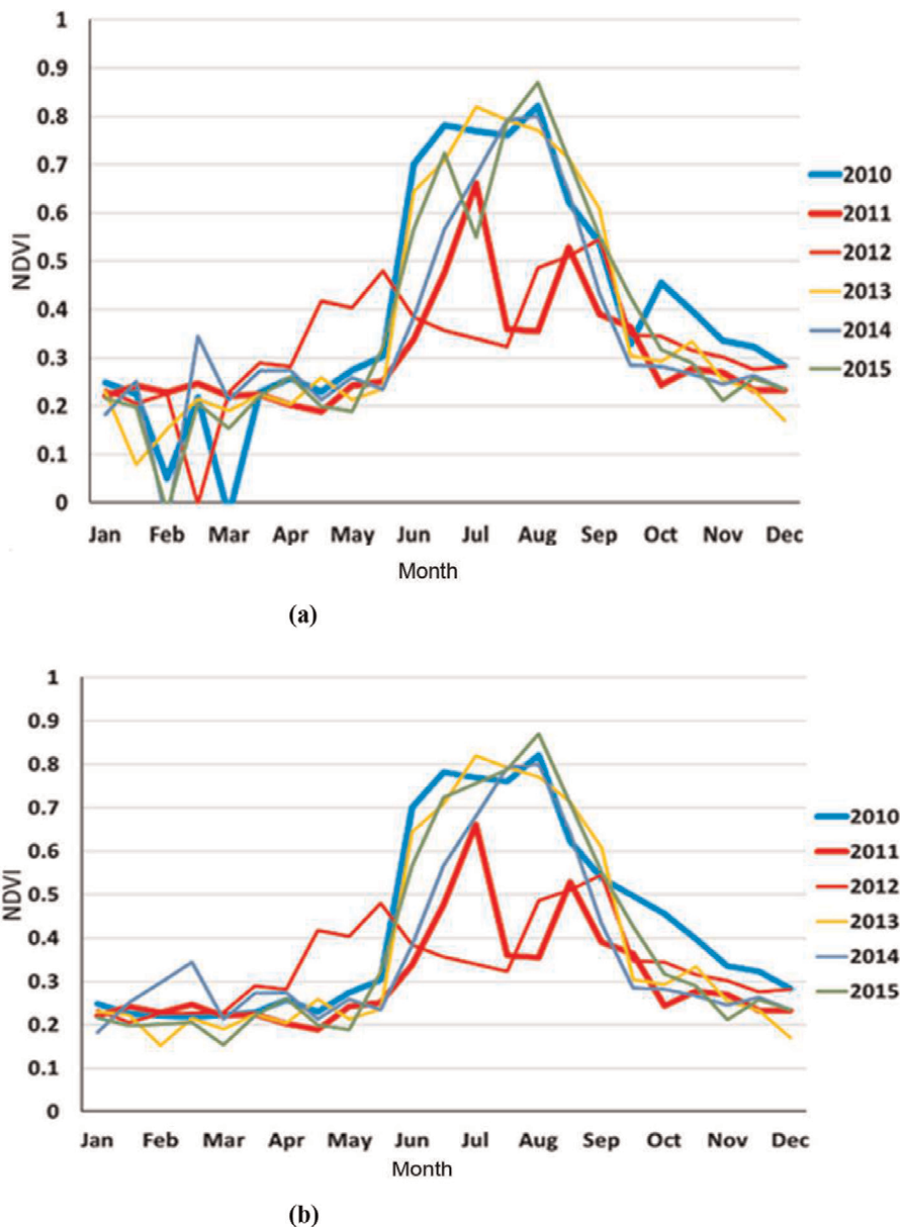
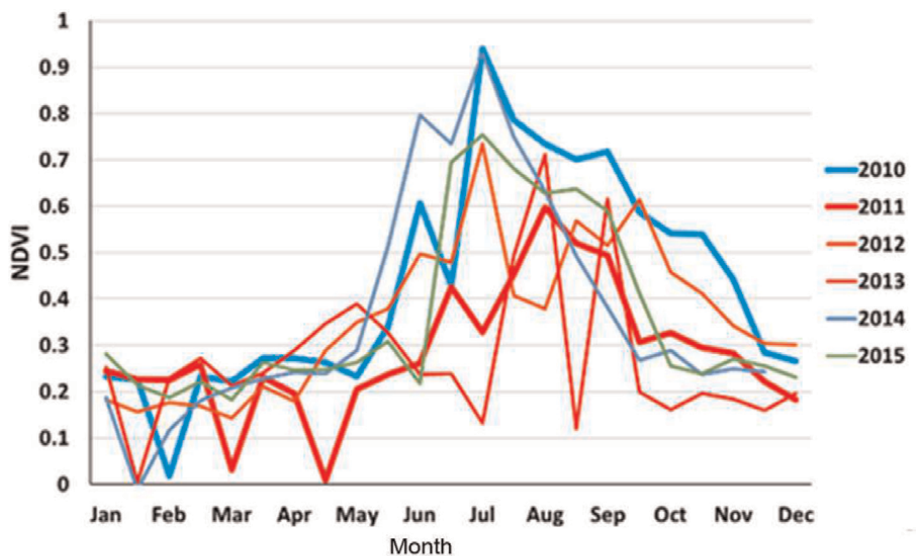


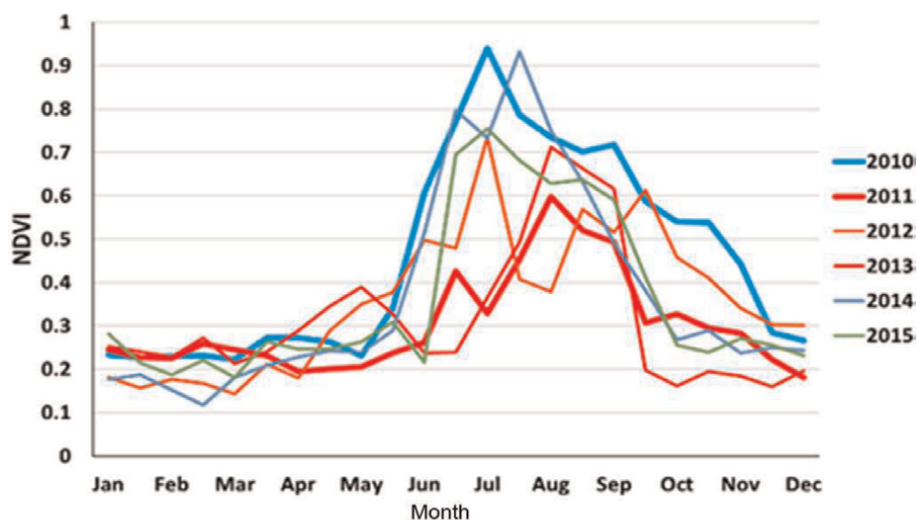
Figure 21.
 MODIS NDVI seasonal variability of inundated inshore paddy field (sample point P3). (a) Before interpolation and (b) after interpolation.

NDVI reduction patterns in the year 2011 and afterward due to the effects of the tsunami were well preserved after applying the interpolation method.

The NDVI values from July to August were averaged and plotted from 2010 to 2014 for the four sample points as shown in **Figure 23**. If we assume that the paddy fields whose NDVI values were less than 0.65 were damaged by the tsunami, we may conclude as follows. The NDVI values of sample point P1, the normal paddy field, are



(a)



(b)

Figure 22.
MODIS NDVI seasonal variability of seriously inundated inshore paddy field (sample point P4). (a) Before interpolation and (b) after interpolation.

all over 0.7 reflecting the no damage from the tsunami. As for sample point P2, the inundated paddy field where the recovery project started in 2011 reduced the NDVI value from 0.83 to 0.63 in 2011, but recovered to 0.83 in 2012. As for sample point P3, the inundated inshore paddy field where the recovery project started in 2012 reduced the NDVI value from 0.79 to 0.35 in 2011 and 0.4 in 2012, but recovered to 0.78 in 2013. As for sample point P4, the inundated inshore paddy field where the recovery project started in 2013 reduced the NDVI value from 0.76 to 0.53 in 2011, and 0.60 in 2012 and 2013, but recovered to 0.83 in 2014. The result suggests that the recovery

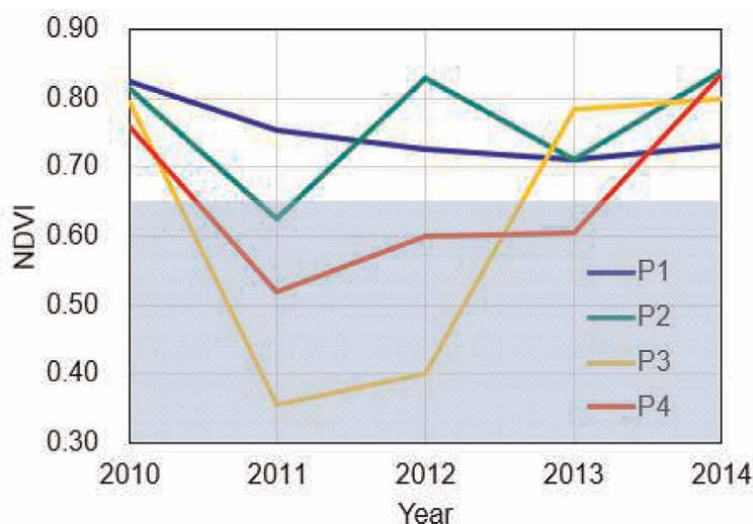


Figure 23.
 MODIS NDVI variability of the four sample points for each summer.

project was performed steadily, and the recovery of the paddy fields was achieved within a year in each project.

6. Conclusion

In this study, the authors have investigated how the NDVI seasonal variability of paddy fields changes before and after the tsunami that struck the Tohoku Region of Japan on March 11, 2011. The authors have selected two areas, namely the paddy fields along the Kitakami River and in the Sennan Plain of Miyagi Prefecture, as the test sites of this study.

As for the Kitakami River, the difference in the damages of the tsunami was clearly reflected in the seasonal variability of NDVI. The inundated paddy fields located on the upper side of the River shows similar NDVI seasonal variability with normal paddy field in 2011 and also in 2012. This means that the inundated paddy fields on the upper side of the river were not as serious as the lower side of the river. However, the NDVI seasonal variability pattern of the inundated paddy fields near the mouth of the river was quite different for 2011 and 2012. The result reflected the heavy damage to the paddy fields in this area.

Time series of the 16-day composite of MODIS NDVI data were analyzed for evaluating the recovery speed of paddy fields in the Sennan Plain. As a result, in the inland area where the agricultural recovery project started in 2011, the paddy fields recovered within 1 year. As for the paddy fields located between the inland and inshore, the agricultural recovery project started in 2012 and the paddy fields recovered in 2012. The agricultural recovery project started in 2012 for the paddy fields located at inshore, and the paddy fields were recovered in 2013. By looking only at the results, you may say that every damaged paddy field analyzed in this study recovered within 1 year after performing the agricultural recovery project. But, maybe this is not true. The local government may have investigated the damages of the inundated paddy fields and systematically scheduled the agricultural recovery project. As a

result, not all, but most of the paddy fields in this region successfully recovered within 3 years.

As the conclusion of this study, we may say that the seasonal variability evaluation of MODIS NDVI is quite useful for monitoring the damage and recovery condition of paddy fields. However, the spatial resolution of MODIS is too low for applying the classification method to evaluate the recovery condition of the damaged paddy fields. The paddy field of this region is not so large to be identified with MODIS data, and the mixed pixel problem may reduce the accuracy of the result. A higher resolution optical sensor such as the Sentinel-2/MSI with a revisit cycle of fewer days may be needed for applying the classification method.

Acknowledgements


This study was performed under the framework of “Monitoring Environmental Recovery of Damaged Area in Tohoku, Japan from Space & Ground for Environmental Education” under the Grants-in-Aid for Scientific Research sponsorship by MEXT (Ministry of Education, Culture, Sports, Science and Technology) and JSPS (The Japan Society for the Promotion of Science). The financial support from the Remote Sensing Technology Center (RESTEC) was also very helpful. The author would like to thank them for their kind support. The author also would like to thank the students of his lab, namely Mr. Ryota Uemachi and Mr. Kota Yamamoto, who worked hard with me in the past. Their contribution was outstanding.

Author details

Kohei Cho
Tokai University, Research & Information Center, 2-3-23, Takanawa, Minato-ku,
Tokyo

*Address all correspondence to: kohei.cho@tokai-u.jp

IntechOpen

© 2023 The Author(s). Licensee IntechOpen. This chapter is distributed under the terms of the Creative Commons Attribution License (<http://creativecommons.org/licenses/by/3.0>), which permits unrestricted use, distribution, and reproduction in any medium, provided the original work is properly cited. 

References

- [1] JMA. The 2011 Off the Pacific Coast of Tohoku Earthquake Observed Tsunami. 2011. Available from: http://www.jma.go.jp/jma/en/2011_Earthquake/chart/2011_Earthquake_Tsunami.pdf
- [2] Nagayama T, Inaba K, Hayashi T, Nakai H. How the National Mapping Organization of Japan responded to the Great East Japan Earthquake? Proceedings of FIG Working Week. 2012;2012(TS03K-5791):1-15
- [3] Fire and Disaster Management Agency (FDMA). 2016. Available from: <http://www.fdma.go.jp/bn/higaihou/pdf/jishin/158.pdf>
- [4] Sendai City. 2023. Available from: <https://www.city.sendai.jp/shiminkoho/shise/daishinsai/zenkoku/photoarchive/engan/index.html>
- [5] Takahashi M, Shimada M. 2012, Disaster monitoring by JAXA for Japan Earthquake using satellites. Journal of the Japan Society of Photogrammetry and Remote Sensing. 2011;50(4): 198-205
- [6] International Charter. 2022. Available from: <https://www.disasterscharter.org/>
- [7] Sentinel Asia. 2022. Available from: <https://sentinel-asia.org/index.html>
- [8] JAXA. Report on JAXA's Response to the Great East Japan Earthquake. 2012. Available from: <https://earth.jaxa.jp/en/application/disaster/20110311report-e/index.html>
- [9] Koshimura S, Moya L, Mas E, Bai Y. Tsunami damage detection with remote sensing: A review. Geosciences. 2020; 10(5):177. DOI: 10.3390/geosciences10050177
- [10] Liou Y, Sha H, Chen T, Wang T, Li Y, Lai Y, et al. Assessment of disaster losses in rice field and yield after tsunami induced by the 2011 Great East Japan earthquake. Journal of Marine Science and Technology. 2012;20(6): 618-623. DOI: 10.6119/JMST-012-0328-2
- [11] Cho K, Fukue K, Uchida O, Terada K, Chen CF. Monitoring environmental recovery of damaged area in Tohoku, Japan from Space & Ground for Environmental Education. In: Proceedings of the 34th Asian Conference on Remote Sensing, SC03. AARS. 2013. pp. 709-716
- [12] Cho K, Baltsavias E, Remondino F, Soergel U, Wakabayashi H. RAPIDMAP project for disaster monitoring. In: Proceedings of the 35th Asian Conference on Remote Sensing, OS-145. AARS. 2014. pp. 1-6
- [13] Cho K, Fukue K, Uchida O, Terada K, Wakabayashi H, Sato T, et al. A study on detecting disaster damaged areas. In: Proceedings of the 36th Asian Conference on Remote Sensing, SP.FR2. AARS. 2015. pp. 1-4
- [14] Cho K, Uchida O, Terada K, Wakabayashi H, Sato T. Monitoring the recovery of the Tsunami damaged areas using satellite observation and field survey for environmental education. In: Proceedings of the 43rd Asian Conference on Remote Sensing, ACRS22_106. AARS. 2022. pp. 1-10
- [15] Uemachi R, Naoki K, Cho K. Monitoring the recovery of tsunami damaged paddy fields using MODIS NDVI. In: Proceedings of the 38th Asian Conference on Remote Sensing, PS-04-ID-844. 2017. pp. 1-4

- [16] Kappa club. 2014. Available from: <http://www.michinoku.ne.jp/~kappa/>
- [17] Weier J., D. Herring, 2000. Available from: <http://earthobservatory.nasa.gov/Features/MeasuringVegetation/>
- [18] NASA. 2017. MODIS Specifications. Available from: <https://modis.gsfc.nasa.gov/about/specifications.php>
- [19] GSI. 2012. Available from: <https://www.gsi.go.jp/kankyochiri/ndvi.html> (In Japanese)
- [20] NASA. 2017. MODIS Specifications. Available from: <https://modis.gsfc.nasa.gov/about/specifications.php>
- [21] Huete A, Didan K, Miura T, Rodriguez EP, Gao X, Ferreira LG. Overview of the radiometric and biophysical performance of the MODIS vegetation indices. *Remote Sensing of Environment*. 2002;**83**:195-213
- [22] Solano R., K. Didan, A. Jacobson, A. Huete. MODIS Vegetation Index User's Guide. 2012. Available from: https://vip.arizona.edu/documents/MODIS/MODIS_VI_UsersGuide_01_2012.pdf
- [23] NASA LAADS DAAC. 2023. Available from: <https://ladsweb.modaps.eosdis.nasa.gov/search/>
- [24] JAXA. AVNIR-2 Advanced Visible and Near Infrared Radiometer Type 2. 2018. Available from: https://www.eorc.jaxa.jp/ALOS/en/alos/sensor/avnir2_e.htm
- [25] Miyagi Prefectural Government. 2015. Available from: <http://www.pref.miyagi.jp/site/touhoku-saigai/nn-pamphlet-h27.html>

Estimating Rice LAI Using NDVI: A Method for Plant Conservation Education

Rushikesh Kulkarni and Kiyoshi Honda

Abstract

In the field of plant conservation, it has become increasingly important to incorporate advancements to make informed decisions and effectively monitor the situation. This chapter focuses on the use of the Normalized Difference Vegetation Index (NDVI), a tool derived from satellite observations like Landsat 8/9 and the Moderate Resolution Imaging Spectroradiometer (MODIS) to estimate the Leaf Area Index (LAI) of rice, a staple crop. The LAI, which indicates the amount of leaf surface area for photosynthesis, plays a role in determining crop yield and overall health. By utilizing NDVI for LAI estimation we can monitor rice crops on a scale without methods enabling early detection of potential threats or deficiencies. Moreover, this chapter highlights how integrating satellite-based sensing into plant conservation education holds potential for advancing our understanding and practices in this field. While the focus remains on rice, the principles and techniques elucidated have broader implications, making them adaptable to diverse crops and vegetation types. As plant diversity continues to face challenges from various anthropogenic factors, leveraging technological tools like NDVI becomes indispensable. This chapter emphasizes the intersection of technology and conservation, offering insights into novel methodologies that hold promise for the future of plant diversity and conservation education.

Keywords: NDVI, leaf area index, rice conservation, remote sensing, plant diversity education

1. Introduction

Plant conservation is a critical global issue that has been garnering significant attention in recent years [1]. The world's ecosystems, whether terrestrial, aquatic, or marine, hinge on the variety and vitality of plant species [2]. As primary producers, plants form the base of food chains, driving ecosystem functions and providing services that are indispensable for human survival. Hence, it is imperative to have a comprehensive understanding of plant diversity and its conservation status.

Tragically, the planet has been witnessing an alarming loss of plant diversity [3]. A myriad of factors, including habitat destruction, overexploitation, pollution, and

climate change, have led to the extinction of numerous plant species, with many more teetering on the brink [4]. This is a loss especially when we consider the roles that plants play in capturing carbon, producing oxygen, stabilizing soil, and purifying water.

Considering the importance of preserving plants, observing and monitoring crops becomes extremely important. This helps in identifying any signs of stress caused by diseases, pests, or environmental factors allowing for intervention to minimize harm. In addition, crop monitoring plays a role, in maximizing resource utilization, improving crop yields, and ultimately ensuring food security.

The progress in technology has accelerated the progress of crop monitoring based on sensing [5]. This includes using satellite and aerial images to keep an eye on the growth well-being and productivity of crops. Remote sensing offers an invasive way to collect up-to-date information across vast areas making it an extremely valuable tool for monitoring crops.

Vegetation indices play a role in monitoring crops using remote sensing. Two important indices are the Normalized Difference Vegetation Index (NDVI) and the Leaf Area Index (LAI). These indices utilize the reflectance values of types of radiation to gain insights into the health and vitality of crops. NDVI for example measures the greenness of vegetation. It is commonly used to evaluate plant health, growth stage, and biomass. On the other hand, LAI quantifies the amount of leaf material in crops, giving an indication of photosynthesis and overall yield.

When we consider the context of ‘Methodologies, for Teaching Plant Diversity and Conservation Status’ we can see that it’s crucial to include techniques such as remote sensing and the utilization of vegetation indices in comprehensive plant conservation education. It’s not only about grasping the aspects of plant diversity and conservation but also about applying contemporary technologies and methodologies for practical real-world purposes.

By incorporating these techniques into the curriculum we can provide the upcoming generation of conservationists, farmers, and environmentalists with the necessary skills and knowledge to effectively monitor, safeguard, and preserve the diverse range of plant species, in our world [6]. Moreover, comprehending and utilizing these approaches will empower them to maximize resource utilization, improve productivity, and make significant contributions towards global food security. Ultimately teaching these methodologies is a part of an education on plant diversity and its conservation status.

In the field of plant conservation, it has become clear that relying on methods is not enough to fully grasp the complex relationships found in diverse ecosystems [7]. The introduction of Remote Sensing technologies has brought about a change in our approach allowing us to have a ranging perspective of vast landscapes and the intricate interactions between different plants. Specifically Vegetation Indices like NDVI serve as indicators by translating data from satellites into metrics that reflect the health and vitality of vegetation [8]. This fusion of technology with knowledge not only benefits conservationists but also forms the foundation for modern plant conservation education. By introducing ecologists and conservationists to these tools we ensure a comprehensive, knowledgeable, and adaptable approach, to safeguarding our planet’s rich tapestry of plant life.

In this chapter, we explore the process of estimating LAI using NDVI. We specifically highlight its significance in educating about plant conservation. It is crucial to comprehend the relationship between these vegetation indices and plant growth to ensure the preservation of plant diversity and the overall health of our planet’s ecosystems.

2. The role of crop monitoring in plant conservation

2.1 Importance of regular crop monitoring

Regularly monitoring crops is a task in agriculture that also contributes to plant conservation [9]. It involves assessing the condition of crops, their growth stages, and potential risks to ensure they grow healthily and produce yields. This does not guarantee food security. It also plays a significant role in preserving the diversity of plants. By conducting crop monitoring, farmers can identify signs of diseases, pest infestations, or environmental stressors [10]. Taking action can minimize the impact of these factors, promote healthy crop growth, and reduce the risk of losing plant species.

Frequent crop monitoring is also important for optimizing resource utilization. Agriculture requires amounts of water, nutrients, and other resources. By monitoring crop conditions and requirements, farmers can optimize the use of these resources effectively while minimizing waste and environmental harm [9]. For example, employing precision irrigation systems based on data collected through crop monitoring can significantly reduce water consumption while ensuring that plants receive moisture.

Furthermore, regular crop monitoring enables data collection on crop growth and development. These data are invaluable for researchers and policymakers involved in efforts to conserve plants. It helps them understand the needs and challenges faced by crop species facilitating the development of more efficient conservation strategies.

2.2 Implications of crop monitoring on plant conservation

Crop monitoring plays a crucial role in plant conservation for several reasons. Firstly it aids in detecting and managing diseases, pests, and environmental stressors at a stage. By acting, we can minimize the impact of these factors on crop growth and reduce the risk of losing important species. This is especially important for crops that are vital for food security and have limited diversity.

Secondly, crop monitoring allows us to optimize resource utilization effectively. By monitoring the conditions and requirements of crops, agriculturists can make use of water, nutrients, and other resources while minimizing waste and environmental harm. This approach is essential for agriculture practices that aim to conserve resources.

Thirdly, comprehensive data collected through crop monitoring provide insights for developing conservation strategies. Understanding the needs and challenges faced by crop species enables us to create more effective conservation plans. Preserving the diversity of crop species is crucial not only for ensuring food security but also for adapting to changing environmental conditions.

Regular crop monitoring is indispensable in preserving plant diversity. It enables the detection and management of threats while optimizing resource utilization and informing conservation strategies. Incorporating technologies such as remote sensing and vegetation indices can further enhance the effectiveness of crop monitoring efforts worldwide in plant conservation [5, 11].

3. Remote sensing in crop monitoring

The field of sensing has experienced advancements in the last few decades. Initially, remote sensing relied on photographs taken from aircraft, which provided a

down view of the land surface and were primarily used for mapping and land use planning. However, these methods had limitations in agriculture due to their level of detail and inability to capture data across spectral bands.

The introduction of satellite technology brought about a breakthrough in sensing. Satellites equipped with sensors of capture data across spectral bands at varying spatial and temporal resolutions opened up new opportunities for agricultural applications. The development of hyperspectral sensors further enhanced this capability by providing information about vegetation and soil properties through data collection in specific narrow spectral bands.

In recent times, unmanned aerial vehicles (UAVs) have emerged as tools for agricultural remote sensing. Equipped with sensors such as hyperspectral and thermal sensors, UAVs can capture high-resolution data at a relatively lower cost [12]. This accessibility has made remote sensing more feasible for medium farms while also facilitating the growth of precision agriculture [13].

Crop monitoring heavily relies on continuous monitoring. It involves the use of various important measurements to assess plant health, vitality, and response to stress. One of the indicators is the LAI, which measures the amount of green leaf area in relation to the ground area. LAI's utility is manifold: it not only delineates canopy structure but also serves as a proxy for plant photosynthetic capacity. Its significance is further magnified when compared with other indicators like evapotranspiration (ET). ET, which encompasses the combined processes of water evaporation from the soil and transpiration from plants, is another salient crop growth indicator. However, monitoring ET presents inherent challenges, particularly in accurately discerning the proportional contributions of evaporation and plant transpiration [14]. Additionally, ET's dependency on various meteorological parameters complicates its direct estimation from remote sensing data [15]. In contrast, LAI provides a more straightforward, albeit equally profound, insight into crop status [16]. While other indicators, such as soil moisture and chlorophyll content, complement the understanding of crop health, LAI holds a comparative advantage due to its direct correlation with plant physiological activities and its lesser susceptibility to external variabilities, unlike ET. Thus, within the intricate tapestry of remote sensing indicators, the prominence and utility of LAI are undeniably paramount.

4. Vegetation indices in remote sensing

Vegetation remote sensing primarily involves capturing the reflectance of electromagnetic waves from plant canopies using passive sensors. It's widely recognized that this reflectance varies based on the type of plant, the moisture content in its tissues, and other inherent characteristics [17]. Vegetation indices in remote sensing provide essential quantitative measures of vegetation properties, revealing critical insights about land surface characteristics. These signatures provide details regarding the condition, biochemical composition [18], and configuration of a leaf area or canopy. These mathematical combinations of different bands of the electromagnetic spectrum are designed to enhance the contribution of vegetation properties while minimizing the influence of soil and atmospheric conditions. By exploiting the spectral characteristics of vegetation, indices such as the NDVI and LAI have become invaluable tools in monitoring vegetation growth, assessing plant health, and estimating crop yield.

The information regarding the biochemical characteristics of vegetation and the soil beneath it is carried by the radiation that is either reflected or emitted by the Earth's surface. Vegetation has a tendency to absorb light in the red parts of the

spectrum while reflecting light in the near-infrared parts. The absorption of light in the portion can be attributed to chlorophyll whereas other pigments and water contribute to the absorption in the portion. The reflection occurring in the infrared area is a result of how light scatters off leaf cell structures.

Vegetation indices take advantage of these characteristics to measure vegetation properties that are not significantly affected by changes in soil and atmospheric conditions. For instance, the NDVI is calculated by comparing the reflectances of red light and then normalizing the difference by their sum. This index offers a way to determine how green the vegetation is and is widely used to evaluate plant health, growth stage, and biomass.

NDVI is commonly used as an indicator of growth or strength. Because of this, many studies have compared it with the LAI [19], which quantifies the LAI in relation to the surrounding soil area [20].

4.1 Normalized difference vegetation index (NDVI)

NDVI is a used measure for assessing vegetation. It is calculated using the following formula:

$$NDVI = \frac{NIR - RED}{NIR + RED} \quad (1)$$

In the infrared region, NIR represents the reflectance while RED represents the reflectance, in the region. The NDVI values range from -1 to $+1$, where negative values indicate areas without vegetation, values close to zero indicate bare soil or sparse vegetation, and positive values indicate vegetation coverage.

NDVI is a measurement for assessing the greenness of vegetation. It is closely linked to factors such as chlorophyll content, LAI, and biomass. It is commonly utilized to monitor plant growth, evaluate plant health, and estimate crop yield [21].

4.2 Leaf area index (LAI)

LAI is a metric in the field of vegetation. It quantifies the coverage of leaves on the ground per unit area. Assessing LAI is crucial for understanding photosynthesis potential and crop yield. Researchers can determine LAI by establishing connections between sensing data, band reflectance, and leaf area index using either relationships or physical models.

In agriculture, accurately estimating LAI plays a role in evaluating crop growth and predicting yield [22]. It is a parameter in models used for forecasting crop yield, scheduling irrigation, and applying fertilizers [13]. Additionally, it aids in the detection of plant stress and diseases, enabling farmers to take actions to minimize losses.

LAI serves as an indicator of crop growth offering insights that can optimize agricultural practices for higher yields and more sustainable farming. Measuring LAI (Leaf Area Index) can be achieved through various methods, such as destructive methods, indirect methods, and remote sensing techniques.

4.2.1 Destructive methods

This method is considered the precise way to measure LAI. It entails plucking the leaves from the plant and gauging their size [22]. A typical practice involves

harvesting leaves from a group of plants within a ground area. Once harvested, the leaves are scanned for area measurement. Although this approach yields results, it requires labor and, as implied by its name, causes harm to the plants.

4.2.2 Indirect methods

These techniques involve calculating the LAI without the need to physically remove and measure the leaves [21].

4.2.2.1 Optical instruments

Indirect LAI measurements are often conducted using instruments such as the LAI 2000, LAI 2200, or digital hemispherical photography. These instruments gauge the amount of light that passes through the canopy at heights allowing for an estimation of the LAI [22].

4.2.2.2 Remote sensing

This approach involves utilizing satellites or high-altitude aircraft to gather reflectance data from the vegetation surface. Empirical relationships or physical models are then utilized to establish a connection between these reflectance data and the LAI.

Each of these approaches has its strengths and limitations. Destructive methods offer the measurements but require significant manual effort and may not be suitable for monitoring large areas or when continuous observation is needed. Optical instruments are less labor-intensive and enable monitoring, although they may have slightly lower accuracy compared to destructive methods. Remote sensing allows for monitoring. It might be slightly less accurate than ground-based methods due to factors such as cloud cover or soil background influence.

NDVI and LAI are valuable tools for crop monitoring and provide valuable information about plant health, growth stage, and yield potential [23]. Despite some limitations, they provide real-time data over large spatial scales, facilitating the timely detection of stress factors and optimizing resource use. Incorporating NDVI and LAI into crop monitoring practices can contribute to sustainable agriculture and plant conservation efforts.

5. Case study: estimating rice LAI using NDVI

Case studies serve as an indispensable pedagogical tool, providing students with a unique platform to bridge theory and real-world applications, thereby fostering the development of their analytical and problem-solving acumen. The immersive and interactive nature of case studies positions them as a cornerstone in effective teaching and learning, equipping students with the skills necessary for their future professional endeavors.

Within the context of this chapter, we narrow our focus to a case study centered on the utilization of the NDVI, derived from MODIS Surface Reflectance data. Our primary objective is to estimate the LAI of rice, shedding light on the intricate methodologies that underpin our understanding and pedagogical approach to plant diversity and conservation status. This exploration at the intersection of remote sensing technology, agronomy, and conservation education highlights the strides made in the

realm of plant growth, health, and diversity estimation. LAI, a pivotal indicator of crop growth, emerges as a multifaceted tool with applications not only in agriculture but also as a pedagogical catalyst in the realm of plant conservation education.

In this chapter, we venture into the profound implications of retrieving LAI from NDVI, offering an in-depth and original perspective tailored for advanced readers with extensive prior knowledge. By meticulously dissecting the intricate relationship between LAI and NDVI, we pave the way for a deeper comprehension of plant diversity and the delicate equilibrium of conservation within our ecosystem. Our exploration of modern methodologies, notably NDVI-based LAI estimation, illuminates the transformative potential of technical knowledge in cultivating a heightened appreciation for plant life and its preservation.

5.1 Materials and methods

5.1.1 Description of study area

The research focal point for this case study resides within the expansive rice fields of the Song Phi Nong District, located in the heart of the Suphan Buri Province, Thailand. This geographic context, illustrated in **Figure 1**, presents a uniformly characterized terrain, meticulously analyzed utilizing advanced Landsat 7 ETM+, complemented by comprehensive land use maps and aerial imagery. The study period spans from January to April 2006, a critical growth phase for the initial crop cycle in this province.

The topographical essence of the study area reveals a predominantly flat low-land terrain, contributing to the perennial inundation of the rice fields throughout the monsoon season. This region's climatic conditions manifest three distinct seasons: a

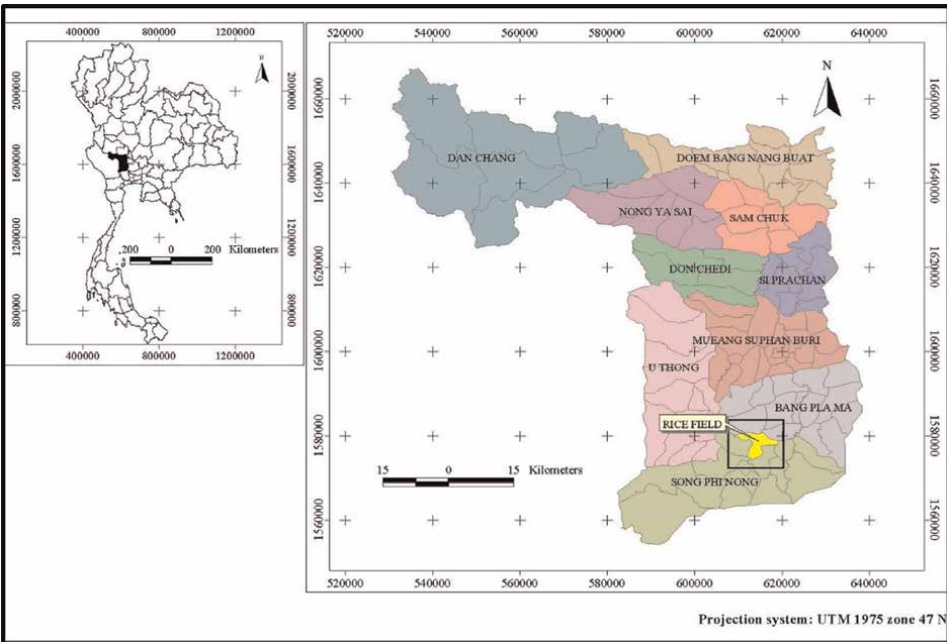


Figure 1.
Location of the Study area in the Suphan Buri Province, Central Thailand.

rainy period from May to October, followed by a cool, dry interlude extending through November to February, and culminating in a hot, dry season from March to May. These cycles influence the annual rainfall, averaging between 900 to 1300 mm, and solar radiation approximating $17 \text{ MJ m}^2 \text{ d}^{-1}$ with temperature fluctuations ranging from a peak of $33 - 34^\circ\text{C}$ to a low of $23 - 24^\circ\text{C}$. This climatic backdrop, interspersed with technological interventions, lays the foundation for the in-depth examination and estimation of Rice LAI employing NDVI within this intricate agricultural landscape.

5.1.2 Field data collection

The acquisition of precise spectral reflectance and Leaf Area Index (LAI) data during the course of this study was a critical component of our research methodology. To ensure the accuracy and reliability of our findings, a meticulous field data collection process was undertaken. This section provides an exhaustive account of the instruments, techniques, and procedures employed for this purpose.

Spectral reflectance, a pivotal parameter for our study, was measured using a state-of-the-art spectroradiometer. The data acquisition process commenced during the initial stages of rice growth and extended through to the harvesting period. Notably, spectral reflectance readings were recorded at specific times between 9:00a.m. and 11:00a.m. This timing was selected deliberately, as the employed LAI-2000 Plant Canopy Analyzer (PCA) does not rely on direct solar radiation for LAI measurements. Furthermore, it is imperative to capture LAI with a low sun elevation angle, which is typically achievable during morning or evening hours.

In order to mimic satellite data acquisition conditions, spectral reflectance readings were captured at five different angles, separately in the East and West directions. This strategic approach aligns with satellite data acquisition patterns, which predominantly move in the North-South direction while capturing reflectance in the East-West direction. Each spectral reflectance measurement involved 150 intervals, ranging from 0° to 60° , as precisely marked on a custom-made clinometer; refer to **Figure 2**. This level of granularity enabled us to examine the Bidirectional Reflectance Distribution Function (BRDF) effect in the field, as illustrated in **Figure 2**. For each day of ground truthing, five readings of spectral reflectance were recorded at each of the five different angles in both the East and West directions. These readings, along with the corresponding five LAI measurements from five sampled locations, were meticulously averaged.

Over the data collection period spanning from 12th February to 2nd April, a total of eight readings of spectral reflectance at each of the five different angles and eight readings of LAI were obtained in the field. The setup involved clamping the fiber optic wire of the spectrometer at each angle, where spectral reflectance readings were recorded in both directions. Consequently, a total of ten readings of spectral reflectance were measured each day during ground truthing activities. The spectrometer utilized in this process covered the spectral range from 304 nm to 1135 nm, with a precision increment of 1 nm.

To facilitate the comparison between in situ NDVI and MODIS data, the average reflectance for the red band was computed within the wavelength range of 620 nm to 670 nm, while for the near-infrared band, calculations were performed within the wavelength range of 841 nm to 876 nm.

The estimation of the NDVI from in situ spectral reflectance readings was conducted on a weekly basis throughout the data collection phase. These in situ NDVI values were subsequently juxtaposed with NDVI estimations derived from 8-day

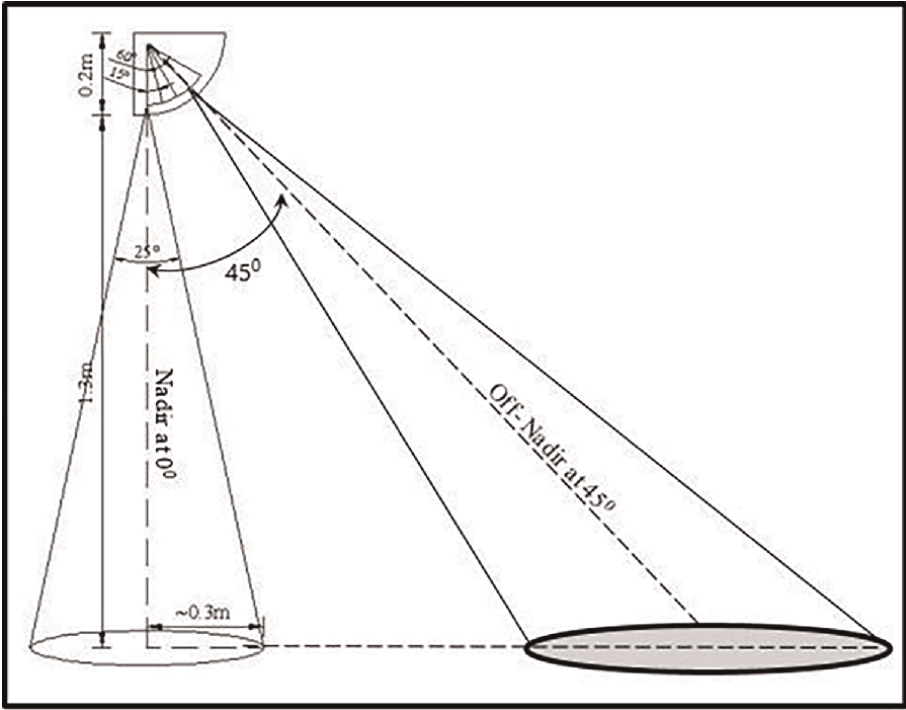


Figure 2.
Schematic diagram of clinometer setup used to measure surface reflectance in the field with various angles.

composite MODIS surface reflectance data acquired during corresponding weeks of ground truthing, as depicted in **Figure 3**. Notably, two of the field data collection dates, namely 26th February and 3rd March, corresponding to the 8-day composite period from 26th February to 5th March (refer to **Table 1** for details).

5.1.3 Methodology

The workflow of the methodology used in this study is presented in **Figure 3**. It entails the acquisition of atmospheric-corrected MODIS surface reflectance

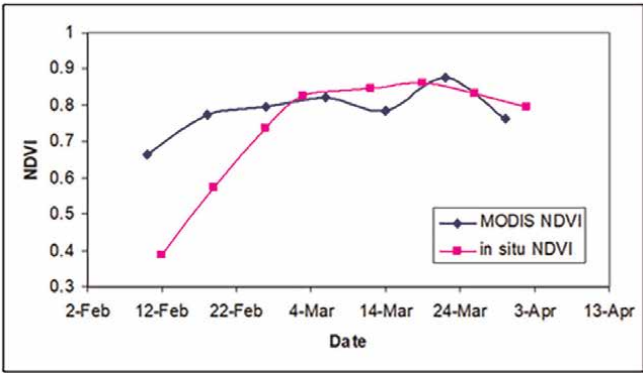


Figure 3.
Comparison of Field-Estimated NDVI at 0° Viewing Angle with MODIS Surface Reflectance-derived NDVI.

Field data collection dates	MODIS 8-day composite dates
12th Feb	10th Feb–17th Feb
19th Feb	18th Feb–25th Feb
26th Feb	26th Feb–5th March
3rd March	26th Feb–5th March
12th March	6th March–13th March
19th March	14th March–21th March
26th March	22th March–29th March
2nd April	30th March–6th April

Table 1.
Comparison of field data collection dates and MODIS 8-day composite reflectance data capture dates.

data, which are then compared to the concurrently gathered field-derived NDVI using a precise fiber optic spectroradiometer. This comparative analysis serves as the cornerstone for establishing the intricate relationship between MODIS-derived NDVI and LAI, as thoughtfully delineated within the methodology’s flowchart in **Figure 4**.

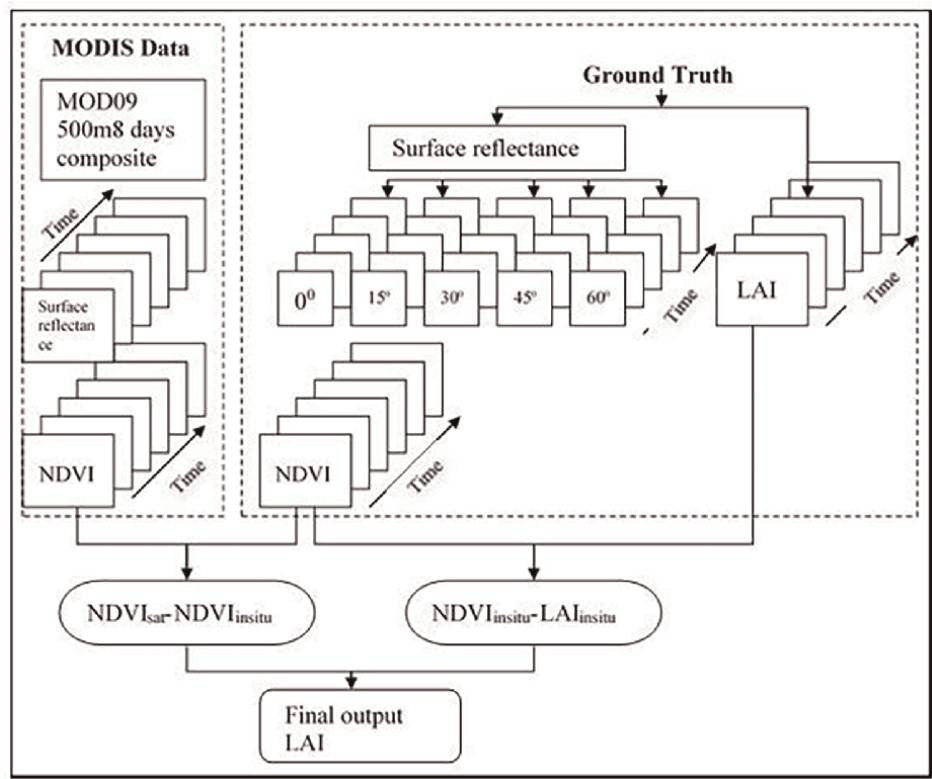


Figure 4.
Workflow of the methodology.

5.2 Results and discussion

5.2.1 Correlation analysis of in situ NDVI and NDVI derived from MODIS

The study focused on contrasting in situ NDVI measurements against those derived from MODIS. Upon comparison of eight in situ NDVI values against seven MODIS-derived NDVI values, distinctions were evident, particularly in early crop development stages. During this phase, the paddy displays a dispersed growth pattern with visible muddy soil amidst the newly germinated rice plants. As evident in **Figure 5**, this exposes the canopy to background contamination errors.

From a satellite observational perspective, the inherent angular effect of the MODIS observation platform can cause the field to appear differently than ground-based observations, as seen by the naked eye. This phenomenon is attributed to the angular effect, which, in this scenario, led to an elevation in MODIS-derived NDVI values. The atmospheric attenuation and the presence of aerosols introduce notable discrepancies between the surface-measured “true” NDVI and space-determined NDVI [24]. The comparison of MODIS BRDF nadir-adjusted 16-day composite data with in situ NDVI, as displayed in **Figure 6**, revealed analogous growth patterns to in situ measurements taken at nadir. However, the integration of 16 days of composite data with data garnered in a single day presents inherent challenges.

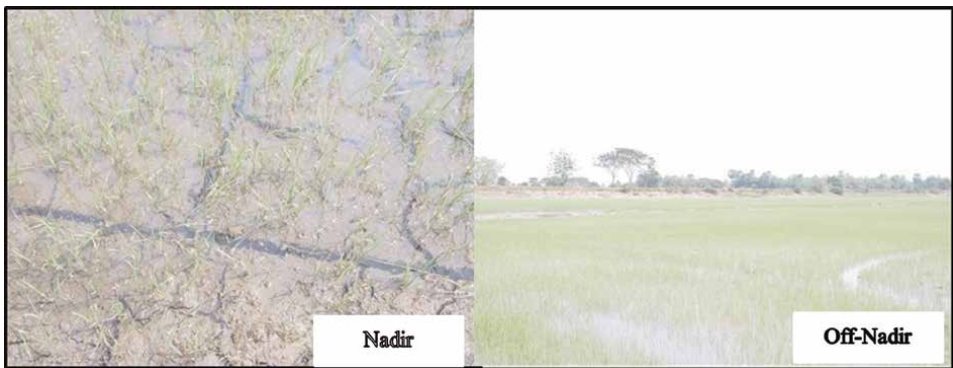


Figure 5.
Comparing Nadir and Off-Nadir Perspectives: The Interplay of Soil and Paddy Leaf Reflectance.

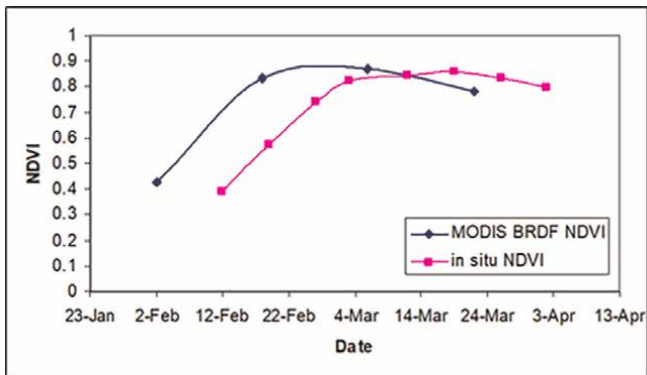


Figure 6.
Comparison of NDVI from MODIS (BRDF) Nadir-Adjusted Data and Field-Estimated NDVI.

Observation angle	Relationship	R ²
0°	$y = 2.447x - 1.1838$	0.65
15°	$y = 2.437x - 1.1793$	0.66
30°	$y = 2.447x - 1.1838$	0.65
45°	$y = 2.532x - 1.2469$	0.67
60°	$y = 2.488x - 1.2068$	0.68

Table 2.
Linear correlations between in situ NDVI acquired from spectrophotometer and clinometer at different angles and the corresponding MODIS NDVI values.

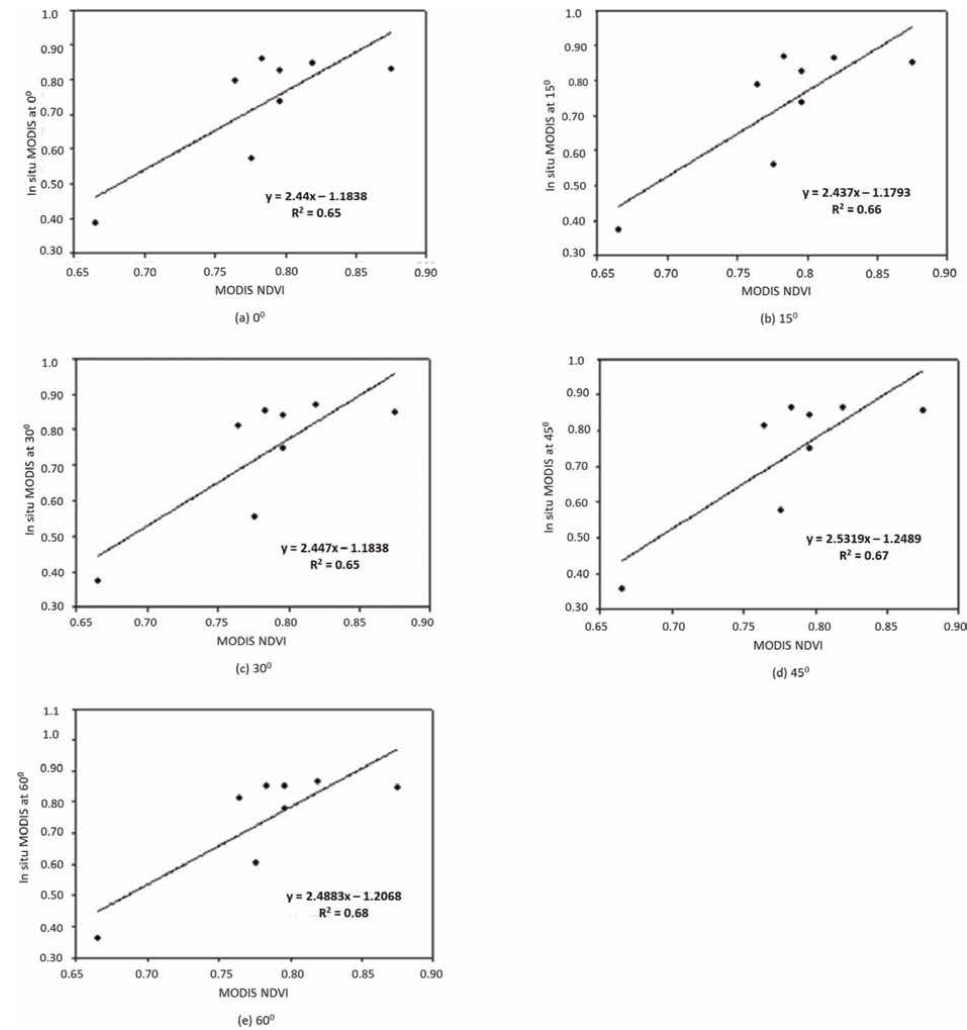


Figure 7.
Correlation of in situ NDVI measurements at varying angles (0°, 15°, 30°, 45° and 60°) with MODIS-derived NDVI values.

A comprehensive assessment was conducted by comparing the MODIS NDVI with the average in situ NDVI, aggregated from measurements taken at five field locations, both in the East and West directions and across five observation angles. It's important to note that the ground truth surface reflectance data were consistently collected during the morning hours, between 9:00 a.m. and 11:00 a.m. To quantify the association, a linear correlation coefficient R^2 was computed between in situ NDVI from five angles and the NDVI derived from MODIS surface reflectance as presented in **Table 2**. The outcome of this exercise is delineated in **Figure 7**, illustrating comparable results across all observations. For preciseness, the in situ NDVI was linearly interpolated to match the view zenith angle of MODIS.

Diving into the technicalities, the MODIS metadata file underscores the specifications intrinsic to the MODIS surface reflectance product, as documented in **Table 3**. The in situ NDVI measurements taken at various angles underwent interpolation to align with the zenith angle of MODIS, and the subsequent results are tabulated in **Table 4** and presented in **Figure 8**.

For standardization, the interpolated in situ NDVI was adjusted to a nadir observation. This elaborate process established a multistage methodology to extract in situ NDVI from MODIS-derived NDVI. Refer **Figure 9**.

MODIS data available day	DOY	View zenith angle	Solar zenith angle	NDVI
02 Feb	33	6.77	39.20	0.5987
10 Feb	41	7.93	36.59	0.6649
18 Feb	49	6.43	30.69	0.7757
26 Feb	57	8.39	32.14	0.7962
06 Mar	65	22.26	28.93	0.8199
14 Mar	73	20.07	29.22	0.7835
22 Mar	81	22.45	24.01	0.8748
30 Mar	89	19.39	25.14	0.7643

Table 3.
Characteristics of MODIS on respective dates.

Field data collection day	Interpolated in situ NDVI
12 Feb	0.3794
19 Feb	0.5675
26 Feb	0.7362
03 Mar	0.8252
12 Mar	0.8642
19 Mar	0.8616
26 Mar	0.8492
02 Apr	0.7941

Table 4.
Interpolated in situ NDVI corresponding to view zenith of MODIS.

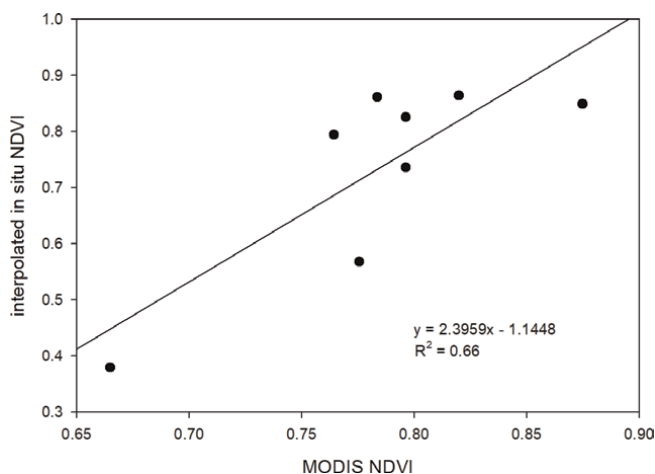


Figure 8.
Relationship between MODIS NDVI and interpolated in situ NDVI.

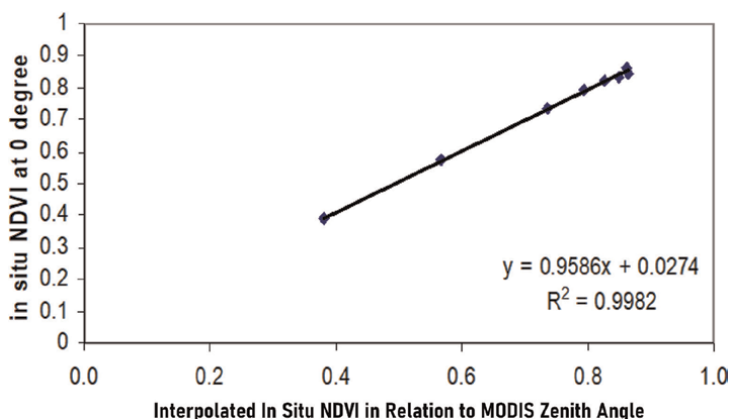


Figure 9.
Comparison of in situ NDVI estimated at 0° in field and in situ NDVI obtained by derived model.

A noteworthy challenge encountered during this study was the presence of clouds, which substantially influenced the dataset. Specifically, the remote sensing data accrued on the 19th and 22nd of March displayed significant inaccuracies, impacting the NDVI and LAI calculations. Moreover, while the initial plan encompassed data collection from seven distinct locations, challenges in rice maintenance at two sites narrowed the scope to five sites by the end of this research.

In summation, while the inherent differences between in situ NDVI and MODIS-derived NDVI exist, particularly during the early growth stages, the methodologies developed and adopted in this study demonstrate the potential to harmonize these measurements, ensuring more accurate representations for educational and research endeavors.

5.2.2 Validation of model

From **Figure 10**, it becomes evident that the model-derived NDVI closely mirrors the in situ NDVI recorded at a 0° observation angle during the initial stages of rice

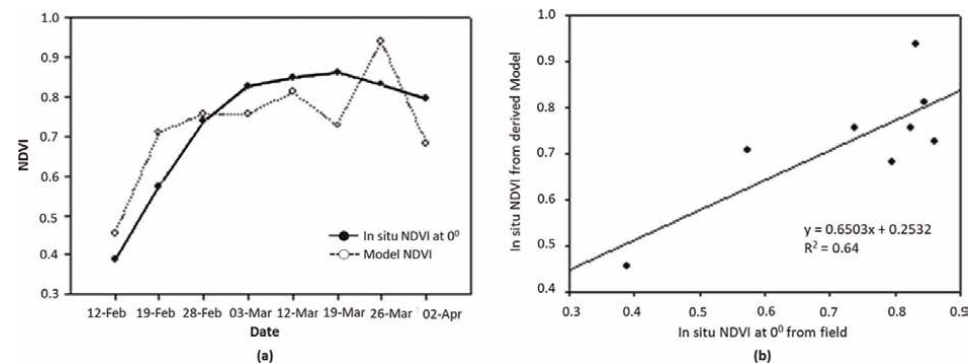


Figure 10.
(a) Comparison of In situ NDVI Measurements at 0° and Model-derived NDVI Over Time and (b) Linear Regression Analysis between In situ NDVI Measured at 0° Sensing Position and Model-derived In situ NDVI.

growth. This alignment signifies the model’s accuracy and relevance, especially in its early phases. However, as the rice matures, discrepancies emerge, likely due to contaminants in the remote sensing data. These irregularities cause the modeled in situ NDVI to deviate from the expected outcomes, highlighting areas for further refinement to ensure the model’s robustness and precision in all growth stages.

5.2.3 Correlation analysis of in situ NDVI and in situ LAI

The relationship between in situ NDVI and in situ LAI proves intricate and multi-faceted (**Figure 11**). While initial observations might suggest a linear association, deeper analysis reveals otherwise. As elucidated in prior studies, the NDVI’s sensitivity to LAI diminishes as the LAI value escalates, typically reaching a threshold between 2 and 3 [21, 24]. Beyond this threshold, NDVI displays an almost linear increase in tandem with LAI until reaching an asymptotic region. Here, the NDVI’s increase becomes markedly lethargic despite further LAI enhancement. This asymptotic phase notably coincides with the scenario where the ground surface is predominantly veiled by foliage. A linear correlation coefficient (R^2) was derived by juxtaposing in situ NDVI at 0° and in situ LAI. Notwithstanding, it’s salient to note that a considerable portion of LAI measurements resided within the 4–5 range,

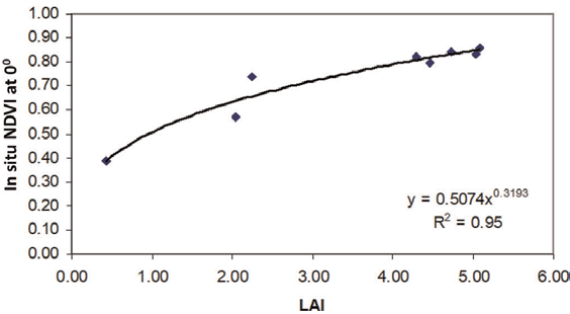


Figure 11.
Regression analysis of In situ NDVI at Nadir against LAI measurements from a rice field using an LAI Canopy analyzer.

rendering a nonlinear correlation analysis between the two in situ parameters more appropriate for this study.

The outcome from the nonlinear correlation analysis between in situ NDVI estimated at 0° and in situ LAI is as in Eq. (2).

$$\text{In situ NDVI at } 0^\circ = 0.5074 \times \text{LAI}^{0.3193} \quad (2)$$

5.2.4 Final model development

The devised model delineates a two-part progression: firstly, the NDVI transformation from satellite data to in situ measurements and subsequently, a translation from in situ NDVI to Leaf Area Index (LAI). In the former segment, analogous variables, predominantly NDVI, are juxtaposed, ensuring a congruent foundation for subsequent analysis. Concurrent measurements of spectral reflectance and in situ, LAI, taken identically in terms of both location and timing within the rice field, comprise the latter part. This methodological bifurcation, characterized by its multi-stage modeling, offers a nuanced perspective, arguably surpassing the realism afforded by single-stage counterparts. Notably, the direct association between MODIS NDVI and in situ LAI remains unexplored in this research. The in situ NDVI yielded an RMSE of 0.603, while the LAI's estimation stood at 2.120. Such heightened RMSE values potentially originate from contamination errors inherent in the remote sensing data. A specific instance on the 22nd of March revealed an overestimated NDVI value, which consequentially skewed the LAI computations.

$$\text{In situ NDVI}_{\text{MODIS}} = 2.2967 \times \text{NDVI}_{\text{MODIS}} - 1.0727 \quad (3)$$

$$\text{LAI} = \left(\frac{\text{NDVI}_{\text{in situ}}}{0.5074} \right)^{3.1318} \quad (4)$$

Refer to **Figure 12** for the model LAI validation against in situ LAI. The discernable trend showcases the LAI derived from our proposed model aligning closely with the empirically measured in situ LAI. The observed coefficient of correlation R^2 registered a value of 0.61, suggesting potential enhancement opportunities through refining the precision of remote sensing datasets.

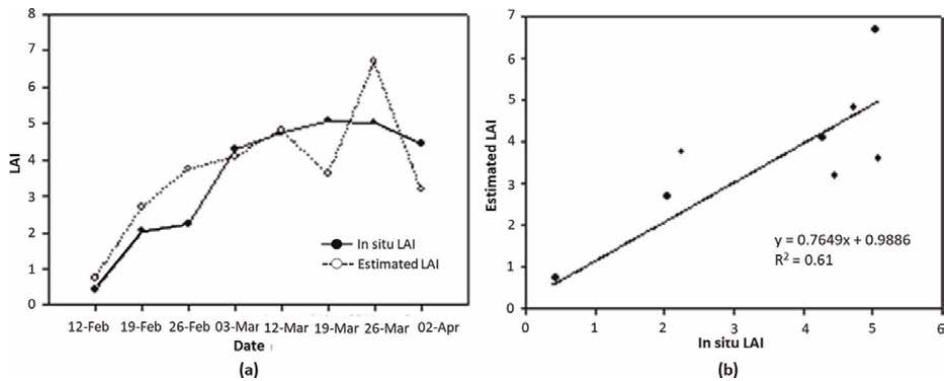


Figure 12. (a) Comparison of In situ LAI measured by LAI canopy analyzer and Estimated LAI by model. (b) Regression Analysis of In situ LAI Against LAI estimated developing relationship with NDVI.

6. Implications for plant conservation education

The incorporation of NDVI methodologies into plant conservation education offers a promising avenue for enhancing both the depth and breadth of students' understanding of plant diversity and conservation. The process of estimating Rice LAI using NDVI serves as a case study that illuminates broader implications for plant conservation education.

6.1 Bridging the gap between theory and practice

Bridging the gap between theory and practice by integrating NDVI-derived methodologies into the curriculum, educators can provide students with hands-on experiences that bridge the gap between theoretical knowledge and practical applications. Such methodologies not only furnish students with a clear understanding of how remote sensing technologies can be employed in monitoring plant health and growth but also demonstrate the transformative potential of these technologies in conservation efforts.

6.2 Fostering critical thinking and analytical skills

The process of analyzing NDVI data, interpreting results, and drawing informed conclusions encourages students to develop robust analytical skills. By navigating the complexities associated with remote sensing data, students cultivate a critical mindset, essential for addressing contemporary challenges in plant conservation.

6.3 Enhancing interdisciplinary learning

NDVI methodologies sit at the nexus of various disciplines including botany, environmental science, remote sensing, and data analytics. Incorporating this interdisciplinary approach into plant conservation education equips students with a holistic understanding, fostering collaboration across diverse fields and promoting innovative solutions.

6.4 Addressing real-world conservation challenges

By focusing on real-world applications, such as the estimation of Rice LAI, NDVI-based education underscores the pressing issues of biodiversity loss and environmental degradation. It compels students to grapple with real-world scenarios, pushing them to devise actionable strategies for conservation.

6.5 Preparing for the future of plant conservation

As technology continues to evolve and play an increasingly significant role in conservation efforts, it's imperative for the next generation of conservationists to be well-versed in cutting-edge methodologies like NDVI. Integrating such tools into educational curricula ensures that students are adequately prepared to leverage technology in future conservation endeavors.

6.6 Challenges and considerations

While NDVI methodologies offer numerous educational benefits, it's vital for educators to be cognizant of potential challenges. These might include the steep learning curve associated with remote sensing technologies, ensuring data accuracy, and addressing the nuances of interpreting NDVI data in varied environmental contexts. An in-depth curriculum, supplemented with hands-on training sessions, can mitigate these challenges.

Eventually, the integration of NDVI methodologies into plant conservation education holds immense potential for shaping the future of the field. By imparting both theoretical knowledge and practical skills, educators can foster a new generation of conservationists, adept at harnessing technology to safeguard our planet's biodiversity.

6.7 Future directions for plant conservation education

The rapidly evolving landscape of plant conservation education, underpinned by technological and ecological advancements, calls for a forward-looking vision. Notably, the integration of vegetation indices, such as NDVI and LAI, into educational frameworks has showcased the transformative potential of these metrics in conservation endeavors. Here, we extrapolate the future trajectories of plant conservation education, with a spotlight on various vegetation indices.

1. **Comprehensive integration of vegetation indices:** The pronounced impact of vegetation indices like NDVI in determining plant health and ecosystem dynamics mandates their comprehensive integration into curricula. Beyond NDVI, there's a need to incorporate a spectrum of indices like the Enhanced Vegetation Index (EVI), Soil-Adjusted Vegetation Index (SAVI), and others, ensuring students gain a holistic understanding of their varied applications.
2. **Delving deeper into the ecological significance of LAI:** LAI is not merely a metric but an ecological barometer reflecting plant health, productivity, and broader ecosystem interactions. Future courses should intensify their focus on LAI, exploring its role in water balance, nutrient cycling, and interspecies interactions within ecosystems.
3. **Embracing advanced technologies for index estimation:** As remote sensing technologies advance, it's essential for conservation education to stay abreast. The advent of high-resolution satellite imagery, drone-based observations, and advanced data analytics platforms promise enhanced accuracy in vegetation index estimation, warranting their inclusion in advanced courses.
4. **Interdisciplinary approaches anchored in vegetation indices:** The multifaceted nature of vegetation indices, spanning botany, geospatial sciences, and data analytics, advocates for interdisciplinary synergies. Future curricula should inspire students to perceive these indices through diverse lenses, fostering comprehensive conservation solutions.
5. **Real-world applications and field studies:** Theoretical knowledge, while foundational, is enriched by practical applications. Emphasizing field studies that

allow students to measure and interpret vegetation indices across different ecosystems can foster a profound understanding of their real-world implications.

6. Policy advocacy with emphasis on vegetation indices: The centrality of vegetation indices in gauging ecosystem health positions them as pivotal metrics in environmental policymaking. Aspiring conservationists should be equipped to champion policies that prioritize these indices, ensuring their prominence in environmental evaluations and conservation strategies.
7. Lifelong learning and continuous updates on vegetation indices: The dynamic nature of the field necessitates an ethos of lifelong learning. As newer vegetation indices are developed and existing ones refined, continuous education opportunities can ensure conservationists remain attuned to cutting-edge methodologies.

As we craft the future of plant conservation education, a harmonious blend of traditional wisdom and avant-garde methodologies, centered around these indices, will be instrumental in nurturing conservationists capable of addressing the multifarious challenges of the modern world.

7. Conclusion

In the contemporary landscape of environmental science and conservation, technological advancements have ushered in novel methods to study and preserve the planet's rich biodiversity. One of the pivotal advancements has been the application of the NDVI derived from satellite observations, such as Landsat 8/9 and the MODIS surface reflectance. This chapter has elucidated the utility of NDVI in estimating the LAI of rice, a staple food crop that plays a significant role in global food security.

The estimation of LAI using NDVI offers multiple advantages. Firstly, it provides an efficient and nondestructive method to gauge the growth and health status of rice crops. The LAI serves as an indicator of the amount of leaf surface area available for photosynthesis, a parameter intrinsically linked to crop yield and health. The ability to remotely assess this metric on a large scale can substantially enhance monitoring capabilities, making it feasible to detect potential threats or deficiencies early on.

Moreover, the use of NDVI-based methodologies exemplifies the integration of modern technology into the realm of plant conservation and education. By leveraging satellite-based remote sensing, educators and conservationists can obtain real-time data, allowing for more dynamic and responsive conservation strategies. This data-driven approach not only enhances the accuracy of monitoring but also offers an opportunity to engage with the broader community, fostering a deeper understanding and appreciation of the intricate dynamics of plant ecosystems.

It is also worth noting that while this chapter has focused on rice LAI estimation, the principles and methodologies discussed are adaptable to other crops and vegetation types. This versatility underscores the potential of NDVI as a tool not just for rice conservation but for broader applications in plant diversity and conservation education.

In the grand narrative of plant conservation, the significance of understanding and preserving biodiversity cannot be understated. As primary producers, plants form the foundation of most terrestrial ecosystems, influencing everything from atmospheric

composition to soil health. The loss of plant diversity, as the chapter highlighted, has far-reaching consequences, affecting not only the health of ecosystems but also the human societies that depend on them.

Eventually, the use of NDVI in estimating rice LAI presents a confluence of technology and conservation, paving the way for more informed and effective strategies to safeguard our planet's biodiversity. As the challenges of environmental degradation and biodiversity loss intensify, it is imperative that educators, researchers, and conservationists harness the power of such innovative methodologies. This chapter serves as a testament to the potential of integrating technology with conservation education, underscoring the need for continuous innovation and collaboration in the quest to preserve the planet's rich tapestry of life.

Abbreviations

BRDF	Bidirectional Reflectance Distribution Function
EVI	Enhanced Vegetation Index
ET	Evapotranspiration
LAI	Leaf Area Index
nm	nano meter
NDVI	Normalized Difference Vegetation Index
MODIS	Moderate Resolution Imaging Spectroradiometer
PCA	Plant Canopy Analyzer
SAVI	Soil Adjusted Vegetation Index
UAV	Unmanned Aerial Vehicles

Author details

Rushikesh Kulkarni^{1*†} and Kiyoshi Honda^{2†}


1 Symbiosis International (Deemed University), Pune, India

2 Chubu University, Aichi, Japan

*Address all correspondence to: rushikeshk@sitpune.edu.in

† These authors contributed equally.

IntechOpen

© 2023 The Author(s). Licensee IntechOpen. This chapter is distributed under the terms of the Creative Commons Attribution License (<http://creativecommons.org/licenses/by/3.0>), which permits unrestricted use, distribution, and reproduction in any medium, provided the original work is properly cited. 

References

- [1] Maunder M. Plant conservation. In: Levin SA, editor. *Encyclopedia of Biodiversity*. Second ed. Waltham: Academic Press; 2013. pp. 76-89. DOI: 10.1016/B978-0-12-384719-5.00280-X
- [2] Sandifer PA, Sutton-Grier AE, Ward BP. Exploring connections among nature, biodiversity, ecosystem services, and human health and well-being: Opportunities to enhance health and biodiversity conservation. *Ecosystem Services*. 2015;**12**:1-15
- [3] Adebayo O. Loss of biodiversity: The burgeoning threat to human health. *Annals of Ibadan Postgraduate Medicine*. 2019;**17**(1):1-3
- [4] Five drivers of the nature crisis. Available at: <https://www.unep.org/news-and-stories/story/five-drivers-nature-crisis>
- [5] Omia E, Bae H, Park E, Kim MS, Baek I, Kabenge I, et al. Remote sensing in field crop monitoring: A comprehensive review of sensor systems, data analyses and recent advances. *Remote Sensing*. 2023;**15**(2): 354. DOI: 10.3390/rs15020354
- [6] Ardoin NM, Bowers AW, Gaillard E. Environmental education outcomes for conservation: A systematic review. *Biological Conservation*. 2020;**241**: 108224
- [7] Corlett RT. Plant diversity in a changing world: Status, trends, and conservation needs. *Plant Diversity*. 2016;**38**(1):10-16
- [8] de la Iglesia A, Martinez SML. Demystifying normalized difference vegetation index (NDVI) for greenness exposure assessments and policy interventions in urban greening. *Environmental Research*. 2023;**220**: 115155
- [9] Dhanaraju M, Chenniappan P, Ramalingam K, Pazhanivelan S, Kaliaperumal R. Smart farming: Internet of things (IoT)-based sustainable agriculture. *Agriculture*. 2022;**12**:1745. DOI: 10.3390/agriculture12101745
- [10] Zhang J, Huang Y, Ruiliang P, Gonzalez-Moreno P, Yuan L, Kaihua W, et al. Monitoring plant diseases and pests through remote sensing technology: A review. *Computers and Electronics in Agriculture*. 2019;**165**:104943
- [11] Bégué A, Arvor D, Bellon B, Betbeder J, de Abelleira D, Ferraz R, et al. Remote sensing and cropping practices: A review. *Remote Sensing*. 2018;**10**:99. DOI: 10.3390/rs10010099
- [12] Zhang Z, Zhu L. A review on unmanned aerial vehicle remote sensing: Platforms, sensors, data processing methods, and applications. *Drones*. 2023;**7**:398. DOI: 10.3390/drones7060398
- [13] Sishodia RP, Ray RL, Singh SK. Applications of remote sensing in precision agriculture: A review. *Remote Sensing*. 2020;**12**:3136. DOI: 10.3390/rs12193136
- [14] Wanniarachchi S, Sarukkalige R. A review on evapotranspiration estimation in agricultural water management: Past, present, and future. *Hydrology*. 2022;**9**: 123. DOI: 10.3390/hydrology9070123
- [15] Wu B, Zhu W, Yan N, Xing Q, Xu J, Ma Z, et al. Regional actual evapotranspiration estimation with land and meteorological variables derived from multi-source satellite data. *Remote*

Sensing. 2020;**12**:332. DOI: 10.3390/rs12020332

[16] Pasqualotto N, Delegido J, Van Wittenberghe S, Rinaldi M, Moreno J. Multi-crop green LAI estimation with a new simple Sentinel-2 LAI index (SeLI). *Sensors*. 2019;**19**:904. DOI: 10.3390/s19040904

[17] Liu C, Sun PS, Liu SR. A review of plant spectral reflectance response to water physiological changes. *Chinese Journal of Plant Ecology*. 2016;**40**(1):80

[18] Huete AR. Vegetation indices, remote sensing, and forest monitoring. *Geography Compass*. 2012;**6**(9):513-532

[19] Sripada RP, Heiniger RW, White JG, Meijer AD. Aerial color infrared photography for determining early in-season nitrogen requirements in corn. *Agronomy Journal*. 2006;**98**(4):968-977

[20] Zhang B, Wu D, Zhang L, Jiao Q, Li Q. Application of hyperspectral remote sensing for environment monitoring in mining areas. *Environmental Earth Sciences*. 2012;**65**: 649-658

[21] Kulkarni R, Honda K. Estimating LAI of Rice using NDVI derived from MODIS surface reflectance. *Advances in Science, Technology and Engineering Systems Journal*. 2020;**5**(6):1047-1053

[22] The Importance of Leaf Area Index (LAI) in Environmental and Crop Research. Available from: <https://cid-inc.com/blog/the-importance-of-leaf-area-index-in-\environmental-and-crop-research/#:~:text=Since%20leaves%20are%20essential%20for,of%20environmental%20factors%20on%20plants>

[23] Vélez S, Martínez-Peña R, Castrillo D. Beyond vegetation: A review unveiling additional insights into

agriculture and forestry through the application of vegetation indices. *J (Multidisciplinary Scientific Journal)*. 2023;**6**:421-436. DOI: 10.3390/j6030028

[24] Carlson T, Ripley D. On the relation between NDVI, fractional vegetation cover, and leaf area index. *Remote Sensing of Environment*. 1997;**62**: 241-252. DOI: 10.1016/S0034-4257(97)00104-1

Plant Diversity in Agro-Pastoral Grasslands of Tanzania

*Pius Yoram Kavana, Bukombe John Kija,
Emmanuel Pagiti Reuben, Ally Kiyenze Nkwabi,
Baraka Naftal Mbwambo, Simula Peres Maijo,
Selemani Rehani Moshi, Shabani Haruna Matwili,
Victor Alexander Kakengi and Stephen Justice Nindi*

Abstract

This chapter delves into the intricate relationship between agro-pastoral activities and plant diversity in Tanzanian grasslands. The study addresses three critical research questions: the current status of plant diversity in agro-pastoral grasslands, the impact of anthropogenic activities on plant diversity, and strategies for maintaining plant diversity in Tanzania's agro-pastoral grasslands. A systematic literature review and primary vegetation sampling were conducted. The impacts of agro-pastoralism on plant diversity were observed to have both detrimental and win-win scenarios. Practices such as deferred and controlled grazing contribute to soil conservation and biodiversity conservation, whereas continuous grazing and land cultivation lead to land degradation and loss of plant diversity. The study underscores the importance of perennial grasses, which contribute to soil improvement and provide a stable feed resource base for grazing animals. However, anthropogenic activities threaten plant diversity, especially in lowlands. Altitude is a significant factor affecting plant diversity, with a decline observed in lowlands subjected to agro-pastoral activities. As human population increased agro-pastoral activities, the chapter concludes by highlighting the potential negative consequences on ecosystem services and biodiversity in lakes. It emphasizes the urgency of adopting sustainable agro-pastoral practices and ecosystem-specific conservation measures to ensure these vital grassland ecosystems' long-term health and resilience.

Keywords: anthropogenic activities, ecosystem services, edible plants, inedible plants, perennial grasses, plant resources

1. Introduction

There are a variety of natural biological resources in grasslands that human beings rely on for their livelihood, survival, and development. People living in grassland ecosystems tend to believe that cultivating crops and maintaining pastures offer more immediate benefits than conserving natural resources and biodiversity [1].

This implies conflicting goals between agro-pastoralism and biodiversity conservation as a tendency to maximize services from agro-pastoralism results in overutilization and removal of plants that consequently affect plant diversity. This challenges the management of plant resources in grassland ecosystems since agro-pastoralism and plant diversity are not independent [2]. There is a progressive growth in human population and conversion of grassland to agriculture [3]. However, little is known about the situation's impact on the diversity of plants that form basal feed resources for grazing livestock and wild animals in grasslands.

The diversity of species in grasslands has functional implications, as the quantity and variety of species in the ecosystem dictate the organismal traits that impact ecosystem processes [4]. Species traits can directly influence energy and material flows or modify abiotic conditions, such as restricting resources, affecting disturbance, and regulating climate processes [5].

The elements of species diversity influencing trait expression encompass species richness, evenness, and composition, and their interactions and variations in time and space [6]. Plant diversity and the complementarity of plant species are important regulators of grassland ecosystem productivity [7]. This happens as a result of plant species' response to nutrient availability and resource use efficiency in a diverse plant community. However, the availability of growth-limiting resources changes along plant diversity gradients under normal conditions. High plant diversity communities tend to contain species that are able to access scarce resources during periods of stress, such as accessing water from deeper soil profiles or plant nutrients from different soil depths in the rhizosphere [8, 9]. It is, therefore, plausible to determine plant diversity in grasslands to get clues about ecosystem health.

1.1 Research questions

- i. What is the plant diversity status in agro-pastoral grasslands?
- ii. Is plant diversity affected by anthropogenic activities practiced in agro-pastoral grasslands?
- iii. What is the way forward to maintain plant diversity in agro-pastoral grasslands of Tanzania?

1.2 Objective of the chapter

- To portray the current situation and future prospects of plant diversity in agro-pastoral grasslands

2. Methodology

2.1 Study sites

The study was conducted in Western Serengeti and Ugalla ecosystems in Western Tanzania (**Figure 1**). Western Serengeti is characterized by savannah vegetation that involves extensive grassland with scattered trees and shrubs. Ugalla ecosystem is found in miombo woodlands where grasslands mainly exist in seasonally flooded areas.

2.2 Data collection and analysis

A systematic review of scientific literature on the impact of agro-pastoralism on plant diversity in grasslands involved collecting secondary data, following the guidelines provided by Pullin and Stewart [10] and Inskip and Zimmermann [11]. Google Scholar and other search engines were used to determine the body of knowledge on the subject. To determine relevance and applicability, the search protocol was preceded by predefined filters for keywords [10, 11]. Primary data on vegetation was collected by vegetation sampling during the peak blooming period of herbaceous plants. Each transect was established by recording GPS readings at the starting and end points within the study area. The foliar cover was determined by visual estimation, and herbaceous plant species within 1 m² quadrats were recorded at every 100 m along each transect. Plant identification followed the nomenclature outlined by Agnew and Agnew [12]. Each plant species encountered was classified based on functional attributes, such as life form (grasses and forbs), life span (annual and perennial), and feeding merit (edible and inedible). The determination of the feeding

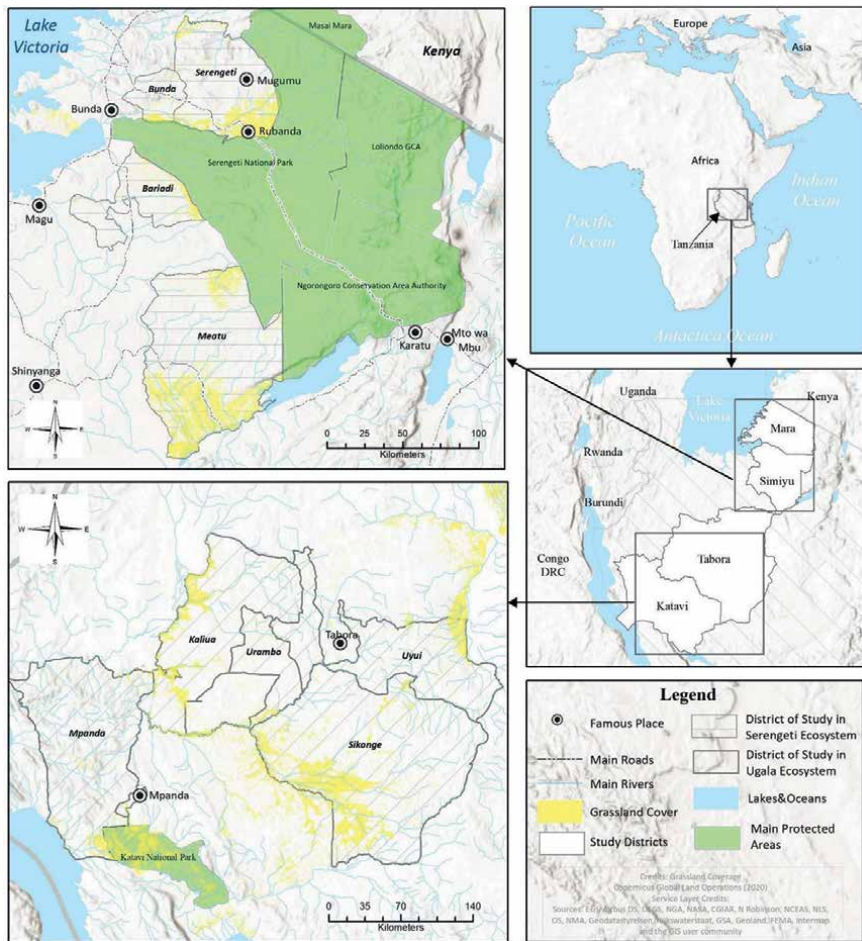


Figure 1.
Map showing the study area.

merit relied on the experience of research workers, the subjective opinions of rangers and livestock keepers, and support from the literature. The relationship between agro-pastoral activities and plant diversity in different ecosystems was analyzed using R software version 4.3.1.

3. Importance of plant diversity for agro-pastoralism

Grasslands serve as a crucial feed resource for grazing animals, and beyond that, grasses play significant roles in water catchments, biodiversity reserves, and cultural and recreational aspects [13]. Additionally, they have the potential to act as a carbon sink, mitigating greenhouse gas emissions [13]. The importance of grasses lies in their content of linoleic acid, with over half of the total fatty acids consisting of ω -3 linoleic acid, including the potent anticarcinogen conjugated linoleic acid (CLA; [14]). Research by Dewhurst and King [15] revealed substantial variations in ω -3 linoleic acid content among grass species and cultivars. CLA is linked to significant fat and protein metabolism regulation, leading to increased muscle formation and decreased fat content [14]. Consequently, milk and meat containing CLA offer higher nutritional value for humans, underscoring the importance of conserving the biodiversity of grass species in grasslands.

The diversity of plants in terms of perennial and annual plants is important in grasslands for ensuring year-round feed resource availability. Perennial grasses, for example, play a crucial role in maintaining grassland health by being more productive, supporting extended grazing periods, and enhancing soil quality [16]. Nevertheless, their extended root zones enable the recapture of leached nutrients and water, contributing to overall soil improvement [16]. Grasslands dominated by annual grasses are of poorer quality during the dry season because the plants mature faster and lose nutritive value faster as well. Perennial grasses are observed to be vulnerable to agro-pastoral activities, and they are replaced by annual grasses [17]. This situation causes changes in plant diversity in grasslands subjected to anthropogenic activities.

4. Impacts of agro-pastoralism on plant diversity

In Tanzania, agro-pastoral livelihood involves a combination of traditional and modern practices to fulfill production needs. The choice of agro-pastoralism practices significantly impacts both herbaceous plant biodiversity and the livelihood of the local population. Practices such as keeping large herds of grazing animals within confined areas or grazing continuously on the same range throughout the year lead to land degradation. This degradation results from the high pressure exerted on plant species and soil disturbance due to trampling. Additionally, the unrestricted expansion of cultivated land negatively affects herbaceous plant species, reducing the feed resource base for grazing animals. Animal trampling causes soil compaction, impacting soil density and porosity resulting in poor water infiltration. The removal of plants due to the large number of grazing animals leaves the land bare, contributing to surface water runoff during the rainy season leading to soil erosion.

Clearing land and cultivating for crop production fundamentally alter and disturb a previously stable ecosystem. The cultivated area undergoes immediate succession, with plant species adapted to bare land conditions and disrupted soil invading and establishing themselves. This process leads to shifts in plant species composition and,

consequently, changes in plant biodiversity. Some herbaceous plant species within the community may become more prevalent, while new species may invade the community from neighboring ecosystems.

Erosion of soil from exposed cultivated land during the rainy season leads to the loss of the top fertile soil, resulting in decreased soil fertility. This diminished fertility contributes to the establishment of a limited number of plant species, leading to a reduction in herbaceous plant composition. The decline in herbaceous plant composition results in lower above-ground biomass production, creating an inadequate feed

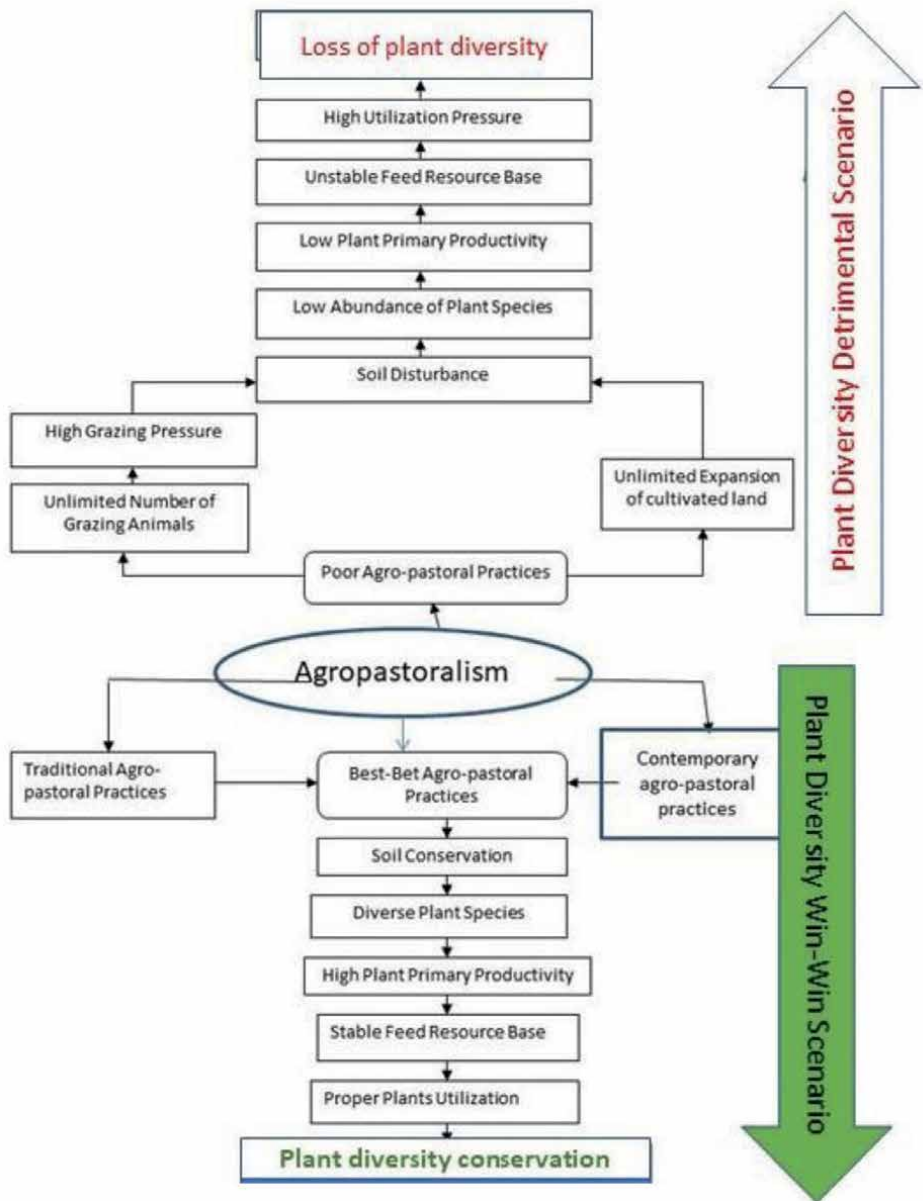


Figure 2.
Conceptual framework on the impact of agro-pastoralism on plant diversity. Adopted from [18].

resource base for grazing animals. The high number of grazing animals in a shrinking grazing land, coupled with insufficient feed resources in terms of both quantity and quality, increases grazing pressure. This elevated grazing pressure on palatable herbaceous plant species leads to the disappearance of these plants and, subsequently, the loss of herbaceous plant biodiversity. The sequence of events described in this scenario can be termed as “herbaceous plant biodiversity detrimental scenario.”

On the flip side, agro-pastoralism, as a livelihood strategy, encompasses various traditional and contemporary best-bet practices, such as deferred grazing (Ngitiri or Alalili), grass band cultivation, zay pit cultivation (Ngoro system), and controlled grazing based on proper stocking rates. These optimal agro-pastoralism practices contribute to soil conservation by minimizing disturbances to the soil and native plants, resulting in the availability of diverse plant species that contribute to high primary productivity. Sustained high primary productivity ensures a stable feed resource base in terms of both quantity and quality to support grazing animals. This situation allows grazing animals to selectively remove herbaceous plants through grazing while providing an opportunity for the regeneration of plants. This, in turn, contributes to the biodiversity conservation of herbaceous plants. The sequence of events described in this scenario can be termed as “herbaceous plant biodiversity win-win scenario.” Both the “herbaceous plant biodiversity detrimental scenario” and the “herbaceous plant biodiversity win-win scenario” impact the livelihood of agro-pastoralists, either negatively or positively. This conceptual framework can be represented by a schematic diagram as follows (**Figure 2**).

5. Effect of agro-pastoralism on plant diversity in Western Serengeti and Ugalla grasslands

Changes in plant diversity are attributed to human activities and their effects are exacerbated by the climatic condition of the site. Vegetation changes in many countries are associated with climate change, human population growth, and extensive agriculture [19]. The decline in plant diversity affects negatively ecosystem functions and services because many species are needed to maintain ecosystem functioning and services [20]. Anthropogenic activities (**Figure 3**) contribute to the reduction of plant diversity [17]. However, their effects differ between different ecosystems due to differences in plant species composition and environmental factors such as soil and precipitation.



Figure 3.
Anthropogenic activities in the Western Serengeti and Ugalla ecosystem.

This study showed relatively higher plant diversity ($p < 0.001$) in Western Serengeti than Ugalla ecosystem (**Figure 4**). This could be attributed to differences in physiognomic aspects of savannah in Western Serengeti and Miombo woodlands in Ugalla ecosystem.

Grasses form a basal diet for wild and domestic grazing animals, implying that a grassland ecosystem with a high diversity of grass species supports many grazing animal species. The current study showed a higher diversity of grass species ($p < 0.001$) in Western Serengeti than in Ugalla ecosystem (**Figure 5**). This concurs with the fact that many wildlife species are found in Serengeti grassland while the Ugalla ecosystem harbors few species, particularly specialized feeders such as sable antelope.

This study showed 24 plant species common to grasslands in Ugalla and Western Serengeti, while 84 plant species were exclusively found in the Ugalla ecosystem and Western Serengeti (**Figure 6**).

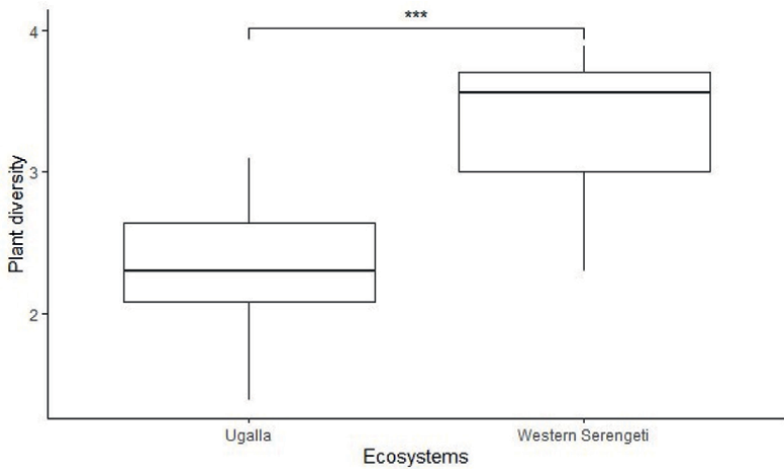


Figure 4.
Plant species diversity in the Ugalla ecosystem and Western Serengeti.

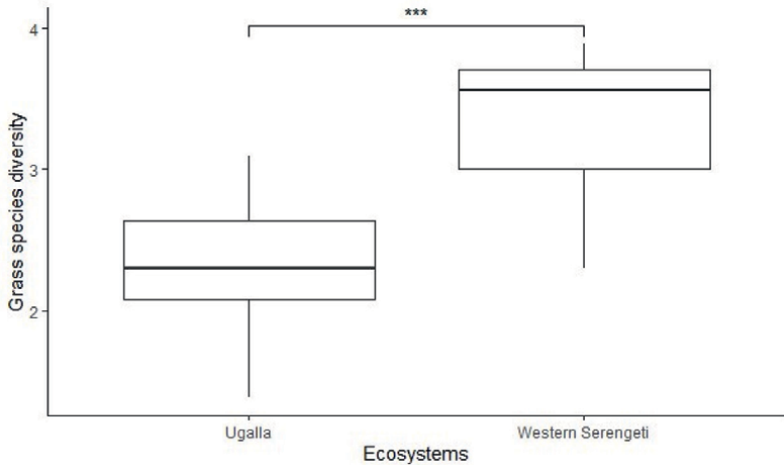


Figure 5.
Diversity of grass species in Western Serengeti and Ugalla ecosystem.

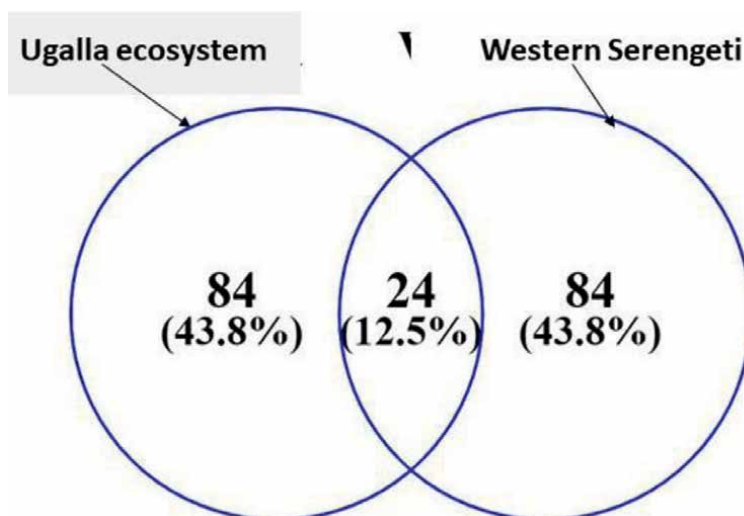


Figure 6.
Existence of plant species in the Ugalla ecosystem and Western Serengeti.

Plant species that were common to the Ugalla ecosystem and Western Serengeti include *Brachiaria brizantha*, *Cynodon dactylon*, *Cynodon plectostachyus*, *Dactyloctenium aegyptium*, *Digitaria macroblephara*, *Digitaria milaniana*, *Digitaria ternate*, *Gutenbergia cordifolia*, *Heliotropium steudneri*, *Hygrophila auriculata*, *Hyparrhenia hirta*, *Justicia exigua*, *Justicia matammensis*, *Panicum coloratum*, *Panicum maximum*, *Senna occidentalis*, *Sesbania sesban*, *Setaria sphacelata*, *Setaria verticillata*, *Sida acuta*, *Solanum incanum*, *Sporobolus festivus*, *Sporobolus pyramidalis*, *Tephrosia pumila*, and *Triumfetta rhomboidea*. Plant species that were exclusively found in each ecosystem are shown in **Table 1**.

The unique plant species in each ecosystem need to be conserved because they mostly support specialized feeders. Local extinction of these species might affect the existence of specialized feeders in the ecosystem.

Perennial grasses provide a better indication of the health status of grasslands than annual grasses. Perennials tend to yield higher dry matter and provide better soil protection than annuals [21]. In that manner, grasslands with a low diversity of grass species are prone to land degradation by water runoff. In this study, perennial plant diversity was higher in Western Serengeti than Ugalla ecosystem (**Figure 7**).

The low diversity of perennial grasses in Ugalla ecosystem makes the ecosystem prone to soil erosion under cultivation. This compelled smallholder farmers in Ugalla ecosystem to adopt ridge cultivation to limit water runoff on cultivated land during the rainy season. The functional role of perennial grasses is both biomass production and soil important for a stable grassland ecosystem.

Grasslands sustain grazing animals by providing edible plants that are not harmful and have nutritional values. A high diversity of edible plants ensures the availability of a balanced ration for the grazing animals to enable their production and reproduction functions. The current study showed higher diversity of edible plants in Western Serengeti than Ugalla ecosystem (**Figure 8**).

The superiority of Western Serengeti in terms of edible plant diversity enables the area to support a large number of different herbivore species. Inedible plant species diversity was not significantly different ($p > 0.05$) in the Ugalla ecosystem

Ugalla ecosystem	Western serengeti
<i>Acalifa indica</i>	<i>Abutilon mauritianum</i>
<i>Albuca abyssinica</i>	<i>Achyranthes aspera</i>
<i>Amaranthus fimbriatus</i>	<i>Altenanthera pungens</i>
<i>Aspilia mossambicensis</i>	<i>Andropogon greenwayi</i>
<i>Blepharis maderaspatensis</i>	<i>Aneilema petersii</i>
<i>Brachiaria deflexa</i>	<i>Aristida adoensis</i>
<i>Brachiaria scalaris</i>	<i>Aristida kenyensis</i>
<i>Bryophyllum pinnatum</i>	<i>Asparagus africanus</i>
<i>Cardiospermum halicacabum</i>	<i>Aspilia mossambicensis</i>
<i>Chloris roxburghiana</i>	<i>Bidens schimperii</i>
<i>Combretum zeyheri</i>	<i>Blepharis linariifolia</i>
<i>Commiphora mossambicensis</i>	<i>Blepharis maderaspatensis</i>
<i>Conyza bonariensis</i>	<i>Bothriochloa insculpta</i>
<i>Conyza stricta</i>	<i>Brachiaria jubata</i>
<i>Crotalaria pallida</i>	<i>Brachiaria semiundulata</i>
<i>Ctenium newtonii</i>	<i>Brachiaria serrata</i>
<i>Cyanotis nodiflora</i>	<i>Cenchrus ciliaris</i>
<i>Cyperus cyperoides</i>	<i>Chloris gayana</i>
<i>Cyperus esculentus</i>	<i>Chloris pycnothrix</i>
<i>Cyperus fimbriatus</i>	<i>Chloris virgata</i>
<i>Cyperus involucratus</i>	<i>Chrysochloa orientalis</i>
<i>Cyperus rotundus</i>	<i>Clitoria ternatea</i>
<i>Cyperus volkielloides</i>	<i>Commelina africana</i>
<i>Digitaria brazzae</i>	<i>Commelina benghalensis</i>
<i>Digitaria mombasana</i>	<i>Corchorus aestuans</i>
<i>Digitaria obtusifolia</i>	<i>Craterostigma plantagineum</i>
<i>Digitaria scalarum</i>	<i>Crotalaria spinosa</i>
<i>Dissotis rotundifolia</i>	<i>Cynium tubulosum</i>
<i>Dolichos kilimandscharicus</i>	<i>Cyperus pulchellus</i>
<i>Echinochloa colona</i>	<i>Cyperus triceps</i>
<i>Echinochloa haploclada</i>	<i>Digitaria bicornis</i>
<i>Emilia blittersdorffii</i>	<i>Digitaria eriantha</i>
<i>Emilia coccinea</i>	<i>Digitaria longiflora</i>
<i>Eragrostis chapelieri</i>	<i>Dyschoriste radicans</i>
<i>Eragrostis leptostachya</i>	<i>Echinochloa pyramidalis</i>
<i>Eragrostis setulifera</i>	<i>Eleusine indica</i>
<i>Eragrostis spectabilis</i>	<i>Eragrostis aspera</i>
<i>Eragrostis superba</i>	<i>Eragrostis cilianensis</i>
<i>Eriochloa fatmensis</i>	<i>Eragrostis racemosa</i>

Ugalla ecosystem	Western serengeti
<i>Eriosema glomeratum</i>	<i>Eragrostis tenuifolia</i>
<i>Euphorbia candelabrum</i>	<i>Euphorbia inaequilatera</i>
<i>Euphorbia grantii</i>	<i>Eustachys paspaloides</i>
<i>Euphorbia hirta</i>	<i>Gomphrena globosa</i>
<i>Fadogia cienkowskii</i>	<i>Gutenbergia petersii</i>
<i>Fuirena umbellata</i>	<i>Harpachne schimperii</i>
<i>Gardenia ternifolia</i>	<i>Heliotropium nelsonii</i>
<i>Hibiscus cannabinus</i>	<i>Heteropogon contortus</i>
<i>Hyparrhenia newtonii</i>	<i>Hyperthelia dissoluta</i>
<i>Hyparrhenia rufa</i>	<i>Hypoxis hirsuta</i>
<i>Indigofera taborensis</i>	<i>Indigofera basiflora</i>
<i>Indigofera arrecta</i>	<i>Indigofera hochstetteri</i>
<i>Indigofera capitata</i>	<i>Indigofera spicata</i>
<i>Indigofera conferta</i>	<i>Indigofera volkensii</i>
<i>Indigofera microcarpa</i>	<i>Ipomea mombassana</i>
<i>Indigofera swaziensis</i>	<i>Justicia betonica</i>
<i>Ipomoea cairica</i>	<i>Justicia glabra</i>
<i>Ipomoea involucrate</i>	<i>Kyllinga nervosa</i>
<i>Kohautia caespitosa</i>	<i>Kyllinga triceps</i>
<i>Kyllinga nervosa</i>	<i>Lepidagathis scabra</i>
<i>Launaea cornuta</i>	<i>Leucas aspera</i>
<i>Leersia denudata</i>	<i>Leucas deflexa</i>
<i>Melhanina velutina</i>	<i>Macroptilium atropurpureum</i>
<i>Pennisetum polystachion</i>	<i>Microchloa kunthii</i>
<i>Perotis hildebrandtii</i>	<i>Mollugo nudicaulis</i>
<i>Phyllanthus amara</i>	<i>Ocimum basilicum</i>
<i>Phyllanthus engleri</i>	<i>Ocimum suave</i>
<i>Phyllanthus reticulatus</i>	<i>Omorcapum kirkii</i>
<i>Pittosporum floribundum</i>	<i>Omorcapum trichocarpum</i>
<i>Polygala ruwenzoriensis</i>	<i>Ornithogalum kirkii</i>
<i>Richardia scabra</i>	<i>Oxygonum sinuatum</i>
<i>Senna hildebrandtii</i>	<i>Pennisetum mezianum</i>
<i>Sesamum angustifolium</i>	<i>Portulaca oleracea</i>
<i>Sesamum indicum</i>	<i>Portulaca quadrifida</i>
<i>Sida ovata</i>	<i>Setaria pumila</i>
<i>Smilax anceps</i>	<i>Sporobolus africanus</i>
<i>Spermacoce princeae</i>	<i>Sporobolus cordofanus</i>
<i>Sporobolus spicatus</i>	<i>Sporobolus ioclados</i>
<i>Stylosanthes fruticosa</i>	<i>Sporobolus marginatus</i>

Ugalla ecosystem	Western serengeti
<i>Tephrosia lupinifolia</i>	<i>Talinum portulacifolium</i>
<i>Tephrosia vogelii</i>	<i>Themeda triandra</i>
<i>Terminalia sericea</i>	<i>Tragus berteronianus</i>
<i>Vernonia petersii</i>	<i>Tribulus terrestris</i>
<i>Vigna vexillata</i>	<i>Vernonia galamensis</i>

Table 1.
Plant species exclusively found in the Ugalla ecosystem and Western Serengeti.

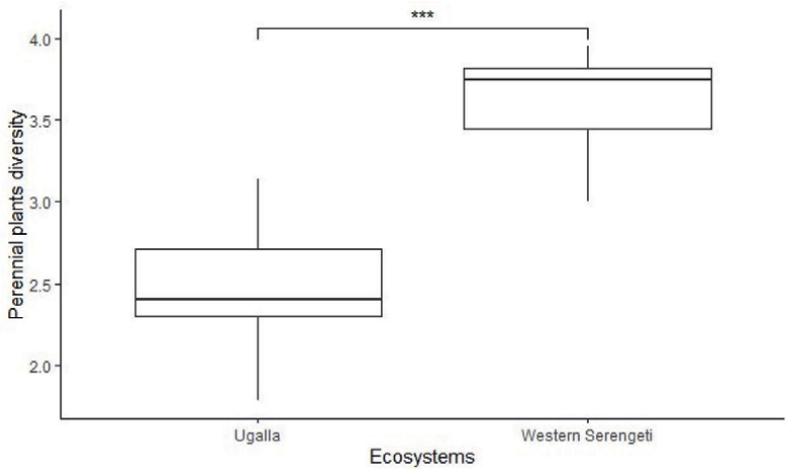


Figure 7.
Diversity of perennial grasses in Ugalla ecosystem and western Serengeti.

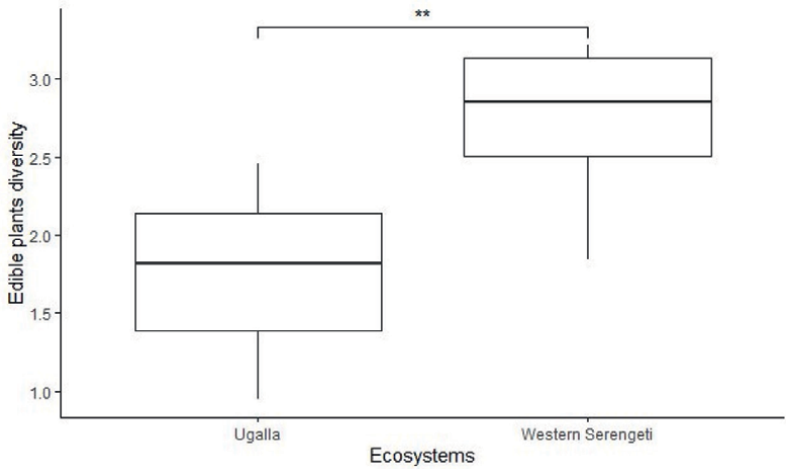


Figure 8.
Diversity of edible plants in the Ugalla ecosystem and Western Serengeti.

and Western Serengeti (**Figure 9**). However, the uneven size of the boxplot in Ugalla indicates more variation of inedible plant diversity in different locations within the ecosystem. This suggests variations in the phenology of plants in different locations in the Ugalla ecosystem. This situation provides an opportunity for non-herbivores such as birds and bees to get resources for surviving in the ecosystem.

Generally, this study showed that plant diversity increased with an increase in altitude and the optimum altitude for plant diversity lies between 1600 and 1800 m above sea level (**Figure 10**).

Results shown in **Figure 10** suggest that plant diversity in lowlands is affected negatively by agro-pastoral activities. In most cases, lowlands are considered suitable for cultivation and livestock grazing in the Ugalla ecosystem and Western Serengeti.

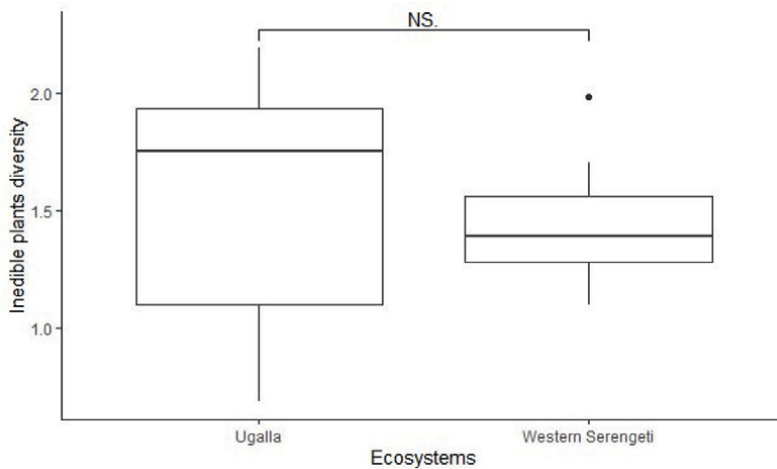


Figure 9.
Diversity of inedible plants in the Ugalla ecosystem and Western Serengeti.

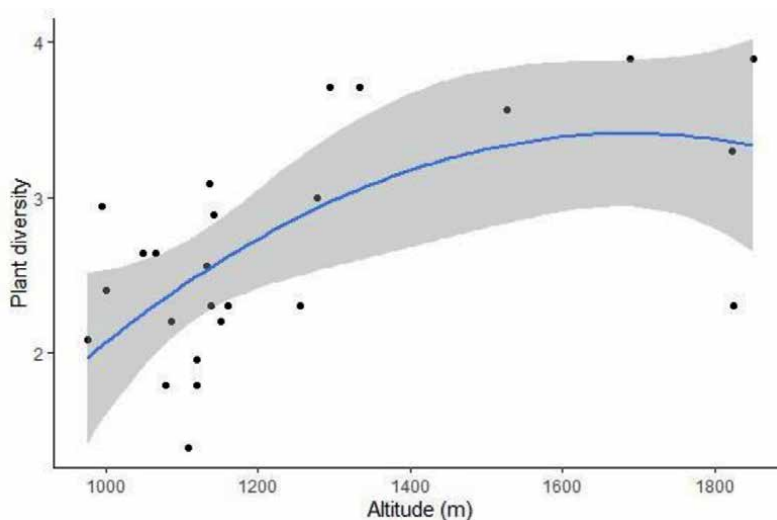


Figure 10.
Variation of plant diversity with altitude.

On the other hand, steep areas are subject to a decline in plant diversity due to soil erosion especially when disturbed by agro-pastoral activities.

6. Prospects of plant diversity in agro-pastoral grasslands of Serengeti and Ugalla ecosystems

The increase in human population causes an increase in food demand that consequently increases agro-pastoral activities in lowlands of the Ugalla ecosystem and Western Serengeti. This situation might negatively affect ecosystem functions due to the decline of plant diversity. Some of the effects have been manifested by an increase in siltation of water bodies found within the ecosystems with consequent decline of biodiversity in lakes [22].

7. Conclusions

- The magnitude of agro-pastoral activities' effect on plant diversity in grasslands differs between ecosystems. The grassland with a low diversity of perennial grass species is much more affected when subjected to cultivation.
- Poor maintenance of plant diversity in grasslands negatively affects ecosystem services provided by plants, and consequent effects are manifested in water bodies by the decline of biodiversity.
- The impact of agro-pastoral activities on plant diversity is conspicuous in lowlands but much more negative when practiced on steep slopes.
- Variations in the phenology of inedible plants within an ecosystem provide temporal and spatial opportunities for non-herbivore animals and invertebrates to access plant resources for their survival.

Way forward

Plant diversity conservation strategies in agro-pastoral grasslands are inevitable to alleviate negative effects on ecosystem services and consequences manifested in water bodies.

Declaration


Some parts of this chapter are based on an unpublished part of the main author's Ph.D. thesis on "influence of agro-pastoralism on herbaceous plants diversity and livelihood of communities in Western Serengeti" submitted to the Senate of Sokoine University of Agriculture in Tanzania.

Author details

Pius Yoram Kavana*, Bukombe John Kija, Emmanuel Pagiti Reuben,
Ally Kiyenze Nkwabi, Baraka Naftal Mbwambo, Simula Peres Maijo,
Selemani Rehani Moshi, Shabani Haruna Matwili, Victor Alexander Kakengi
and Stephen Justice Nindi
Tanzania Wildlife Research Institute, Western Wildlife Research Centre, Kigoma,
Tanzania

*Address all correspondence to: pykavana@gmail.com

IntechOpen

© 2024 The Author(s). Licensee IntechOpen. This chapter is distributed under the terms of the Creative Commons Attribution License (<http://creativecommons.org/licenses/by/3.0>), which permits unrestricted use, distribution, and reproduction in any medium, provided the original work is properly cited. 

References

- [1] Mligo C. Plant species composition and distribution in relation to land use patterns in Serengeti ecosystem Tanzania. *Open Journal of Forestry*. 2015;5:607-620
- [2] Grace JB, Anderson TM, Olff H, Scheiner SM. On the specification of structural equation models for ecological systems. *Ecological Monographs*. 2010;80:67-87
- [3] Estes AB, Kuemmerle T, Kushnir H, Radeloff VC, Shugart HH. Land-cover change and human population trends in the greater Serengeti ecosystem from 1984-2003. *Biological Conservation*. 2012;147(1):255-263
- [4] Chapin F, Zavaleta E, Eviner V, Naylor R, Vitousek PM, Reynolds HL, et al. Consequences of changing biodiversity. *Nature*. 2000;405(6783):234-242
- [5] Hooper DU, Vitousek PM. The effects of plant composition and diversity in ecosystem processes. *Sciences*. 1997;227:1302-1305
- [6] Volvenko IV. The importance of species diversity and its components as criteria for selecting nature conservation areas. *Russian Journal of Marine Biology*. 2011;37(7):604-607
- [7] Craven D et al. Plant diversity effects on grassland productivity are robust to both nutrient enrichment and drought. *Philosophical Transactions. Royal Society B*. 2016;371:20150277. DOI: 10.1098/rstb.2015.0277
- [8] Mueller KE, Tilman D, Fornara DA, Hobbie SE. Root depth distribution and the diversity – Productivity relationship in a long-term grassland experiment. *Ecology*. 2012;94:787-793. DOI: 10.1890/12-1399.1
- [9] Dimitrakopoulos PG, Schmid B. Biodiversity effects increase linearly with biotope space. *Ecology Letters*. 2004;7:574-583. DOI: 10.1111/j.1461-0248.2004.00607.x
- [10] Pullin AS, Stewart GB. Guidelines for systematic review in conservation and environmental management. *Conservation Biology*. 2006;20(6):1647-1656
- [11] Inskip C, Zimmermann A. Human-felid conflict: A review of patterns and priorities worldwide. *Oryx*. 2009;43(1):18-34
- [12] Agnew ADQ, Agnew S. Upland Kenya Wild Flowers: A Flora of the Ferns and Herbaceous Flowering Plants of Upland Kenya. Nairobi: East African Natural History Society; 1994
- [13] Boval M, Dixon RM. The importance of grasslands for animal production and other functions: A review on management and methodological progress in the tropics. *Animal*. 2012;6(5):748-762
- [14] Carlier L, Rotar I, Vlahova M, Vidican R. Importance and functions of grasslands. *Notulae Botanicae Horti Agrobotanici Cluj-Napoca*. 2009;37(1):25-30. Available from: <http://www.notulaeobotanicae.ro>
- [15] Dewhurst RJ, King PJ. Effects of extended wilting, shading and chemical additives on the fatty acids in laboratory grass silages. *Grass and Forage Science*. 1998;53:219-224
- [16] Manahan SE. *Environmental Science and Technology: A Sustainable Approach to Green Science and Technology*. Philadelphia, PA: Taylor & Francis; 2007. p. 672

[17] Kavana PY, Sangeda AZ, Mtengeti EJ, Mahonge C, Bukombe J, Fyumagwa R, et al. Herbaceous plant species diversity in communal agro-pastoral and conservation areas in western Serengeti, Tanzania. *Tropical Grasslands-Forrajes Tropicales*. 2019;7(5):502-518. DOI: 10.17138/TGFT(7)502-518

[18] Kavana PY. Influence of Agro-Pastoralism on Herbaceous Plant Diversity and Livelihood of Communities in Western Serengeti. [Ph.D. Thesis]. Tanzania: Sokoine University of Agriculture; 2021. p. 181

[19] FAO. The State of Food and Agriculture. Climate Change, Agriculture and Food Security. Rome, Italy: Food and Agriculture Organization of the United Nations (FAO); 2016. p. 194

[20] Isbell F, Calcagno V, Hector A, Connolly J, Harpole WS, Reich PB, et al. High plant diversity is needed to maintain ecosystem services. *Nature*. 2011;477(7363):199-202. DOI: 10.1038/nature10282

[21] Van Wyk E, Van Oudtshoorn F. Guide to Grasses of Southern Africa. First ed. Pretoria, South Africa: Briza Publications; 1999

[22] McGlue MM, Yeager KM, Soreghan MJ, Behm M, Kimirei IA, Cohen AS, et al. Spatial variability in nearshore sediment pollution in Lake Tanganyika (East Africa) and implications for fisheries conservation. *Anthropocene*. 2021;33:100281. ISSN 2213-3054. DOI: 10.1016/j.ancene.2021.100281

Methods and Practices for Analyzing Vegetation Shift Using Phytosociological Hierarchical Data

Koji Shimano, Yui Oyake and Tsuyoshi Kobayashi

Abstract

We introduce a procedure to predict the vegetation shift using traditional phytosociological survey (cover data). The cover value is generally obtained for each layer of the layered plant community, but usually maximum cover value over the layers used for the vegetation classification and recognition (*C-max* procedure). As an ameliorate procedure, we propose the procedure of every coverage of all layers used to evaluate vegetation shift (*C-all* procedure). The *C-all* procedure enables us to embrace the information on vertical gradient of species distribution in the surveyed communities. In the case of our observations and analyses, tree species with smaller (or no) cover in the upper layer but greater cover in the lower layer can be dominant in the upper layer in the future, resulting in vegetation shift (changes in dominant species of the community). Every general community analysis (cluster analysis, INSPAN, and TWINSpan) followed by *C-all* procedure supports such prediction for some types of Japanese forests. In the forests, changes in species composition have been conventionally predicted by measuring the trunk diameter and height of trees. Our proposal suggests that traditional phytosociological survey is also convenient for studying forest succession and regeneration.

Keywords: cover data, cluster analysis, INSPAN, TWINSpan, phytosociological survey

1. Introduction

In this article, we would like to describe our method for predicting vegetation changes using phytosociological vegetation data, which is usually collected for vegetation classification. Our hope is that the accumulated data of phytosociological vegetation surveys will provide a method for not only community classification but also a method to know vegetation dynamics and future prediction of vegetation in a certain procedure. For this purpose, we introduce ameliorated analyzing procedure using the information on coverage of plants collected from the layered forests at each layer (hierarchical data) and ways to estimate vegetation shifts such as forest regeneration and succession.

2. Plant coverage along the layer

We explain how phytosociological vegetation data are collected in short. Within a certain area selected as a study site for vegetation survey where the occurrence of plants in the community is expected to be uniform, which often means a sample “plot” (quadrat) extracted from a homogeneous stand in an area of a site, we record the existing species in the plot and the above-ground dominance in each layer (along a vertical direction of the community; e.g., tree layer, sub-tree layer, shrub layer, herb layer) over the plot. Then, the abundance of each species is measured, and the dominant species are evaluated.

2.1 Measuring the coverage

Various indices of dominance can be considered, such as the number of individuals, plant volumes, cover, etc. As a traditional standard, the “rank of cover rate” proposed by Braun-Blanquet [1], indicates how much of the projected area of target vegetation is occupied by each species composing the community. The coverage ranks as abundance of each species are 5, 4, 3, 2, 1, and +:

5 : 87.5 (75% ≤ cover ≤ 100%),
4 : 62.5 (50% ≤ < 75%),
3 : 37.5 (25% ≤ < 50%),
2 : 15.0 (5% ≤ < 25%),
1 : 2.5 (0.1% < < 5%),
+ : 0.1%

Here, even if the above-ground parts of a plant (crown and/or trunk of a tree) traverse over the tree layer and the sub-tall-tree layer or lower layers, the cover value of that plant is aggregated as a value of the upper layer and not as other layers. For the plants of other layers, the cover of the plants constituting each layer is determined based on the vertical distribution of plants. This method has been widely accepted and a vast amount of data has been collected around the world.

It is important to note that in the layered forests in the temperate regions, for example, researchers record data according to the following hierarchical levels: the tall-tree layer, which constitutes the forest canopy (overstory); the sub-tall-tree layer, which is slightly lower in height than the tall-tree layer; the shrub layer, which is about 4–5 m high; and the herb layer, which contains herbaceous plants (including grasses, sedges, sometimes ferns, lianas and so on), seedlings, and juveniles of trees and shrubs less than 1 m in height. This work means that the hierarchical structure of the community is faithfully recorded. Not only in the different types of forests in other regions but also in the herbaceous communities and grasslands are such hierarchical data collections useful.

2.2 General uses of coverage (C-max procedure) and demerits

The classical classification and recognition of community type are based on the concept of “Environmental Diagnosis”. A recognized vegetation provides an indicator of the climate and other regional environmental traits, such as dryness or wetness of the soil, which has been established in the plant community.

Generally, in such Environmental Diagnostic studies, the data taken from the idea of Braun-Blanquet are carefully organized and analyzed using the method of Mueller-Dombois and Ellenberg [2], which is the central text in the field. In their methods,

Plot α		Layer/ Stratum	Plot β	
By C-max procedure (species/cover rank)	By C-all procedure (species/cover rank)		By C-all procedure (species/cover rank)	By C-max procedure (species/cover rank)
Max cover Species A /3 Species B /3 Species C /1	Species A /1	I (tall tree)	Species A /3	Max cover Species A /3 Species B /3 Species C /1
	Species B /3	II (sub-tree)	Species B /2	
	Species C /1	III (shrub)	Species C /+ Species B /1	
	Species A /3 Species B /1 Species C/1	IV (herbaceous)	Species B /3 Species A /1 Species C/1	

Table 1.
Treatment of vegetation data in the respective analyses of procedures C-all and C-max. The Braun-Blanquet method records the occurrence species and cover in each layer/stratum separately. In the conventional C-all method, one representative value (i.e. the maximum value) of cover rank/coverage for each layer is extracted and used in the analysis, as shown in the table. In the C-all method introduced here, the same species appearing in different layers are treated as different species by attaching a symbol indicating each layer (e.g. I, II) to the species name.

data recorded by tall-tree, sub-tall-tree, shrub, and herbaceous strata, in other words, along a developmental stage of height growth of plants in the layered forests (although the shrub species do not grow in height even at well-developed stages and have less effect on the varying in community types as compared to the tree species), are used to classify communities. Nevertheless, a maximum value of cover among the stratum alone is selected for each species and then used to predict the forest types of the future, even which are possibly affected by the minor values of other stratum. In many cases, this means that only the cover of the tall tree layer is used as the representative value for that species at the study site (**Table 1**).

We call this maximum coverage (over the layers) selected procedure as ‘C-max’. The conventional C-max procedure is fine on the community classification at the stable phase of community dynamics. However, that does not aim to survey the dynamics of the community at patchy/short-term scales, so it is inconvenient to recognize the community shape in the past and future in a changing environment. In reality, many plant communities are unstable and at a certain phase of those dynamics, especially under natural disturbances and human interferences.

3. Unselected uses of coverage (C-all procedure) and advantages

Here, we introduce the ameliorated procedures using data from the traditional Braun-Blanquet methods on the coverage of plants collected from the layered forests to consider the vegetation shifts such as forest regeneration and succession.

Imagine that a land is cleared in a temperate region. After a few decades, pioneer trees such as red pine *Pinus densiflora* would occupy forest overstory. However, beneath the overstory, the pine seedlings could not grow as a next generation of overstory because of the shading from their mother trees. Then the pine forest would shift to an oak forest dominated by *Quercus serrata* that is with much shade tolerance

and grow up to the overstory from the saplings and seedlings at the shrub layer and the herbaceous layer. In phytosociological vegetation surveys, the presence of species is recorded separately for tree, sub-tree, shrub, and herbaceous layers. If all pieces of information from the vertical distribution of plants are used, it is possible to estimate such successional change (**Table 1**).

Therefore, we conduct every coverage of all layers selected procedure (*C-all* procedure) and show useful results to infer successional change drawn by the multivariate analyses (cluster analysis, INSPAN, and TWINSPAN) for community recognition. How to handle stratified data and the results of found possible vegetation shift are presented as below.

3.1 Handling the values of cover in the *C-all* procedure

As mentioned above, there are six cover ranks, and the median of their cover ranges was used in the following analysis (similar to the cluster analysis of Goto and Shimano [3], and Oyake et al. [4, 5]).

For the *C-all* procedure, when a species occurs in more than one stratum, cover values are treated separately for each stratum. For example, tall tree stratum = I, sub-tree stratum = II, shrub stratum = III, and herbaceous stratum = IV are recognized in a survey plot, and the cover rank of Species A is observed as

- 5 in the tall tree layer
- no occurrence in the sub-tall-tree layer
- 3 in the shrub layer
- 1 in the herbaceous layer,

then treated as

- Species A I is 5
- Species A II is no occurrence
- Species A III is 3
- Species A IV is 1,

respectively. Such handling seems to be only natural but note that it is different from the conventional handling method, *C-max* procedure (**Table 1**).

3.2 Evaluation of vegetation status on the artificial green

The research group of Oyake, one of the authors, investigated the established vegetation on the embankment slopes of Japanese expressways approximately 50 years after construction. Such artificial greens are often needed to evaluate vegetation shifts to manage the lands, and the expected *C-all* procedure is useful for the evaluation.

Seven 5-m² study plots with different stand of the sites were established along the Meishin Expressway (Shiga Prefecture, Japan [4]), four plots on the Kyushu

Study site	Plot	Num. of Species	Dominant species	Life form
Meishin Expressway [4]	M1	5	<i>Pleioblastus simonii</i>	Dwarf bamboo
	M2	34	<i>Quercus serrata</i> , <i>Padus grayana</i>	Deciduous broadleaf tree
	M3	41	<i>Pueraria lobata</i>	Vine
	M4	36	<i>Cerasus jamasakura</i>	Deciduous broadleaf tree
	M5	17	<i>Pueraria lobata</i> , <i>Rhus javanica</i> var. <i>chinensis</i>	Vine, Deciduous broadleaf tree
	M6	24	<i>Padus grayana</i> , <i>Cerasus jamasakura</i>	Deciduous broadleaf tree
	M7	47	<i>Padus grayana</i> , <i>Fatsia japonica</i>	Deciduous broadleaf tree, Evergreen broadleaf tree
Kyushu Expressway [5]	K1	11	<i>Pleioblastus simonii</i>	Dwarf bamboo
	K2	15	<i>Pleioblastus simonii</i>	Dwarf bamboo
	K3	18	<i>Quercus acutissima</i> , <i>Phyllostachys edulis</i>	Deciduous broadleaf tree, Giant bamboo
	K4	13	<i>Cryptomeria japonica</i> , <i>Phyllostachys reticulata</i>	Evergreen conifer, Giant bamboo
Chuo Expressway [5]	C1	49	<i>Cerasus jamasakura</i> , <i>Acer crataegifolium</i>	Deciduous broadleaf tree
	C2	30	<i>Toxicodendron sylvestre</i> , <i>Eurya japonica</i>	Deciduous broadleaf tree, Evergreen broadleaf tree
	C3	44	<i>Clethra barbinervis</i> , <i>Quercus glauca</i>	Deciduous broadleaf tree, Evergreen broadleaf tree
	C4	45	<i>Pinus densiflora</i> , <i>Cerasus jamasakura</i>	Evergreen conifer, Deciduous broadleaf tree

Table 2.
 Number of species and dominant species at each survey artificial slope of expressway [4, 5].

Expressway (Kumamoto Pref., Japan), and four plots on the Chuo Expressway (Aichi and Gifu Prefectures, Japan. [5]). For each plot, established vegetation was recorded using the Braun-Blanquet method. When conducting the vegetation survey, the stratification method was used to record the occurrence species name and cover by species in each stratified layer (≥ 10 m: 1st (canopy) layer, 5–10 m: 2nd (sub-canopy) layer, 1.3–5 m: 3rd (lower tree) layer, 0.5–1.3 m: 4th (shrub) layer, < 0.5 m: 5th (understory) layer).

The number of species and dominant species found in each plot are shown in **Table 2**. The vegetation at each plot was characterized as deciduous broadleaf forests (M2, M4, M6, M7, C1, C2, and C3 plots); plot C4 was Japanese red pine *Pinus densiflora*-dominated forest at an earlier successional stage; the plots M1, K1, and K2 were dwarf-bamboo communities dominated by *Pleioblastus simonii*; the plot M2 was dominated by herbaceous vine *Pueraria lobata*; the plot K3 was a community dominated by a giant bamboo *Phyllostachys edulis*, and the plots M5 and K4 were invaded by a giant bamboo *Phyllostachys reticulata*.

A stratified cluster analysis was performed based on the results of the stratified vegetation survey obtained for the three routes. When the same species were

recorded in different strata, two patterns of analysis were conducted: *C-max* and *C-all* procedures. Based on the clusters obtained, Indicator Species Analysis (INSPAN, see **Box 1**) was performed.

3.2.1 Applications to cluster analysis and INSPAN

The results of cluster analysis based on *C-all* procedures and the indicator species indicated by INSPAN are shown in **Figure 1**. The results of cluster analysis by the conventional *C-max* procedure and the indicator species indicated by INSPAN are shown in **Figure 2**.

Looking at the results of INSPAN, it appears that dominant species have a significant influence on cluster partitioning in cluster analysis using the conventional *C-max* procedure (**Figure 2**). On the other hand, cluster analysis using the *C-all* procedure can extract species that characterize the vegetation, although they are not highly covered, such as the understory vegetation.

For example, plot M2, which was dominated by *P. lobata*, was classified as cluster 5 in the stratified cluster analysis, where many deciduous broadleaf forest plots were classified. In INSPAN, these understory/floor vegetations are shared with other deciduous broadleaf forest plots. Thus, the *C-all* procedure can detect similarities in communities that are difficult to discern from the dominant species. On the other hand, when split into eight clusters, plot M2 is classified in a different cluster from the deciduous broadleaf forest plots (see **Box 1**).

Thus, cluster analysis using the *C-all* procedure and INSPAN can be useful to predict future vegetation shifts.

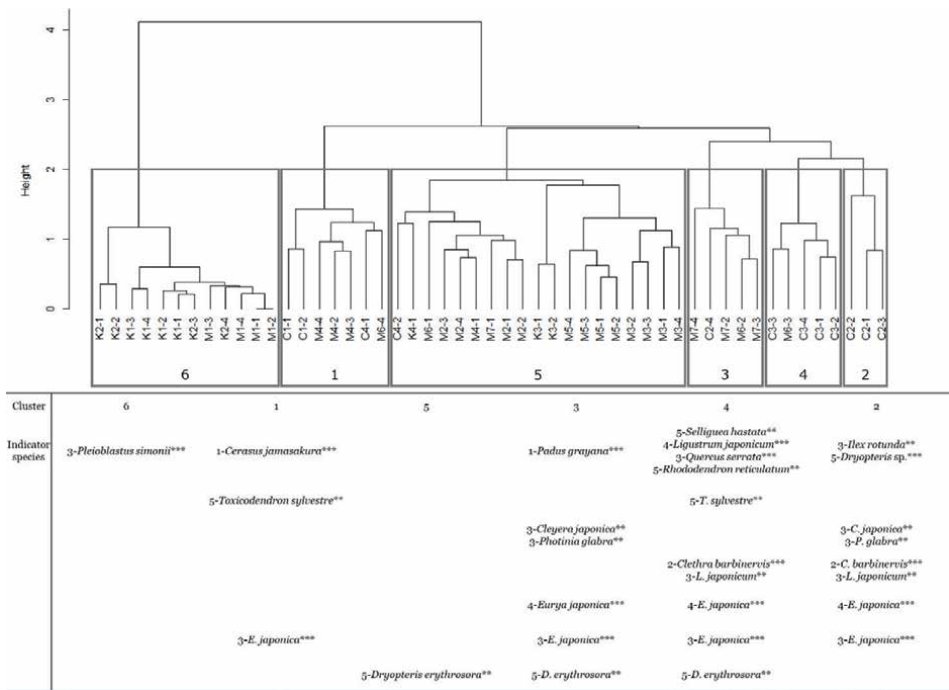


Figure 1.
Dendrogram of cluster analysis results and indicator species for each cluster from INSPAN by *C-all* procedure.

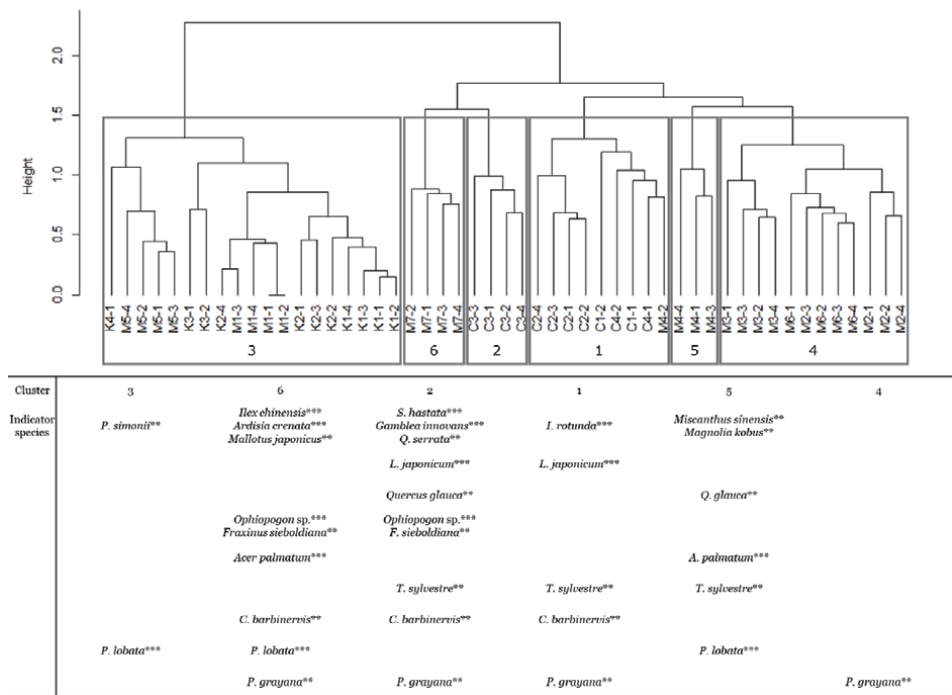


Figure 2.
Dendrogram of cluster analysis results and indicator species for each cluster from INSPAN by C-max procedure.

Cluster analysis summarizes groups of sites with similarities in species and displays a dendrogram. However, the dendrogram does not tell us which species contributed to that grouping. Here, INSPAN (Indicator Species Analysis) can be used to find representative species, which are significantly selected for each community grouping. It should be noted, however, that the indicator species selected will vary by grouping. For example, if one community is divided into two, the indicator species of the undivided community will be the indicator species of one of the two communities, and the other indicator species will be selected for the other community. Thus, it is important to determine how many groups are divided. In mentioned in **Figure 3** is useful in determining the number of divisions. In general, a higher value of the “gap statistic” indicates an appropriate number of groups.

Box 1.
Cluster analysis and INSPAN.

3.3 Evaluation of the invading process of alien species to a natural vegetation

As a next example, we conducted a survey in a riparian forest in central Japan to obtain data, which is suitable to evaluate the vegetation dynamics, fearing that native Japanese willow *Salix serissaefolia* forest, which is unique to Japanese riverbanks and might be replaced by invaded black locust *Robinia pseudoacacia*. Based on this data, we show that two-way indicator species analysis (TWINSPAN, see **Box 2**) followed by the *C-all* procedure is suitable for such vegetation shift.

The data were obtained from a Braun-Blanquet’s phytosociological vegetation survey of 107 plots in the summer of 2008 along the banks of the Saigawa River (Matsumoto and Azumino cities, Nagano Prefecture), central Japan, to determine the

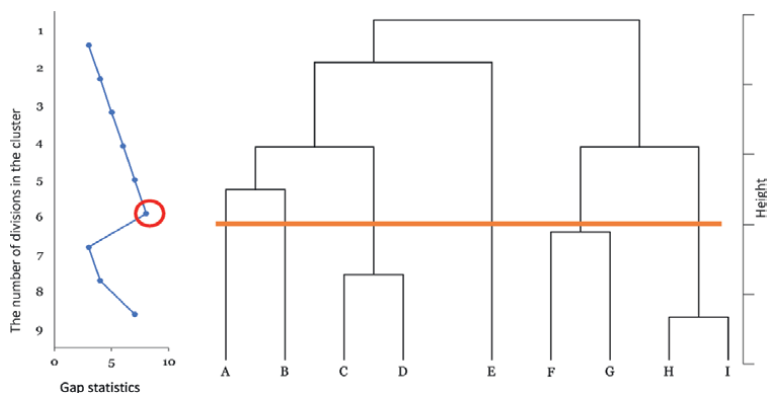


Figure 3.

Schematic diagram of how the number of cluster divisions is determined using the gap statistic. Usually, the highest value of gap statistic, the number of division, is optimum. Characters from A to I are community groups in the cluster. Here, six is the number of optimum division. Note that the number 6 has nothing to do with the value of height (dissimilarity) in the cluster analysis. The position (height) of the horizontal line separating the groups in the cluster diagram can be anywhere as long as the number of group divisions is six.

TWINSPAN is one of the standard analyses on vegetation classification. That is a top-down community classification method, similar to phytosociological tabulation, in which all sites in the study area are firstly divided into two groups based on species composition, and then the divided groups are further divided into two groups (Figure 4). Another representative method of classifying communities by species composition is cluster analysis, which is also used in [3], and is a bottom-up method in which sites with similar species compositions are grouped together based on the similarity of their compositions. Incidentally, Mineda et al. [6] pointed out that cluster analysis is appropriate when the species composition among sites is discontinuous and intermittent, while TWINSPAN is appropriate when it is continuous [6].

Here, we show the differences between the cluster analysis and TWINSPAN, and the output results from common software. Suppose we have data on plant species and their dominance for 100 stands (plots). In the case of cluster analysis, the occurrence of plant species at each site is evaluated numerically to determine how similar the occurrence of each species is and how similar the amount of occurrence is between the stands. TWINSPAN, on the other hand, overviews all plant communities of interest and divides them into broader communities; first there are two groups. After that, the groups will be divided into groups (Table 3).

Box 2.

TWINSPAN.

species composition and characteristics of plant communities [3]. At each plot, the cover rank and community height of all species in each layer including the tall-tree layer ($10 \text{ m} \leq \text{tree height}$), sub-tall-tree layer ($5 \text{ m} \leq <10 \text{ m}$), shrub layer ($0.7 \text{ m} \leq <5 \text{ m}$), and herbaceous layer ($<0.7 \text{ m}$) were recorded.

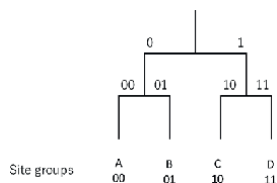


Figure 4.

Schematic diagram of the result of site group division with TWINSPAN. This method divide sites into two groups first, then the groups also do into two in the next step secondly. Characters from A to D mean the divided groups.

Species with layer	Plot number										Species division
	3	2	8	4	9	7	6	1	5	7	
Tree Species AI	5	4	5	5	3						0
Tree Species AII	1	2	1	1	2						0
Shrub Species CIII	1	+	1						+	+	0
Herb Species DIII		+	+		+				+	+	0
Herb Species DIV	+										0
Tree Species BI						5	4	3	5	4	1
Tree Species BII						1	2	3	1	2	1
Tree Species BIII		1			2	1			1		1
Tree Species BIV	1	+			1		+	+		+	1
Shrub Species CIII							+	+			1
Plot division	0	0	0	0	0	1	1	1	1	1	

Table 3.
Image of a result of TWINSpan. Using the occurrence similarity, all species with the layer and all sites were divided into twice. The image here shows only the first two divisions of species and plots. Roman numerical, I, II, III and IV, means tree, subtree, shrub and herb layer, respectively. As you will find, tree species B can be found beneath the overstory of tree species A, but tree species A plants was not beneath tree species B layer. This indicates the forest dominated by tree species A will be the forest dominated by tree species B in the future.

In the study site, several community phases along an invasion intensity of *R. pseudoacacia* populations into *S. serissaefolia* stand were observed. Data were collected by the method of Braun-Blanquet.

3.3.1 Application to TWINSpan

In the present study, TWINSpan was conducted using values compiled by the *C-max* and *C-all* procedures to determine the likelihood of coexistence of species groups that characterize the community within a grouped community (plot group), and the sympatry and exclusivity within and among species between the upper and lower layer [7]. The analysis was performed using the “twinspan” function of the “twinspanR” package (ver. 0.19) on the statistical analysis software R (ver. 3.5.0; R Core Team [8]). Here, only the result with *C-all* procedure was shown.

The TWINSpan results originated from [7] allowed us to recognize the communities as four major groups. The first two divisions from the top of the dendrogram were herb/shrub and forest communities. In the next division, “the herb/shrub community” was divided into *R. pseudoacacia* community and *S. serissaefolia* shrub/grass community. On the other hand, “the tall tree community” was divided into *R. pseudoacacia* and *S. serissaefolia* communities. However, it is noteworthy that *R. pseudoacacia* forests had *R. pseudoacacia* shrubs and seedlings, while *S. serissaefolia* forests did not have *S. serissaefolia* seedlings or shrubs, but *R. pseudoacacia* seedlings and shrubs (Figure 5). Although the TWINSpan analysis can be divided into further small groups, no further dividing was necessary to determine the vegetation shift between *R. pseudoacacia* and *S. serissaefolia* communities.

That is, *R. pseudoacacia* IV, which is a seedling or juvenile tree, grows both beneath the forest overstory of *S. serissaefolia* I and *R. pseudoacacia* I, whereas *S. serissaefolia* IV seedlings would not grow under the canopy of *R. pseudoacacia*. *S. serissaefolia* IV mainly occurred in sandy bare soil sites. This asymmetric distribution of *R.*

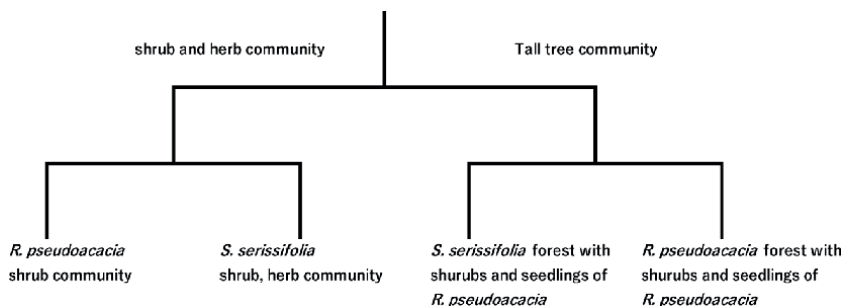


Figure 5.
Summarized result of plot groups with TWINSpan. Community types and key species are described.

pseudoacacia seedlings and juvenile trees allowed them to invade *S. serissaefolia* tall forests, while *S. serissaefolia* seedlings and juvenile trees could not invade either *S. serissaefolia* forests or *R. pseudoacacia* forests. These suggest that, in the future, *S. serissaefolia* willow forests may be replaced by *R. pseudoacacia* forests, but *R. pseudoacacia* forests will remain as *R. pseudoacacia* forests.

Thus, in contrast to the conventional *C-max* procedure, TWINSpan based on the *C-all* procedure made it possible to infer what species will replace and also diagnose future changes in dominant species. Combining further studies on variations in ecophysiological traits, population dynamics, and relationships among species would be nice with long monitoring of vegetation change.

4. Conclusions

In the classical phytosociological vegetation surveys, the values of plant coverage are obtained for layered communities. In the conventional classification and/or recognition of vegetation, only the maximum coverage over the layers is selected (*C-max* procedure). We use our original *C-all* procedure (every coverage of all layers selected procedure) and new success to reveal the vegetation shift such as successional processes from the phytosociological data. The *C-all* procedure will be useful to not only the layered forests but also the herbaceous communities and grasslands (see [5]).

Other dominant indices such as diameter and height of trees would be able to apply similarly other than cover value. However, general tree-by-tree surveys often miss information on the plant layer with less than 1.3 m in height. The manner of phytosociological surveys, which basically intends lower layer(s), and *C-all* procedure complements such problems easily. Re-analyzing vastly accumulated cover data from the past would give additional valuable information on vegetation history by *C-all* procedure.

Recently, new informatics to measure vegetation structure has been developed, and the data from those could be also applied by the *C-all* procedure in the future. However, the convenient cover data by the traditional phytosociological surveys should continue to use important information in many fields.

Conflict of interest

There is no conflict of interest.

Notes/thanks/other declarations

We, the authors, would like to thank our editor, who invited us to publish this book and was patient with our late submission of the manuscript.

Author details

Koji Shimano^{1*}, Yui Oyake² and Tsuyoshi Kobayashi³


1 Faculty of Design Technology, Osaka Sangyo University, Osaka, Japan

2 Faculty of Engineering and Design, Kagawa University, Kagawa, Japan

3 Faculty of Agriculture, Kagawa University, Kagawa, Japan

*Address all correspondence to: shimano@est.osaka-sandai.ac.jp

IntechOpen

© 2023 The Author(s). Licensee IntechOpen. This chapter is distributed under the terms of the Creative Commons Attribution License (<http://creativecommons.org/licenses/by/3.0>), which permits unrestricted use, distribution, and reproduction in any medium, provided the original work is properly cited. 

References

- [1] Braun-Blanquet J. Pflanzensoziologie, Grundzüge der Vegetationskunde. 3rd ed. Berlin: Springer-Verlag; 1964
- [2] Mueller-Dombois D, Ellenberg H. Aims and Methods of Vegetation Ecology. New Jersey: The Blackburn Press; 1974
- [3] Goto S, Shimano K. Riparian forest invasion by *Robinia pseudoacacia* and its effects of riverside vegetation. *Vegetation Science*. 2018;**35**:49-65
- [4] Oyake Y, Imanishi J, Ishihara K, Ogura I, Shibata S. Long-term vegetation transition on man-made slopes 53 years after construction in Central Japan. *Landscape and Ecological Engineering*. 2019;**15**:363-378
- [5] Oyake Y, Mimaki R, Oda K. Vegetation on artificial embankment slopes of the expressways approximate 50 years after construction in two express ways: Kyushu and Chuo Expressway. *Journal of the Japanese Society of Revegetation Technology*. 2023;**48**:507-515 (in Japanese with English Abstract)
- [6] Mineta T, Yamanaka T, Hamasaki K. Statistical analysis for biological and social research (8): Classification (cluster analysis, and indicator species analysis). *Journal of the Japanese Society of Irrigation, Drainage and Rural Engineering*. 2005:221-226 (in Japanese)
- [7] Shimano K, Goto S, Kobayashi T. Shifts from native to non-native riparian plant communities analyzed using hierarchical phytosociological data. *Japanese Journal of Ecology*. 2022;**72**:13-25 (in Japanese with English Synopsys)
- [8] R Core Team. R: A Language and Environment for Statistical Computing. Vienna, Austria: R Foundation for Statistical Computing; 2018

*Edited by Eusebio Cano Carmona
and Ana Cano Ortiz*

This book contemplates methodologies that can be used in the teaching of future experts in agriculture and plant cultivation. It expresses the need for knowledge transfer for good territorial management in the current era of climate change. In most cases, land management at the planetary level is sustainable, but today's society demands sustainable development. To improve the training of technicians in sustainable development methodologies, this book presents some methods and techniques compatible with ecodevelopment.

Published in London, UK

© 2024 IntechOpen

© sweetsake / iStock

IntechOpen

